A role for the hearing gene *Cib2* in somatic sensation

Inaugural-Dissertation
to obtain the academic degree
Doctor rerum naturalium (Dr. rer. nat.)

submitted to the Department of Biology, Chemistry, Pharmacy
of Freie Universität Berlin

by
Dimitra Mazaraki
from Evia, Greece
2022

The present work was carried out under the supervision of Prof. Dr. Gary R. Lewin from April 2017 to June 2022 at the Max Delbrück Centre for Molecular Medicine in the Helmholtz Association.

1st reviewer: Prof. Dr. Gary R. Lewin
Department of Disorders of the Nervous System
Max-Delbrück Centre for Molecular Medicine Berlin

2nd reviewer: Prof. Dr. Ursula Koch
Institute of Biology, Neurophysiology
Freie Universität Berlin

Date of the defense: 13th of February 2023

Declaration of Independence

Herewith I certify that I have prepared and written my thesis independently and that I have not used any sources and aids other than those indicated by me. Intellectual property of other authors has been marked accordingly. I also declare that I have not applied for an examination procedure at any other institution and that I have not submitted the dissertation in this or any other form to any other faculty as a dissertation.

1 Table of Contents

2 APPENDIX

2.1 List of Figures

2.2 List of tables

2.3 List of Abbreviations

AM	A-fibre mechanonociceptor
AP	Action potential
ASIC	Acid-sensing ion channels
BABB	Benzyl Alcohol/ Benzyl Benzoate
BSA	Bovine serum albumin
CGRP	Calcitonin gene-related peptide
CHO	Chinese hamster ovary
CIB	Calcium And Integrin Binding protein
CK20	Cytokeratin 20
CM	C-mechanonociceptors
CNS	Central Nervous System
DH	D-Hair
DMEM	Dulbecco's Modified Eagle Medium
DMSO	Dimethyl sulfoxide
DNA	Deoxyribonucleic acid
DRG	Dorsal root ganglia
EDTA	Ethylenediaminetetraacetic acid
EF	Elongation factor
EGTA	Aminopolycarboxylic acid
FBS	Fetal bovine serum
GFP	Green fluorescent protein
HTMR	High-threshold mechanoreceptor
IHC	Immunohistochemistry
KCNQ	Potassium voltage-gated channel subfamily Q
LHFPL5	Lipoma HMGIC fusion partner-like 5
LSM700	Laser Scanning Microscopy 700
LTMR	low-threshold mechanoreceptor
NF200	Neurofilament 200
NGF	Nerve growth factor
NMDA	N-methyl-D-aspartate
OCT	Optimal cutting temperature
OHC	Outer hair cells
PBS	Phosphate buffered saline
PCDH15	Protocadherin-15
PCR	Polymerase chain reaction
PFA	Paraformaldehyde
PLL	Poly-L-lysine
RA	Rapidly-adapting
RAM	Rapidly-adapting mechanoreceptor
RNA	Ribonucleic acid
RT	Room temperature
SA	Slowly-adapting
SAM	Slowly-adapting mechanoreceptor
SIF	Synthetic inerstitial fluid
STOML3	Stomatin-like protein 3
TH	Tyrosine hydroxylase
TMC	Transmembrane Channel Like

TMEM	Transmembrane (TMEM) protein family members
TMHS	Tetraspan membrane protein in hair cell stereocilia
TMIE	Transmembrane Inner Ear Protein
TRAAK	TWIK-related arachidonic acid-activated K^+ channel
TRK	Tyrosine kinase receptor
TRPV1	Transient receptor potential vanilloid
USH2A	Usherin

3 Summary

Hearing and touch are two of our senses that rely on mechanotransduction to convert mechanical stimulus into electrochemical activity. Several studies have demonstrated that touch and hearing share common genetic determinants; mutations in genes causing deafness are also associated with reduced tactile sensitivity. Furthermore, transcriptome analysis from several studies has revealed that the same genes are expressed in both systems. However, the role of these genes has yet to be determined.

In this work, I demonstrated that the calcium and integrin binding protein 2 (CIB2), a key component of mechanotransduction in the auditory system, is also implicated in somatosensory mechanosensation. CIB2 is an auxiliary subunit of the mechanotransduction channel in the auditory system that modulates channel function and determines correct channel positioning. Mutations in *Cib2* cause hearing loss in humans and mice, as well as the cessation of mechanotransduction in the auditory system.

By applying immunohistochemistry, I demonstrated the expression of CIB2 in a subset of DRG neurons, mainly nociceptors and, to a lesser extent, mechanoreceptors. CIB2 was also present in the terminal endings of sensory neurons that innervate skin end organs. In particular, CIB2 was found in terminal afferents innervating Meissner's corpuscles and hair follicles, both associated with rapidly adapting mechanoreceptors. The impact of CIB2 on the physiological properties of different types of mechanoreceptors and nociceptors was investigated using an ex-vivo skin nerve preparation from the saphenous and tibial nerve. I showed that genetic ablation of *Cib2* had a profound impact on rapidly adapting mechanoreceptors (RAMs). In a velocity and vibration experiment, RAMs lacking *Cib2* exhibited dramatically higher frequency sensitivity. Thus, CIB2 influences RAM adaption rate and functions as a brake on their velocity sensitivity.

CIB2 exhibits structural similarities with KChIP proteins, which are like CIB2, calcium sensors. Additionally, KChIP proteins have been shown to modulate Kv4 channel surface expression, assembly, and kinetics, leading us to the hypothesis that CIB2 influences RAM adaptation by interacting with and regulating a potassium channel. KCNQ4 inhibition or genetic deletion in RAMs had previously been shown to enhance velocity and vibration responses, similarly to observations in *Cib2* knockout mice. I found that inhibiting KCNQ4 did not affect RAM responses in *Wnt1-Cre; Cib2*$^{fl/\,fl}$ mice, showing that in mice lacking *Cib2*, KCNQ4 does not function effectively in RAMs. We were able to study the influence of CIB2 on KCNQ4 kinetics by employing a whole-cell patch clamp and transiently overexpressing CIB2 and KCNQ4 in the CHO cell line. We discovered that the deactivation time for KCNQ4 was slower after CIB2

overexpression. Furthermore, *KCNQ4* mRNA was found in 60% of *Cib2*-positive neurons. Thus, we conclude that CIB2 interacts with and modulates KCNQ4.

The absence of CIB2 in C-fibers, clearly altered their physiological properties. C-fires lacking *Cib2* showed signs of sensitization as they displayed a prominent increase in after-charge responses. However, genetic deletion of *Cib2* did not affect another type of nociceptor, the Aδ nociceptors.

Finally, we assessed the behavioral impact of peripheral *Cib2* ablation on light touch and mechanical pain. By using multiple behavioral assays, I found that mice lacking *Cib2* exhibit a profound loss of touch sensation. Therefore, I performed an electrical search experiment using an ex-vivo skin nerve preparation to search for mechanically insensitive fibers and found that half of the Aβ-fibers were mechanically silent. These findings suggest that CIB2 is interacting with a mechanosensitive channel, the nature of which is yet to be investigated.

This study allowed us to conclude that CIB2 interacts with and modulates ion channels (potassium and mechanosensitive channels) in the somatosensory system and therefore regulates sensory mechanotransduction. We hypothesize that CIB2, as in the auditory system, is an auxiliary subunit of channels in the somatosensory system.

3.1 Zusammenfassung

Hören und Tasten sind zwei unserer Sinne, die auf Mechanotransduktion beruhen, um mechanische Reize in elektrochemische Aktivität umzuwandeln. Mehrere Studien haben gezeigt, dass Tastsinn und Gehör gemeinsame genetische Determinanten haben; Mutationen in Genen, die Taubheit verursachen, werden auch mit einer verringerten Tastsensibilität in Verbindung gebracht. Darüber hinaus haben Transkriptomanalysen in mehreren Studien ergeben, dass in beiden Systemen die gleichen Gene exprimiert werden. Die Rolle dieser Gene ist jedoch noch nicht geklärt.

In dieser Arbeit habe ich gezeigt, dass das Calcium- und Integrin-bindende Protein 2 (CIB2), eine Schlüsselkomponente der Mechanotransduktion im auditorischen System, auch an der somatosensorischen Mechanosensation beteiligt ist. CIB2 ist eine Hilfsuntereinheit des Mechanotransduktionskanals im auditorischen System, die die Kanalfunktion moduliert und die korrekte Kanalpositionierung bestimmt. Mutationen in *Cib2* führen bei Menschen und Mäusen zu Hörverlust und zur Unterbrechung der Mechanotransduktion im auditorischen System.

Mit Hilfe der Immunhistochemie konnte ich die Expression von CIB2 in einer Untergruppe von DRG-Neuronen nachweisen, hauptsächlich in Nozizeptoren und in geringerem Maße in Mechanorezeptoren. CIB2 war auch in den Endigungen der sensorischen Neuronen vorhanden, die die Endorgane der Haut innervieren. Insbesondere wurde CIB2 in terminalen Afferenzen gefunden, die Meissner-Körperchen und Haarfollikel innervieren, die beide mit schnell adaptierenden Mechanorezeptoren assoziiert sind. Die Auswirkungen von CIB2 auf die physiologischen Eigenschaften verschiedener Arten von Mechanorezeptoren und Nozizeptoren wurden anhand eines Ex-vivo-Hautnervenpräparats aus dem Nervus saphenus und dem Nervus tibialis untersucht. Ich konnte zeigen, dass die genetische Ablation von *Cib2* eine tiefgreifende Auswirkung auf die sich schnell anpassenden Mechanorezeptoren (RAMs) hat. In einem Geschwindigkeits- und Vibrationsexperiment zeigten RAMs, denen *Cib2* fehlte, eine dramatisch höhere Frequenzempfindlichkeit. Somit beeinflusst CIB2 die Anpassungsgeschwindigkeit der RAMs und wirkt als Bremse für ihre Geschwindigkeitsempfindlichkeit.

CIB2 weist strukturelle Ähnlichkeiten mit KChIP-Proteinen auf, die wie CIB2 Calcium-Sensoren sind. Darüber hinaus wurde gezeigt, dass KChIP-Proteine die Oberflächenexpression, den Zusammenbau und die Kinetik von Kv4-Kanälen modulieren, was uns zu der Hypothese führt, dass CIB2 die RAM-Anpassung durch Interaktion mit einem Kaliumkanal und dessen Regulierung beeinflusst. Die Hemmung oder genetische Deletion

von KCNQ4 in RAMs hatte zuvor gezeigt, dass sich die Reaktionen auf Geschwindigkeit und Vibration verstärken, ähnlich wie bei *Cib2*-Knockout-Mäusen beobachtet wurde. Ich fand heraus, dass die Hemmung von KCNQ4 die RAM-Reaktionen in Wnt1-Cre; $Cib2^{fl/\,fl}$-Mäusen nicht beeinflusste, was zeigt, dass KCNQ4 in Mäusen, denen *Cib2* fehlt, nicht effektiv in RAMs funktioniert. Wir konnten den Einfluss von CIB2 auf die Kinetik von KCNQ4 untersuchen, indem wir eine Ganzzell-Patch-Clamp-Anlage einsetzten und CIB2 und KCNQ4 in CHO-Zellen vorübergehend überexprimierten. Wir entdeckten, dass die Deaktivierungszeit für KCNQ4 bei CIB2-Überexpression langsamer war. Außerdem wurde *KCNQ4* mRNA in 60% der *Cib2*-positiven Neuronen gefunden. Daraus schließen wir, dass CIB2 mit KCNQ4 interagiert und es moduliert.

Das Fehlen von CIB2 in C-Fasern veränderte eindeutig deren physiologische Eigenschaften. C-Fasern, denen *Cib2* fehlte, zeigten Anzeichen einer Sensibilisierung, da sie eine deutliche Zunahme der Nachladungsreaktionen zeigten. Die genetische Deletion von *Cib2* hatte jedoch keine Auswirkungen auf einen anderen Nozizeptortyp, die Aδ-Nozizeptoren.

Schließlich untersuchten wir die verhaltensbezogenen Auswirkungen der peripheren *Cib2*-Ablation auf leichte Berührungen und mechanische Schmerzen. Mit Hilfe mehrerer Verhaltenstests stellte ich fest, dass Mäuse, denen *Cib2* fehlt, einen tiefgreifenden Verlust des Tastsinns aufweisen. Daher führte ich ein elektrisches Suchexperiment mit einem ex-vivo Hautnervenpräparat durch, um nach mechanisch unempfindlichen Fasern zu suchen, und stellte fest, dass die Hälfte der Aβ-Fasern mechanisch stumm waren. Diese Ergebnisse deuten darauf hin, dass CIB2 mit einem mechanosensitiven Kanal interagiert, dessen Natur noch untersucht werden muss.

Diese Studie erlaubt uns die Schlussfolgerung, dass CIB2 mit Ionenkanälen (Kalium- und mechanosensitiven Kanälen) im somatosensorischen System interagiert und diese moduliert und somit die sensorische Mechanotransduktion reguliert. Wir stellen die Hypothese auf, dass CIB2, wie im auditorischen System, eine Hilfsuntereinheit von Kanälen im somatosensorischen System ist.

4 Introduction

The ability to sense the physical world is fundamental for living organisms, which have evolved for this purpose the sensory nervous system. The seven senses that are conveyed by our sensory system are tactile, proprioceptive, vestibular, visual, auditory, olfactory, and gustatory. Unlike the rest of the senses, touch is distinctive, as receptors for touch and its related modalities are dispersed across the skin while receptors for the other senses are concentrated in compact sense organs (the ears for hearing, the eyes for sight, and the nose for smell). As Aristotle noted, who was the first to describe our senses, "touch lacks a single proper sensible." The perception of touch is underpinned by the somatosensory system, which serves three major functions; exteroceptive for detection and response to stimuli arising outside our body, interoceptive, and proprioceptive, which gives rise to the perception of body posture and balance. This work will focus on the cutaneous somatosensory system, which involves sensory receptors in the skin that provide us with the capacity to detect mechanical forces from the environment to identify the shape and texture of objects, and temperature differences, and facilitate social behaviors such as hugging and kissing, as well as to protect us from harm. The conversion of these mechanical stimuli into electrical signals is the process of sensory mechanotransduction (Chalfie, 2009).

4.1 Cutaneous somatosensory system

Cutaneous somatosensory systems carry four basic types of information upon stimulation: modality, location, intensity, and timing (Abraira & Ginty, 2013; Delmas & Coste, 2013). At the receptive site, diverse mechanical, thermal, and chemical stimuli are transduced into a change in membrane potential that is called receptor potential, which eventually triggers action potential initiation (Hu & Lewin, 2006). Stimulus information transduced into an electrical signal depends on the cooperation of auxiliary cells (end organs) in the skin and the sensory nerve endings as well as the properties of the mechanosensitive channels and the current voltage-gated ion channel properties that amplify or repress transducer signals and thus regulate receptor potential and firing (Hao et al., 2015). Specialized mechanoreceptors detect a wide variety of mechanical stimuli, including light brush, stretch, vibration, deflection of hairs, and noxious pressure (Marshall & Lumpkin, 2012; McGlone & Reilly, 2010). This variety of stimuli is matched with a diverse population of somatosensory neurons, a diverse cell population whose cell bodies are located in the dorsal root ganglia (DRG). Each neuron has a single axon that divides into two branches, with a distal process that innervates the skin's various layers and a proximal process that reaches the spinal cord and establishes synapses in the dorsal

horn. Terminal endings of these neurons in the skin convert mechanical inputs into an electrical signal over a particular threshold, resulting in membrane depolarization, action potential initiation, and propagation to the spinal cord and/or brainstem, where they are passed to second-order neurons. The sensory information is then transmitted from the thalamus to the somatosensory cortices, where it is processed and integrated into sensory precepts (Kandel, E.R., 2000). Mechanically-gated ion channels quickly convert mechanical information into electrical impulses and depolarize sensory terminals to create action potentials (Delmas & Coste, 2013; Lumpkin & Caterina, 2007; Ranade et al., 2015).

4.1.1 Skin

Mammalian skin is composed of two layers: a nonvascular epidermis and an inner layer called the dermis. The two layers are connected via finger-like projections (dermal papillae) of the vascular dermis extending into the epidermis (Fig. 1). The epidermis forms a protective barrier over the body's surface. Keratinocytes are organized in the upper layer and form cellular junctions between each other and secrete keratin proteins and lipids which contribute to the formation of an extracellular matrix and provide mechanical strength to the skin (Breitkreutz et al., 2009). The deeper layer of skin, the dermis, is composed of loosely packed fibroblasts and a collagen-rich extracellular matrix. Underneath the dermis, a layer of fat cells forms the hypodermis (Jenkins & Lumpkin, 2017). Skin is the largest sensory organ and the primary tissue that interfaces with environmental stimuli. The skin is innervated by a diverse range of sensory neuron subtypes, including nociceptors, which respond to noxious stimuli; thermoreceptors, which are tuned to detect temperature information; and low-threshold mechanoreceptors (LTMRs), which encode non-painful mechanical stimuli, or light touch. Mammalian skin is divided into hairy and non-hairy (glabrous) layers. Most animals have glabrous skin on their hands and feet (paws). Glabrous skin is thus used for discriminative touch, as well as sensing texture and shape and mediating grip control, reaching, and movement (Zimmerman et al., 2014). More than 90% of the body's surface is covered by hairy skin. The hairs serve as a barrier against temperature loss and physical harm, as well as a crucial part of social interactions and mating behaviour. Furthermore, hair serves as a fundamental, physical process via which many species experience touch, but with far lower spatial acuity than non-hairy skin.

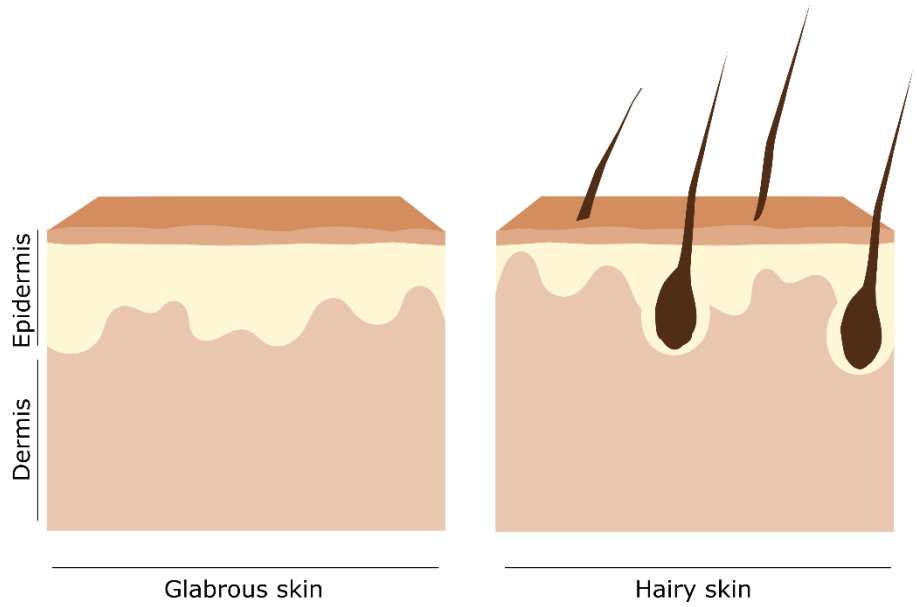

Figure 1. Hairy and glabrous skin in mouse. Mammalian skin includes invaginations of the epidermis called rete ridges, and dermal zones in between are called dermal papillae

The key to our understanding of the neurobiological basis of touch is determining how end organs in the skin encode complex forms of tactile stimulation and how this encoding is then integrated and processed within the central nervous system. In the following sections, the most important receptors found in skin-nerve preparations are described in more detail.

4.1.2 Mechanoreceptors and their associated end-organs

The perception of innocuous and noxious touch sensations is based on special mechanosensitive sensory neurons that are divided into two groups: low-threshold mechanoreceptors (LTMRs) that respond to innocuous mechanical stimulation and high-threshold mechanoreceptors (HTMRs) that detect harmful mechanical stimuli. Furthermore, they can also be classified according to their morphology, level of myelination, and conduction velocity. Large-soma and heavily myelinated neurons with fast conduction velocities (>10m/s) correspond to Aβ LTMRs, medium-soma, and lightly myelinated axons to Aδ-LTMRs or D-hair receptors with intermediated velocities (<10 and >1 m/s) and non-myelinated to nociceptors. which display slow conduction velocities (<1m/s) (A. G. Brown & Iggo, 1967; Koltzenburg et al., 1997; Leem et al., 1993; Milenkovic et al., 2008). Mechanoreceptors respond to mechanical stimulation at variable rates of adaptation, known as rapidly adapting

(RA) and slowly adapting (SA), while nociceptors exclusively exhibit slowly adapting responses (Li et al., 2011; Smith & Lewin, 2009).

4.1.3 Glabrous skin

Distinct cells or sensory corpuscles have been discovered in the glabrous skin, each connected with an LTMR and exhibiting unique tuning properties: Merkel cell–neurite complexes, Ruffini corpuscles, Meissner's corpuscles, and Pacinian corpuscles (McGlone & Reilly, 2010; Munger & Ide, 1988; Zimmerman et al., 2014). The associated LTMRS fall into two main categories: rapidly adapting (RA) and slowly adapting (SA) mechanoreceptors, which each can be subdivided into two variants, type I and type II. SAI mechanoreceptors are linked to epidermal Merkel cell–neurite complexes and are activated by both static and dynamic stimuli. The second SA population is associated with Ruffini endings and is particularly sensitive to stretch (Zimmerman et al., 2014). However, these receptors are not very abundant in mouse glabrous skin (Lewin & Moshourab, 2004). RAI and RAII mechanoreceptors are Meissner's and Pacinian sensory corpuscles, respectively; Meissner's corpuscles detect movement across the skin, and Pacinian corpuscles respond to high-frequency vibrations (Zimmerman et al., 2014). The third member of the glabrous LTMR is the D-hair mechanoreceptors, which are innervating hair shafts, found in the middle of the mouse glabrous skin. These afferents display rapidly-adapting properties and fall into the A-δ LTMR category (Rutlin et al., 2014; Walcher et al., 2018). As this work is mainly focusing on the Meissner's corpuscles associated RAMs and Merkel cell SAMs, these end organs will be described more in detail below.

Meissner's Corpuscles

Meissner's corpuscles (MC) were first discovered by Meissner and Wagner (Meissner, 1853). They reside in the glabrous skin, mainly in areas responsible for light touch like fingertips, lips, tongue, and genitalia (Johnson, 2001). In the skin, they are located in the dermal papillae, the region where the upper layer of the dermis connects with the epidermis via collagen fibers. They have an ellipsoid shape and are filled with several layers of non-myelinating Schwann-related cells (lamellar cells), which are linked with the collagen strands to the epidermis and are spirally innervated by Aβ RAI-LTMR axons (Cauna, 1956; Takahashi-Iwanaga & Shimoda, 2003) (Fig. 2). The central domains of the capsule are covered by a thick layer of basal lamina-like matrix. In these regions, the sensory endings project into the surrounding extracellular matrix (Neubarth et al., 2020). The central domains of the capsule are covered by a thick layer of basal lamina-like matrix. In these regions, the sensory endings project into the surrounding

extracellular matrix (Neubarth et al., 2020). Meissner's corpuscle-associated RAMs are sensitive to dynamic skin deformation and are tuned to detect small-amplitude skin vibrations <80 Hz (Vega-Bermudez & Johnson, 1999), which suggests an important role in sensing slips and, therefore, maintenance of the grip and object manipulation (Srinivasan et al., 1990). They exhibit immediate and fast-adapting firing in response to movement only at the initial and final contacts of a mechanical stimulus, but not at static, with very low thresholds. The receptive field of Meissner's corpuscle-associated RAMs is fairly small compared to other mechanoreceptors.

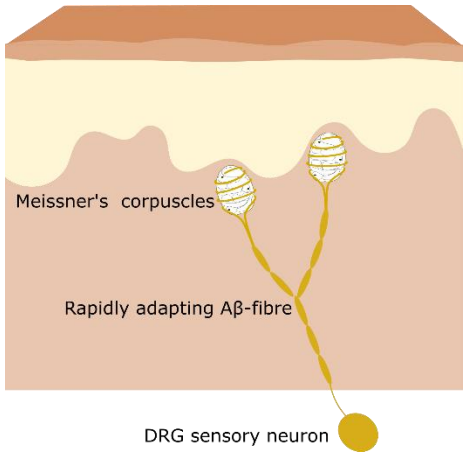

Figure 2. Meissner corpuscle structure and innervation. Meissner's corpuscle innervated by myelinated Aβ-fibres at dermal papillae.

The proposed transduction process is that epidermal deformation causes corpuscle movement. This movement compresses the collagen strands that are linked with the lamellar cells and exerts tension on the nerve fibers leading to the opening of the mechanosensitive channels expressed at the sensory nerve endings. When the pressure is released, the skin returns to its original place, displacing the corpuscle and causing further bending of the nerve fibers (Takahashi-Iwanaga & Shimoda, 2003; Zimmerman et al., 2014). Recent studies have suggested that within most Meissner corpuscles there are two types of Aβ-fiber endings, a TrkB+ population and a Ret+ subtype with distinct responses to tactile stimuli (Neubarth et al., 2020). *In vivo* DRG recordings revealed the TrkB+ population responding only at the onset and offset of skin indentations while, the Ret+ Aβ subtype exhibit variability in the adaptation to static indentation, indicating that not all Meissner Aβ afferents are rapidly adapting to static indentation (Neubarth et al., 2020). It, therefore, seems that the characteristics of the action

potential are known, but the molecular mechanisms involved in mechanoelectrical transmission have yet to be fully elucidated.

Cutaneous end-organ complexes have a heterogeneous protein expression, as was found in many immunohistochemical studies. Numerous calcium-binding proteins, which are implicated in Ca^{2+} homeostasis, are also found in the lamellar cells of the sensory capsules. S-100b, calbindin D28, calretinin, parvalbumin, and neurocalcin are among them (Johansson et al., 1999; Vega et al., 1996). Recent studies have identified ion channels expressed at the Meissner corpuscle which are essential for mechanotransduction. Ion channel subunits of DEG/ENaCC, including acid-sensing ion channels (ASIC), are gated by mechanical forces and have been postulated as mechanotransducers. In a subset of human Meissner corpuscles, DEG/ENaCC subunits and ASIC2 have been identified. (Cabo et al., 2015; Chen & Wong, 2013; Omerbašić et al., 2015). TRPV4 (vanilloid 4) a member of the TRP family has been in the lamellar cells of human Meissner corpuscles (Alonso-González et al., 2017). However, a function for this protein in the lamellar cells of sensory corpuscles has yet to be identified. KCNQ4 (Kv7.4), a voltage-gated K^+ channel has been detected in RAMs which is crucial for setting the velocity and frequency preference in both mice and humans (Heidenreich et al., 2011). Finally, PIEZO2, one of the main mechanotransducer in LTMRs (Ranade et al., 2014) was found to be expressed in Meissner corpuscles, and lanceolate nerve endings (Ikeda et al., 2014). PIEZO2 has been also detected in human Meissner's corpuscle axon, (García-Mesa et al., 2017; Ranade et al., 2014), and functional experiments in the mouse and humans show a role of PIEZO2 in mediating responses in the Meissner sensory axons (Chesler et al., 2016; Ranade et al., 2014)

More recent studies have demonstrated evidence that lamellar cells of Grandry's corpuscles (similar to lamellar cells inside Meissner corpuscles) from duck bill skin detect tactile stimuli, implying that lamellar cells play a critical role in mechanosensation (Nikolaev et al., 2020). Furthermore, Schwaller and collaborators found that a transmembrane, tether-like protein *USH2A*, expressed within the Meissner lamellar cells plays a critical role in shaping low-frequency vibration tuning in the Meissner Aβ RAI-LTMRs which is supported by evidence where extracellular protein tethers have been involved in mechanotransduction of cultured sensory neurons (Hu et al., 2010; Schwaller et al., 2021).

Merkel cells

Merkel cells were discovered in 1875 by Friedrich Merkel (Merkel, 1875). They are keratinocyte-derived epidermal cells located in the stratum basale directly at the dermis-to-epidermis transition, forming finger-like structures between adjacent keratinocytes (Maricich

et al., 2012). Merkel cells are sensory receptor cells that make synapse-like interactions with Aβ SAI-LTMR terminal endings called the Merkel cell-neurite complex (Maksimovic et al., 2014; Maricich et al., 2009) and, may use as neurotransmitters, glutamate, adrenalin or serotonin (Hitchcock et al., 2004; Hoffman et al., 2018). They are located in glabrous skin, particularly on fingertips and lips, and at lower density in hairy skin, in whisker follicles, and guard hairs at specialized patches called touch domes (Lacour et al., 1991). They do not exhibit spontaneous discharge and, in response to sustained skin indentation, they display a sustained and graded dynamic response, followed by an irregular production of neuronal activity in response to static pressure (Hartschuh & Weihe, 1980; Johnson, 2001; Wellnitz et al., 2010). The initial phase is determined by the magnitude and velocity of the force, while the second is force amplitude-dependent (Werner & Mountcastle, 1965). Merkel cells have the greatest spatial resolution (0.5 mm) among the skin end-organs and, therefore, play an important role in texture discrimination and shape recognition (Iggo & Muir, 1969; Maksimovic et al., 2013).

Merkel cells can be identified in the skin by specific markers like Keratin 8 (K8) and Keratin 20 (K20) (Moll & Moll, 1992). In addition, a basic helix-loop-helix transcription factor called Atoh1 is expressed by Merkel cells (Jenkins & Lumpkin, 2017). Recent work has demonstrated that Merkel cells themselves play an active role in mechanotransduction; *Ex vivo* skin nerve preparation recordings from Atoh1 mutant mice demonstrated a necessity for Merkel cells in the Aβ SAI-response LTMRs to skin indentation while optogenetically-evoked depolarization of Merkel cells can produce action potentials showing that they are necessary and sufficient for sustained action-potential firing (Maksimovic et al., 2014; Maricich et al., 2009). In the latter study, it was also demonstrated that the two distinct phases have observed upon indentation and stimulation of the complex arising from both Merkel cells and the terminal afferent; Sensory afferents transduce dynamic stimuli such as moving gratings, while Merkel cells convey static stimuli such as pressure (Maksimovic et al., 2014). Interestingly, the Piezo2 mechanically-activated (MA) cation channel, is expressed in Merkel cells, and mice lacking Piezo2 in Merkel cells, but not in sensory neurons, exhibit a lack of mechanoactivity which shows that Merkel cell mechanosensitivity is dependent on PIEZO2 (Woo et al., 2014).

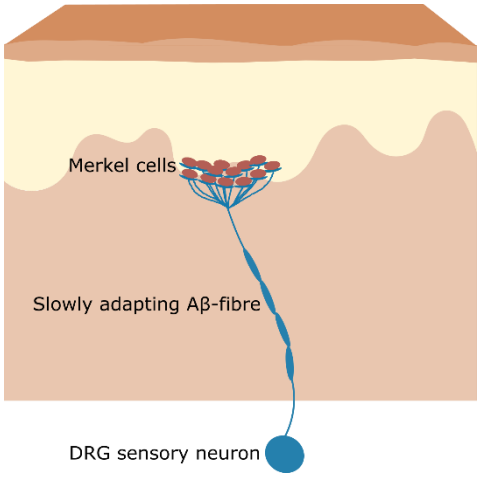

Figure 3. Merkel cells complexes. Merkel cells are innervated by slowly adapting Aβ-fibres at the upper dermis and the epidermis.

4.1.4 Hairy skin

The hair follicles represent end-organs that detect light touch. Mechanoreceptors that are associated with hair follicles respond to hair deflection (A. G. Brown & Iggo, 1967). Three principal types of hair follicles have been identified: zigzag, which accounts for approximately 72 percent of all hair follicles, awl/ auchene around 23%, and guard around 5%. which are densely innervated by functionally distinct sensory nerve fibers. Guard hair follicles are innervated by an RA-LTMR; Awl/auchene hairs are associated with all three types of LTMRs; and Zigzag hair follicles are innervated by both C-LTMRs and Aδ-LTMRs (Li et al., 2011; Wu et al., 2012). Sensory neurons project their axons to more than one hair follicle, and one hair follicle can be innervated by different cells and fibre types. The specific combinations of LTMR subtype terminals associated with hair follicles enable the hairy skin mechanosensory system to detect and convey to the CNS the complex combinations of characteristics that characterize the sense of touch. These sensory endings form lanceolate and circumferential endings around the hair follicle. The longitudinal lanceolate terminations form a palisade around the hair follicle and are partially enclosed by the finger-shaped terminal Schwann cells. Collagen fibers cover the extracellular space between and surround each lanceolate ending-terminal Schwann cell complex, supplying structural support (Li et al., 2011; Takahashi-Iwanaga, 2000)

Aβ RA-LTMRs and Aδ-LTMRs are rapidly adapting and sensitive to movement and low-frequency vibration, and they are silent in the absence of stimulation. Hair follicle-specific Aδ-LTMRs was first described in the small hairs of the cat and rabbit and are considered to be the most sensitive mechanoreceptors in the skin as they exhibit the lowest mechanical thresholds and highest dynamic sensitivity of any other LTMR (A. G. Brown & Iggo, 1967; Koltzenburg et al., 1997). The responses of RA-LTMRs to hair follicle movement show few

action potentials, and their physiological receptive fields are small, with only a few hairs innervated per nerve fiber. The hairy skin population of unmyelinated LTMR axons known as C-LTMRs is nonpeptidergic, small-diameter sensory neurons and are genetically labeled by tyrosine hydroxylase (TH)(Li et al., 2011). Although C-LTMRs are quite widespread in human skin, their existence has been recognized for many decades but is generally overlooked. C-LTMRs have been linked to pleasant feelings, and are generally associated with the social touch (Löken et al., 2009). In addition, Guard hairs of rodents are associated with the Merkel cell complex, forming a touch dome connected to Aβ slowly adapting LTMR, found within the epidermal/dermal junction. Merkel cells were discovered in 1875 by Friedrich Merkel (Merkel, 1875). The LTMR excitation during hair deflection is hypothesized to rely on a physical connection between hair follicle epithelial cells and LTMR lanceolate endings. These filaments function as protein tethers necessary for mechanotransduction of lanceolate-ending LTMRs, similar to what was found in an *in vitro* study where protein tethers extend between cultured somatosensory neuron axons and fibroblasts, and removal of these tethers leads to a loss of mechanosensitivity (Hu et al., 2010).

4.1.5 Nociceptors

Nociception is a submodality of somatic sensation and acts as a critical warning system, alerting to potential or existing injury followed by a reflex withdrawal. It is derived from the Latin verb "*nocēre*", which means "to harm", and it was first described by Charles Scoot Sherrington, who suggested that there are differences in the nociceptive reflexes which depend on the locus and the type of stimulus (Sherrington, 1906). Nociception should not always be associated with pain, as activation of nociceptors does not necessarily lead to the perception of pain, as pain also includes and requires an emotional and therefore subjective response. All animals have nociceptors, but there is a huge debate about whether other animals than humans also feel pain (Sneddon, 2015). Nociceptors detect noxious stimuli such as extremes of temperature (> ~40°, < ~10°C), high mechanical pressure, and injury-related chemicals such as acids, and can be found in both glabrous and hairy skin. Nociceptors include thinly myelinated Aδ-fibres (also known as A-fibre mechanonociceptors or AMs) and or unmyelinated C-fibres (Fig. 4). In contrast to touch receptors, nociceptors exhibit small cell body diameters, slower conduction velocities, and higher mechanical thresholds (Smith & Lewin, 2009). Nociceptors were thought to be free endings that innervate both glabrous and hairy skin's epidermis. However, a recent study indicated that C-fibres endings were tightly associated with Schwann cells, which exhibit a direct nociceptive function on C-fibre terminals and therefore act as initiators in the detection of nociceptive information (Abdo et al., 2019).

Aδ-fibre mechanonociceptors

Aδ-fibre mechanonociceptors, also known as AMs, consist of thinly myelinated axons and, because of their fast conduction velocity, are thought to transmit "initial pain" responses. Their somas are medium in size, and their conduction velocity ranges from 1.5 m/s to 10 m/s (Lewin & Moshourab, 2004). AMs are activated by high mechanical indentation with some minor response to heat or cold stimuli. They have large receptive fields and display slowly-adapting properties (Cain et al., 2001; Koltzenburg et al., 1997). Before reaching the epidermis, AM terminals lose their myelin sheath and are associated with Schwann cells or keratinocytes (Abdo et al., 2019; Lewin & Moshourab, 2004).

C-fibres

The other type of nociceptor that appears as C-fibres corresponds to the biggest population of the afferents that innervate the skin (around 60 %) (Cain et al., 2001; Lewin & Moshourab, 2004). Their speed of transmission is slower than the AMs, with a conduction velocity ranging from 0.4 to 1.4 m/s. Because of their slower conduction velocity, C fibres are thought to be involved in the longer-term sense of pain. C-fibre nociceptors are categorized according to their modality. The most prevalent C-fibre type seen in fibre recordings are afferents reacting to thermal, mechanical, and chemical stimuli and are termed polymodal (Smith & Lewin, 2009) but some types of C-fibre are activated only by noxious mechanical stimuli (C-M), while others can detect noxious heat or cold (C-H/C) (Cain et al., 2001; Lewin & Moshourab, 2004). The latter population exhibit overlapping modalities with C-thermoreceptors which can detect changes in the temperature like cooling and warming. In addition, a ‘’silent’’ population of c-fibres has been described which are insensitive to mechanical or thermal stimulation rather than being activated only after incubation with inflammatory mediators (Meyer et al., 1991; Schmidt et al., 1995). Finally, as has been described above a small subpopulation of c-fibres is activated by innocuous stimuli and responds to gentle touch (C-LTMRs innervating hair follicle).

Based on their neuropeptide expression, nociceptors may be further classified into two primary neurochemical classes: Peptidergic nociceptors which express neuropeptides such as substance P or calcitonin Gene-Related Peptide (CGRP), and non-peptidergic nociceptors which do not express neuropeptides and mainly bind isolectin-B4 (Perry & Lawson, 1998). Differential peripheral distributions of peptidergic and non-peptidergic C fibres imply that the functions of these fibres are distinct (Cavanaugh et al., 2009). Nociceptors have plastic physiology which plays an important role after injury or inflammation as they display increased sensitivity and a reduction in stimulus threshold which can lead to pain responses (Wolf & Ma, 2007) or in more severe cases to neuropathic pain, in which stimuli that were previously considered as innocuous now produce pain (allodynia), or hyperalgesia, in which noxious stimuli provoke more pain.

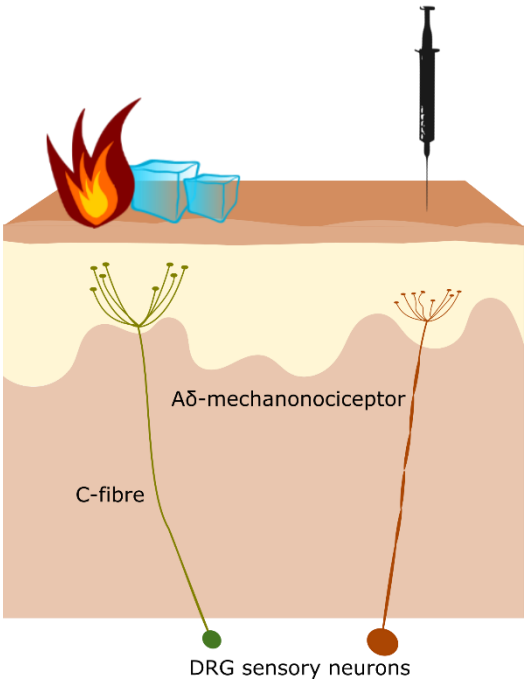

Figure 4. Nociceptors. C-fibers are non-myelinated fibers respond to cold and heat. Aδ-mechanonociceptors are thinly myelinated fibers respond to fast pain.

4.2 Auditory system

Our ability to hear is the principal way we connect and communicate, emotionally and intellectually. It provides us with the information we require to live a safe and social life. Hearing is based on precise frequency discrimination across a wide range of sound frequencies. The responsible system for the detection and processing of sensory information related to sound is the auditory system. Sound waves enter the ear and travel through the ear canal and hit the tympanic membrane (eardrum) which vibrates and set in motion its anchored bones. Subsequently, these bones amplify the vibration and send it to the cochlea, which in Greek

means snail as it has a spiral shape. There, the cochlea duct, a chamber filled with endolymph, is hosting a key structure, the organ of Corti, which is attached to the basilar membrane and contains the mechanosensory hair cells. The vibration reaching the cochlear duct induces endolymph fluid waves, which stimulate the hair cells and in turn convert this movement into electrical signals. (Kandel, E.R., 2000; Pickles, 2012). Our capacity to detect subtle changes in sound is related to the cochlea's special anatomical properties, which enable differentiation across frequency components and alert us to the presence and amplitudes of existing tones.

4.2.1 Hair cells

Hair cells in the cochlea are classified into two categories, each of which performs a unique role throughout the transduction process, the inner and the outer hair cells (IHC, OHC). The IHC detects and transmits most of the sound-derived vibrations from the endolymph fluid to the brain via the auditory nerve to the auditory brainstem and finally to the auditory cortex. On the other hand, OHC enhances the sounds entering the cochlea through an active process, therefore acting as pre-amplifiers. The inner hair cells are organized into a single row of roughly 3,500 cells, whereas the outside hair cells are organized into three rows of around 12,000 cells each in the human ear (Hudspeth, 2014). They get their name from the hair bundles which consist of stereocilia and extend from the apical surface of the cell into the fluid-filled cochlear duct. Stereocilia are specialized actin-filled microvilli structured in ascending rows (McPherson, 2018). At the edge of which the IHCs and OHCs reside is placed the basilar membrane which exhibits a variation in width and stiffness to regulate the frequencies best perceived by the hair cells. At the cochlear base, the basal membrane is narrow and stiff reflecting the high frequencies, whereas at the cochlear tip it is broad and less stiff corresponding to low frequencies. On the apical part, the hair cells are connected with the tectorial membrane (TM) which contributes to the sound amplification by triggering OHC and IHC activation through endolymph vibrations. TM width and stiffness mirror BM's and similarly assist in frequency differentiation (Meaud & Grosh, 2010).

Hair cells are very sensitive, and the best-characterized mechanoreceptors in vertebrates. This sensor is highly specialized to detect stimuli with amplitudes of a few nanometres and frequencies considerably larger than one kilohertz (Hudspeth & Corey, 1977). The root of their sensitivity relies on mechanotransduction and the corresponding mechanosensitive ion channel. In early studies on hair cells, the lab of Hudspeth demonstrated that these cells upon movement of their hair bundle produced electrical signals just 40μs after deflection, therefore it was hypothesized that should not be chemical intermediates involved in

mechanotransduction; instead, a channel-protein is directly gated, which allows for ion inflow to occur (Corey & Hudspeth, 1979; Hudspeth & Jacobs, 1979). Impairment in the mechanotransduction process of the hair cell results in deafness and balance abnormalities (Petit & Richardson, 2009), highlighting the crucial function of mechanotransduction in the nervous system.

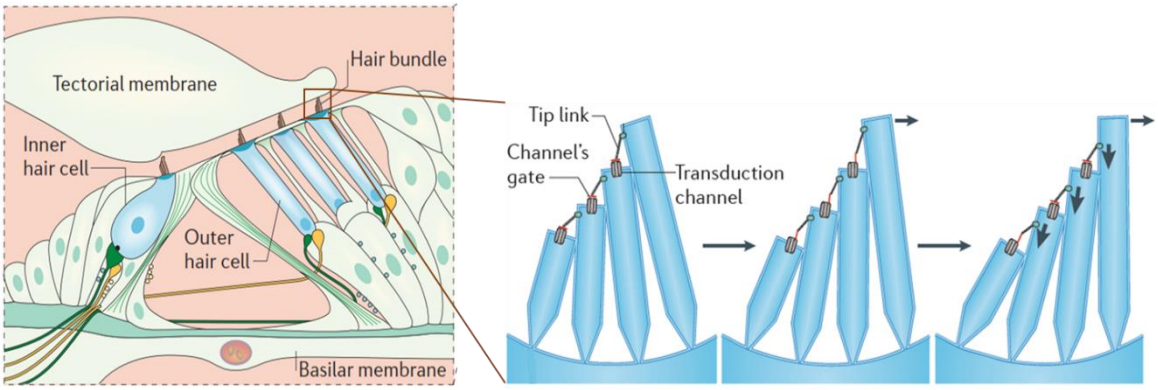

Figure 5. Organ of Corti and hair cells. Deflection of hair cell towards the highest raw of stereocilia open the mechanosensitive channel. Figure modified from A. J. Hudspeth 2014.

The mechanotransduction complex is localized at the tips of the stereocilia (Pickles, 2012). The rows of stereocilia are connected with extracellular filaments, the tip links, which are thought to convey mechanical force to the transduction channels (Assad et al., 1991). In a healthy hair cell, deflection of the hair bundle toward the longest row of stereocilia increases the tension in tip links which is conveyed to the mechanotransduction channel complex to gate the channel. Hair cells do not generate action potentials; the depolarization of the cell is caused by the inflow of positive ions from the endolymph and results in the generation of graded receptor potentials. Small displacements of the hair bundle resulted in numerous millivolts of depolarizing receptor potentials. Currents produced by the movement of the stereocilia are carried primarily by potassium since they are the most prevalent cation in the endolymph; yet, despite its low concentration, Ca^{+2} may contribute up to 10% of the inward current (Gillespie & Müller, 2009). Depolarization caused by the inward current at the apical membrane leads to the basolateral opening of voltage-gated potassium channels like KCNQ4 channels. Mutations in the *KCNQ4* gene cause a dominant form of hereditary deafness (Kharkovets et al., 2000). Deflections in the opposite direction decrease the channel open probability and produce the reverse polarity current (Kim & Fettiplace, 2013; Kindt et al., 2012; Marcotti et al., 2014; Waguespack et al., 2007) which are also observed during hair cell development and after tip-link breakage (Alagramam et al., 2011; Kim & Fettiplace, 2013; Marcotti et al., 2014). Hair cell recordings from hair bundle stimulation have been widely

documented in both non-mammals (Holton & Hudspeth, 1986) and mammals (Kros et al., 1992).

4.2.2 The molecular composition of the mechanotransduction complex

Multiple genes and proteins that are involved in deafness are linked to the mechanotransduction apparatus in the auditory system. Amongst them are Cadherin 23 (CDH23) and protocadherin 15 (PCDH15) proteins that form the tip link (Siemens et al., 2004), which conveys tension force to the mechanotransduction channel and thus leads to channel opening; Mutations in the genes encoding *CDH23* and *PCDH15*, are associate to Usher syndrome, a syndrome with hearing, vestibular, and visual abnormalities (Alagramam et al., 2011; Bolz et al., 2001; Bork et al., 2001). While significant progress has been made in the identification of some of the mechanically-gated ion channels involved in the somatosensory system (Coste et al., 2010; Ranade et al., 2015), the proteins that contribute to the formation of the mechanotransduction channels that are critical for sound perception remain somewhat a controversy. It has been shown that these ion channels are located in the stereocilia of cochlear hair cells towards the lower end of tip links (Beurg et al., 2009). There is evidence that the proteins TMC1, TMC2, LHFPL5, and TMIE are components of the mechanotransduction channel of hair cells and interact with PCDH15 (Beurg, Xiong, et al., 2015; Xiong et al., 2012; Zhao et al., 2014).

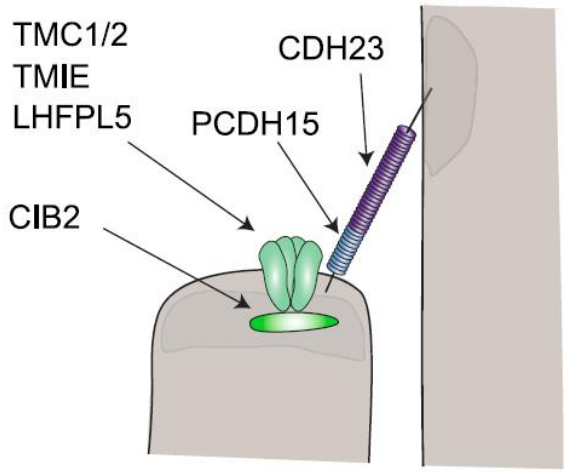

Figure 6. Diagram of the mechanotransduction complex. Tip link proteins and mechanotransduction channel at the tip of stereocilia with CIB2. Figure modified from Liang et al., 2021

TMC1/2

The function of the transmembrane channel-like protein (TMC) in mechanotransduction has been discussed for many years since it was initially proposed as a channel candidate (Beurg et al., 2019, 2021; Beurg, Xiong, et al., 2015; Kawashima et al., 2011; Pan et al., 2013). TMC1 and TMC2 are both localized at the tips of shorter-row stereocilia (Kawashima et al., 2011; Kurima et al., 2002), where transduction channels are localized. Recent research indicates that TMC1 and TMC2 are pore-forming subunits of the hair cell mechanotransduction channel (Ballesteros et al., 2018; Jeong et al., 2022, p. 1; Jia et al., 2020; Pan et al., 2018). However, researchers have not succeeded to express TMC1/2 in any heterologous expression systems to show mechanosensitivity, and no reports of mammalian TMC1/2 in expression systems exhibiting ion channel activity have been found. Recent studies have revealed the structure of *C. elegans* mechanotransduction complex showing the TMC1 as the pore-forming subunits with TMIE and CIB2 as auxiliary subunits (Jeong et al., 2022).

TMIE

TMIE the transmembrane inner ear protein is associated with deafness in humans, mice, and zebrafish (Chung et al., 2007; Gleason et al., 2009; Mitchem et al., 2002). Recent research on cochlear hair cells has shown that TMIE is a required subunit of the mechanotransduction complex and that TMC1/2 cannot form a channel complex without TMIE (C. Cunningham et al., 2020).

LHFPL5

Finally, Lipoma HMGIC fusion partner-like 5 protein (LHFPL5), also known as the tetraspan membrane protein of hair cell stereocilia (TMHS) is a protein with four predicted transmembrane domains. LHFPL5 is expressed in vestibular hair cells and localized at the tip of the stereocilia. Mutations in *lhfpl5* gene can cause deafness in humans and mice. (Longo-Guess et al., 2005; Shabbir et al., 2006). Mutations in *lhfpl5* cause reduced current, single-channel conductance, and slowed channel activation, and the animal exhibit circling behavior (Beurg, Goldring, et al., 2015; Xiong et al., 2012)

4.2.3 CIB2

Calcium and integrin-binding protein 2 (CIB2) plays a critical role in hair cell mechanotransduction and is an auxiliary mechanotransduction channel subunit in worms and vertebrates (Jeong et al., 2022, p. 1; Liang et al., 2021). CIB2 is a 21.6 kDa protein and one of the four members of a family of calcium and-integrin binding proteins (CIB1, CIB2, CIB3, and CIB4). All members of this family have elongation factor-hand (EF-hand) domains that can bind $Ca2^{+}$ and $Mg2^{+}$ through EF3 and EF4 hand motifs, and their N-terminal regions bind the alpha-chain of integrin heterodimers (Jacoszek et al., 2017; Naik et al., 1997; Riazuddin et al., 2012). The CIB2 protein interacts with DNA-dependent protein kinases and is ubiquitously expressed (Seki et al., 1999). CIB2 has been found in skeletal muscle, the brain, the eye, and the inner ear of mammals (Blazejczyk et al., 2009; Häger et al., 2008, p. 2; Riazuddin et al., 2012). Mutations in *Cib2* gene have been linked to non-syndromic deafness and Usher Syndrome 1J (Patel et al., 2015; Riazuddin et al., 2012; Seco et al., 2016), however, a role in usher syndrome has been challenged by research (Booth et al., 2018) showing no retinal deficits in *Cib2* mutant mice. CIB2 is localized along the stereocilia with an accumulation towards the tip of the shorter stereocilia, where the mechanotransduction channel is harbored, in both cochlea and vestibular hair cells. CIB2 interacts with the pore-forming subunits of the channel TMCI and TMC2 at their n-terminus and disruption of this interaction by a single *Cib2* missense mutation results in deafness and the loss of mechanosensory transduction in mice, indicating that CIB2 is also an important component of the mechanotransduction complex in this model (Giese et al., 2017). Furthermore, these mutations lead to the degeneration of sensory hair cells in adult mice which is followed by the degeneration of spiral ganglion neurons (Giese et al., 2017). In young postnatal mice, the hair cells were still intact, however, the architecture of the stereocilia was disrupted mainly in the shorter row where the mechanotransduction channel is based (Giese et al., 2017; Michel et al., 2017). *C. elegans* expresses the ortholog of *Cib2*, called *calm-1,* which is an auxiliary subunit of the mechanotransduction complex, indicating the evolutionary-conserved role in the mechanotransduction of CIB2 proteins (Jeong et al., 2022, p. 1). *Calm-1* is required for mechanosensation mediated by TMC1 and binds the intracellular tether, ankyrin that transmits force to TMC mechanotransduction channels (Tang et al., 2020). CIB2 is required for the proper localization of integrin and adaptor proteins like whirlin in cochlear hair cells (Michel et al., 2017) and more recently was demonstrated that CIB2 is responsible for the localization of TMC1/2 in stereocilia (Liang et al., 2021). However, there are no observable signs of vestibular impairment, such as circling. CIB3, another member of the CIB family, is expressed mainly in vestibular hair cells and less in cochlear samples. Therefore, the absence of vestibular impairment in *Cib2* mutants is probably due to CIB3 compensation in vestibular hair cells

(Giese et al., 2017; Liang et al., 2021; Tang et al., 2020). CIB2 and CIB3 are similarly essential in cochlear hair cells and control both the formation and function of the mechanotransduction channel complex acting as auxiliary subunits of the mechanotransduction channel (Liang et al., 2021). CIB2 and CIB3 have a similar structural arrangement to KChIP proteins, which function as auxiliary subunits of voltage-gated Kv4 channels. KChIP proteins interact with the N-terminal cytoplasmic tail of Kv4 and control channel formation, expression, and activity (An et al., 2000; K. Wang, 2008) in a similar way CIB2/3 binds and regulates TMC1/2 MT channels (Liang et al., 2021).

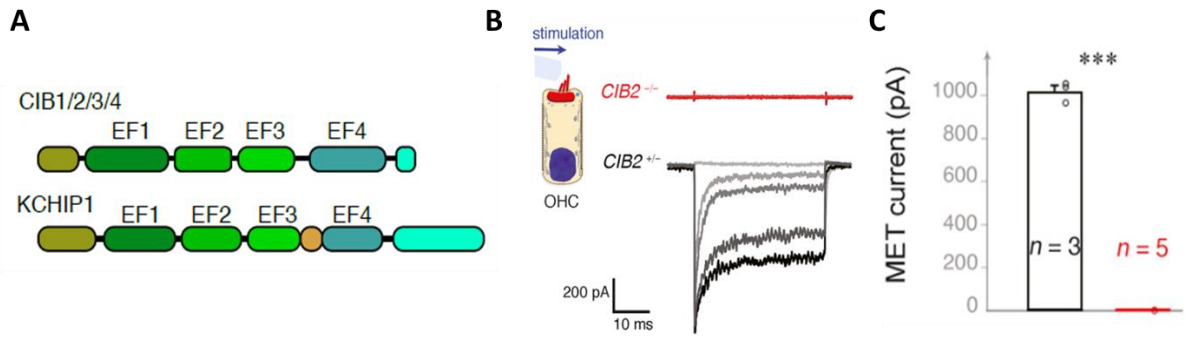

Figure 7. A: CIB1–CIB4 and KChIP1. B. C. CIB2 mutation abolish mechanotransduction in hair cells. Figure modified from Liang et al., 2021

4.3 Ion channels contribute to mechanosensation

4.3.1 Mechanosensitive ion channels

Mechanotransduction is the conversion of mechanical stimuli into a biological response and mechanosensitivity is the ability to detect mechanical stimuli. The detection of touch and sound waves necessitates the use of specific mechanosensitive ion-gated channels allowing sensory cells to respond within a millisecond (Corey & Hudspeth, 1979). There are four established criteria for a protein to be considered a mechanosensitive ion channel (Arnadóttir & Chalfie, 2010):

1. Expression in mechanosensitive cells (such as DRG or hair cells)

2. Changes in the protein sequencing cause mechanosensing defects (changes to the properties of the mechanical response)

3. Rapid-opening properties mediated by mechanical stimulus (such as stretch or indentation)

The best-characterized MS channels are the bacterial mechanosensitive channels of large conductance (MscL) and mechanosensitive channels of short conductance (MscS), which match all the above requirements for mechanosensitive channels (Sukharev et al., 1994). Furthermore, the TRAAK and TREK-1 K+ channels (Berrier et al., 2013; Maingret et al., 1999), Piezo 1 and 2 (Coste et al., 2010) have been suggested as mechanosensitive ion channels. Recently, OSCA1 (Murthy, Dubin, et al., 2018), Elkin-1 (Patkunarajah et al., 2020), and in hair cells, TMC1 and 2 (Jia et al., 2020) associated with TMIE (C. L. Cunningham et al., 2020) have been identified as well. Finally, the transmembrane protein TACAN had been suggested as a mechanosensitive channel (Beaulieu-Laroche et al., 2020). Another lab, however, challenged this conclusion by employing patch recordings and membrane reconstitution techniques, demonstrating a lack of evidence for TACAN being a mechanosensitive channel (Niu et al., 2021).

4.3.2 Voltage-gated ion channels

Although the properties of mechanotransducer channels shape the receptor potential, voltage-gated ion channels modulate generator currents and control AP thresholds, AP firing patterns, propagation, and synaptic transmission, and thus are determinants of DRG sensory neuron function (Sundt et al., 2015; Tsantoulas et al., 2012; Waxman & Zamponi, 2014). The mechanical response is determined by the balance of subthreshold currents (Heidenreich et al., 2011; Muqeem et al., 2018; R. Wang & Lewin, 2011). Activation of voltage-gated inward currents can extend the duration of receptor potential and increase its magnitude, activation of voltage-gated outward currents can reduce the amplitude of receptor potential (Hao et al., 2015). Deep transcriptome analysis of genetically labeled sensory neuron subtypes has shown a wide range of expression of voltage-gated ion channels (Usoskin et al., 2015; Zheng et al., 2019). Voltage-gated sodium channels are crucial factors in the excitability of sensory neurons and their distinct expression patterns in sensory neuron subtypes characterize their functional significance in pain signaling (Bennett et al., 2019; Bird et al., 2013; Dib-Hajj et al., 2015). Distinct combinations of Kv channel expression patterns in DRG sensory neuron subtypes show that expression patterns of these individual ion channels are important indicators of subtype-specific physiological features (Zheng et al., 2019). The focus of the present study was on the Kv7.4 potassium channel which belongs to the Kv7 family.

4.3.3 KCNQ channels

There are five members of this family – Kv7.1 to Kv7.5, which are coded by the *KCNQ1-KCNQ5* genes. They constitute subunits of low-threshold voltage-gated K+ channels, which generate inward M-currents (D. A. Brown, 1988; D. A. Brown & Adams, 1980), which modulate the excitability of neurons (Delmas & Brown, 2005). M-channels activate at subthreshold potentials, of around -60 mV. They are non-inactivating; they provide a constant, voltage-dependent outward current. This helps to stabilize the membrane potential and therefore contributes to the resting membrane potential. Due to their slow activation, they do not significantly contribute to the repolarization of action potentials. However, they have a significant role in moderating repeated or burst firing as well as in the overall excitability of neurons (D. A. Brown, 1988).

Genetic manipulation and drugs that selectively inhibit (e.g. linopirdine, XE991) or enhance (e.g. retigabine) M-channel activity have provided more information about their function (Jentsch, 2000; Maljevic et al., 2008). Inhibition of M-channels leads to depolarization, a decrease in the threshold, while their activation hyperpolarizes the neuronal membrane potential and decreases input resistance, making the neuron more resistant to action potential firing (Gamper N, Shapiro MS, 2015). Studies have demonstrated that Kv7 channel inhibition increases the excitability of central and peripheral neurons, while loss-of-function mutations in *KCNQ* genes cause excitability diseases such as epilepsy, deafness, and cardiac arrhythmia (Delmas & Brown, 2005; Gamper N, Shapiro MS, 2015; Jentsch, 2000).

KCNQ channels in peripheral somatosensory pathways

Functional Kv7 channels have been detected in the somatosensory pathway, including dorsal root ganglion (DRG), dorsal horn (DH) neurons, peripheral nerve axons, and peripheral terminals of primary afferents (Du et al., 2018; Heidenreich et al., 2011; Lang et al., 2008; Passmore et al., 2003, 2012; Rivera-Arconada & Lopez-Garcia, 2005; Vetter et al., 2013).

Nociceptors, that respond to capsaicin express KCNQ2, KCNQ3, and/or KCNQ5 and display distinct M-currents when subjected to voltage clamp protocols (Passmore et al., 2003). In addition, the administration of enhancers of these channels decreases the transmission of Aδ and C-fibre responses into the dorsal horn of the spinal cord (Passmore et al., 2003), and it also hyperpolarizes primary afferent fibres (Rivera-Arconada & Lopez-Garcia, 2005). Moreover, inhibitors reduced discharges of sensory Aδ and C-fibre induced by heat stimulation when applied to the peripheral endings of sensory fibres in the rat skin nerve preparation

(Passmore et al., 2012). On the other hand, inhibition of the channels greatly amplifies peripheral Aδ discharges induced by heat or mechanical stimulation (Passmore et al., 2012).

KCNQ4

As has been already mentioned above, KCNQ4 is playing an important role both in hearing and touch. *KCNQ4* was found to be mutated in humans with DFNA2, a slowly progressive autosomal dominant type of hearing loss (Kubisch et al., 1999). In the cochlea, KCNQ4 is present in mechanosensitive outer hair cells which helps to maintain their resting membrane potential (Kharkovets et al., 2000). KCNQ4 deficiency affects hearing by interfering with the electromotility of sensory outer hair cells and, causing their gradual degeneration (Kharkovets et al., 2006). In the somatosensory system, the KCNQ4 protein is present at the skin's peripheral terminals of Meissner's corpuscles and lanceolate and circular nerve endings (Heidenreich et al., 2011). The location of the protein near the mechanotransduction site implies involvement in the receptor potential process. Kcnq4 gene deletion in mice affects the frequency response of rapidly adapting mechanoreceptors and is required for tuning these mechanoreceptors to higher frequencies of vibrotactile stimuli in mice (Heidenreich et al., 2011). In a human cohort with DFNA2 that carries a loss of function mutation of *KCNQ4*, vibration detection thresholds were much lower in comparison to the healthy cohort (Heidenreich et al., 2011). KCNQ4 channels are not mechanosensitive but are responsible for regulating the excitability of a subpopulation of RAMs by bringing the membrane potential back to its resting state (Hammami et al., 2009).

Ion channel modulators play a critical part in the mechanotransduction process. The study of these proteins' functions will help us better comprehend mechanosensation in both hair cells and sensory neurons. I aim to identify these modulators and the processes by which they influence mechanotransduction.

5 Aims

Calcium and integrin-binding protein 2 (CIB2) is an auxiliary component of the auditory system's mechanotransduction channel that modulates channel function and affects its localization. *Cib2* mutations have been linked to hearing loss in humans and mice. RNA sequencing data indicated that *Cib2* is expressed in a subset of DRG sensory neurons.

We hypothesized that CIB2 protein plays a common role in mechanotransduction of hair cells and sensory neurons. The purpose of my work was to investigate the anatomical distribution of CIB2 in somatosensory neurons and mechanosensitive end-organs at the skin, as well as its functional significance in the mechanotransduction process in the somatosensory system.

To achieve these goals, I aimed to:

1. Use immunofluorescence in C57BL/6N DRG and skin sections.
2. Investigate physiological changes of the different types of mechanoreceptors and nociceptors in *Cib2* conditional knockout mice (wnt1-Cre; *cib2*$^{fl/fl}$).
3. Explore the mechanism by which CIB2 exerts its effects on sensory neurons.
4. Assess the behavioral impact of peripheral genetic deletion of *Cib2* by using light touch and mechanical pain assays.

6 Materials and Methods

6.1 Materials

6.1.1 Chemicals and Kit

Name	Supplier
2’2-thiodiethanol (TDE)	Sigma Aldrich
Agarose	Sigma Aldrich
Bovine serum albumin (BSA)	Sigma Aldrich
Calcium chloride (CaCl2)	Sigma Aldrich
Cut smart buffer	NEB
Dako Mounting Medium	Agilent Technologies
Dimethyl sulfoxide (DMSO)	PanReac AppliChem
DNA polymerase	Thermo Fisher Scientific
dNTPs	Invitrogen
Donkey Serum	Jackson
(D)-Saccharose	Carl Roth
DMEM/F12 - Dulbecco's Modified Eagle Medium: Nutrient Mixture F-12	Gibco
EGTA	Sigma Aldrich
Ethanol Ethidium bromide Roth	Roth
Ethidium bromide	Sigma Aldrich
Fetal calf serum (FCS)	Sigma Aldrich
Fugene	Promega
Gelatine	Sigma-Aldrich
Glucose	PanReac AppliChem
Goat serum	GE Healthcare
Horse serum	Biochrom
Ladder 1Kb	Gibco
Ligase	Thermo Fisher Scientific
Linopirdine	Sigma Aldrich
LB broth	Sigma Aldrich
Magnesium chloride (MgCl2)	Merck
Methanol	Roth
Mineral oil	Sigma Aldrich

OCT Tissue Tek	Sakura, Alphen aan den Rijn
Opti-MEM	Thermo Fisher Scientific
Paraformaldehyde	Sigma Aldrich
Pap Pen (Liquid Blocker)	Biognost
Penicillin/Streptomycin	Sigma Aldrich
Phosphate-buffered saline (PBS)	Gibco
Phusion High-Fidelity Buffer Pack	NEB
Phusion High-Fidelity DNA Polymerase	NEB
Polydimethylsiloxane (PDMS) Sylgard 184 silicone elastomer	Dow Corning Corporation
Poly-L-lysine (PLL)	Sigma Aldrich
Potassium chloride (KCL)	Carl Roth
PureYield Plasmid Midiprep System	Promega
RNAscope® Multiplex Fluorescent Kit v2	ACDBio
Sodium chloride (NaCl)	Carl Roth
Sodium hydroxide (NaOH)	Carl Roth
Taq Polymerase	NEB
Taq Polymerase buffer	NEB
TaqMan Universal PCR Master Mix	Roche
TOP10 Competent E. coli	Thermo Fisher Scientific
Triton X-100	Sigma Aldrich
Trypsin	Sigma-Aldrich
Wizard SV Gel and PCR Clean-Up System	Promega

6.1.2 Plasmids

Name	**Obtained/Constructed from**
N3HA-mscib2	Uli Mueller's lab
pRK8-IRES-DSRed	Dr. Mirko Moroni
pRK8-IRES-GFP	Dr. Mirko Moroni
pCMV6_Kcnq4 (Myc-DDK-tagged)	Origene
pRK8-cib2-IRES-DSRed	Dimitra Mazaraki

pRK8-Kcnq4IRES-GFP	Dimitra Mazaraki

6.1.3 Buffers and solutions

Name	Composition
Extracellular solution for whole-cell patch clamp	140 mM NaCl, 4 mM KCl, 2 mM CaCl2, 1 mM MgCl2, 4 mM glucose, 10 mM HEPES; adjusted to pH 7.4 with NaOH
Intracellular solution whole-cell patch clamp	110 mM KCl, 10 mM NaCl, 1 mM MgCl, 10 mM HEPES, 1 mM EGTA; adjusted to pH 7.3; 290 mOsm
SIF (synthetic interstitial fluid)	2 mM CaCl2, 5.5 mM glucose, 10 mM HEPES, 3.5 mM KCl, 0.7 mM MgSO4, 123 mM NaCl, 1.5 mM NaH2PO4, 7.5 mM saccharose, 9.5 mM Na-gluconate; adjusted to pH 8.4 with 10 N NaOH; during constant carbonation the pH was maintained at pH 7.4
Blocking for DRGs	5% of normal goat/donkey serum, 95% PBS
Blocking for skin	5% of Invitrogen normal goat serum, 20% DMSO, 75% PBS
Washing buffer	0.1% Triton X-100/PBS
Dent's Bleach	10% H2O2, 13.3% DMSO and 53.3% methanol
Dent's Fix	20% DMSO, 80% methanol

6.1.4 Antibodies

Name	Supplier
Anti-NF200 Chicken	Abcam AB72998
Anti-S100 Rabbit	Dako Z0311
Anti-TrpV1 Guinea pig	Novus Biologicals NB300-122

Anti-TrkC goat	Rnd systems AF1404
Anti-TrkA goat	Rnd systems AF1056
Anti-Cytokeratin 20 guinea pig	Citeab BP5080
Anti- CIB2 rabbit	LifeSpan BioSciences LS-C416040
Goat anti-Chicken, Alexa Fluo 647	Thermofisher
Goat Anti-Rabbit Alexa Fluor 488	Sigma Aldrich
Goat Anti-Rabbit Alexa Fluor 555	Invitrogen
Donkey anti-Goat Alexa Fluor 647	Thermofisher
Goat Anti-Guinea pig Alexa Fluor 647	Abcam ab150187
DAPI	Thermo Fisher Scientific 62248

6.1.5 Technical equipment

Name	Supplier
AS30 airstone	Tetratec
Camera HD IC80	Leica
Camera CoolSnapEZ	Visitron Systems
Confocal microscope	Carl-Zeiss, catalog no. LSM700
Electrode wire	Advent-Silverstone (No. AG54864)
EPC-10	HEKA Elektronik
Force sensor (Ultra-precise Force Measurement System FMS-LS)	Kleindiek Nanotechnik
Glass coverslips	VWR
Glass coverslips, 12mm diameter	Thermo Fisher Scientific
Headstage NL 100	Digitimer
Laser scanning microscope LSM710	Carl Zeiss
Lamp LCD KL1500	Leica
Light microscope DM5000B	Leica
Magnetic Base	Kametec
Microelectrode platinium Kaptom (1mΩ)	World Precision Instruments
Micro Forge MF-830	Narishige

Micromanipulator MMA3-LS	Kleindiek Nanotechnik
Micromanipulator MM33	Märzhäuser Wetzlar
Microscope for dissection MS5/M26	Leica
Nanodrop spectrometer 2000	Kleindiek Nanotechnik
Nanomotor	Kleindiek Nanotechnik
NeuroLog System including Stimulatorand Amplifier Modules	Digitimer Ltd
Oscilloscope (Digital Storage Oscilloscope TDS 220)	Tektronix
Piezo actuator	Physik Instrumente (PI)
Piezo amplifier	Physik Instrumente (PI)
PowerLab 4/30	ADInstruments Ltd
Puller	Werner Zeitz
Pump Minipuls 3 Peristaltic	Gilson
Skin-nerve chamber	Custom-made at the Max Delbrück Center for Molecular Medicine in the Helmholtz Association
Soldering iron	Weller WS51
Table (IG Breadboard)	Newport
Tubing (E-3603)	Tygon
Waterbath	Julabo
von Frey Filaments	

6.1.6 Software

Fiji (ImageJ)	Open source
Fitmaster	HEKA Elekectronik
GraphPad Prism 8	Graphpad Software
Igor Pro	Wavemetrics Inc.
LabChart 8 (including Spike Histogram extension	ADInstruments Ltd
Office 365	Microsoft

6.2 Methods

6.2.1 Animals

All animal experiments were carried out according to the German and EU animal protection laws and were approved by the Berlin Animal Ethics Committee (Landesamt fur Gesundheit und Soziales). Mice were kept and handle through animal house of the Max Delbrück Center. All mice strains genetically modified were bred under a C57BL/6N background.

The *Cib2* gene has six exons. Conditional *Cib2* knockout were generated by using *Cib2*$^{fl/fl}$ mice with two flox sites flanking exon 4 which is common to all *Cib2* isoforms and predicted to encode the EF-hand domain region. This mouse line was crossed with Wnt1-Cre mice expressing Cre under the control of Wnt1 gene promoter. Wnt1 is neural crest specific, present in lineages of all peripheral- and enteric nerves, glia and smooth muscle cells among others (X. Huang & Saint-Jeannet, 2004) and thus crossing with wnt1-cre reporter mice resulted in selective constitutive ablation of *Cib2* in the peripheral nervous system. Analysing animals with a genetic ablation of *Cib2* spatially restricted to the somatosensory system allows for a differentiated analysis of peripheral contributions of CIB2 in sensory biology. Ten male animals in the age of 10 to 30 weeks were used for the *Cib2* ablation experiments. Controls in this section will be referred to as controls (*Cib2*$^{fl/fl}$) and conditional knockouts of *Cib2* as *Cib2* conditional deletion (wnt1-Cre; *cib2*$^{fl/fl}$).

Mutation details: The L1L2_Bact_P cassette was inserted at position 54455350 of Chromosome 9 upstream of the critical exon(s) (Build GRCm39). The cassette is composed of an FRT site followed by lacZ sequence and a loxP site. This first loxP site is followed by a neomycin resistance gene under the control of the human beta-actin promoter, SV40 polyA, a second FRT site and a second loxP site. A third loxP site is inserted downstream of the targeted exon(s) at position 54456232. The critical exon(s) is/are thus flanked by loxP sites. A "conditional ready" (floxed) allele can be created by flp recombinase expression in mice carrying this allele. Subsequent cre expression results in a knockout mouse. If cre expression occurs without flp expression, a reporter knockout mouse will be created.

6.2.2 Genotyping

To genotype *Wnt1-Cre; Cib2*$^{fl/fl}$ mice, a piece of tail was taken from E18 embryos and P6 pups. Tissues were incubated for 10 min at 95° C while shaking at 800 rpm in a lysis buffer containing (in mM) 200 NaCl, 100 Tris pH 8.5, 5 EDTA, 0.2% of SDS and Prot K (10 mg/mL, Carl Roth).

PCRs were performed using supernatant of the lysis preparation as DNA template (20-100 ng), 1X Taq PRC buffer, 2 mM MgCl2, 0.2 mM dNTPs, 1.25U Taq-polymerase (Thermofisher Scientific) and 0.5 mM of forward- and reverse-specific primers targeting Cib2 and cre (Table 1).

Gene	**Primers**	
Cib2 flox	Forward	CTGAGCAGCTGTGATGGAAG
	Reverse	TGCATACATGAGCACAGCAA
Wnt1-cre	Forward	TAAGAGGCCTATAAGAGGCGG
	Reverse	AGCCCGGACCGACGATGAA

Table 1. Primers for CIB2 mice genotyping

6.2.3 Skin nerve preparation

Electrophysiological recordings from cutaneous sensory fibres of the tibial nerve and saphenous nerve were made using an *ex vivo* skin nerve preparation following the method described previously by Koltzenburg et al., 1997; Walcher et al., 2018).

Hind paw hairy skin – saphenous nerve preparation

After the animal was euthanized by cervical dislocation, the hair of the hind limb was shaved off. Using fine dissection scissors the saphenous nerve was cleared from the hip to the shin bone. The hairy skin connected with the saphenous nerve was transferred into a heated (32 °C) oxygen-saturated interstitial fluid and fixed “outside-out” using insect needles. The nerve was transferred via a narrow channel into an adjacent chamber filled with mineral oil for nerve teasing and single fibre recordings. For the linopirdine experiments, the orientation of the skin was the opposite of that used in the rest of the experiments, as it is recommended the inside-out configuration of the skin for drug application.

Glabrous skin

After the experimental animal was euthanized the tips of the toes were cut off and the skin was removed up to the ankle. A circumferential cut was made around the ankle. An incision

was made at the hip level and the sciatic nerve was freed from surrounding connective tissue. The finger bones were cut at the tarsal-metatarsal joints and carefully detached from the glabrous skin. The foot with the tibial nerve (up to the sciatic trifurcation) was transferred into the organ bath chamber in the organ bath chamber (with superfused 32°C SIF buffer) the remaining muscle tissue, digital bones as well as tendons were cut out and the skin was fixed to the “outside-out” configuration. The tibial nerve was transferred to the adjacent insulation chamber filled with mineral oil. In the oil chamber, the tibial nerve was cleared from surrounding connective tissue as well as the epineural sheath, and fine filaments were teased out of the nerve and put on the recording electrode to perform single-unit recordings (Fig.7).

Isolation of single units

Small nerve bundles were teased using fine forceps. Using mechanical stimuli administered with a glass rod, single mechanically sensitive units were discovered and categorized based on conduction velocity, spike pattern, and sensitivity to stimulus velocity. A more vigorous and punctuated search was applied for nociceptors. The filaments should be tiny enough that there is no overlap of receptive fields, and single units should be stimulated mechanically. The raw electrophysiological data were recorded using a Powerlab 4/30 system and LabChart 8 software with the spike-histogram extension supported by an oscilloscope for visual identification.

Measurement of conduction velocity

To measure the conduction velocity, an electrical impulse was used while the triggered action potential conducted by the nerve fiber was delayed depending on the nerve fiber type and distance from the electrode. All future mechanical characterizations were corrected for this time delay. After measuring the total distance from the receptor site to the electrode, the conductance velocity (CV) could be calculated using the formula CV = distance/time delay. Typical conduction velocities for each fiber types were > 10 m/s for Aβ, < 10 m/s for Aδ and < 1.5 m/s for C-fibers.

Mechanical stimulation protocol

Mechanical sensitive receptors were stimulated from the epidermis side using either a piezo actuator (dynamic and vibration) or a nanomotor (static) connected to a force sensor and mounted on a manual micromanipulator. Different mechanical stimulation protocols were used

to identify and characterize the sensory afferents. Dynamic mechanical stimulus: A ramp and hold stimulus was used with a constant force (40 mN) and repeated with varying probe movement velocity (0.075 mm/s, 0.15 mm/s, 0.45 mm/s, 1.5 mm/s, and 15 mm/s). Only the firing activity evoked during the dynamic phase was analyzed. Vibrating mechanical stimulus: A vibrating stimulus of 6 steps with increasing amplitude was used with 3 different vibration frequencies (5, 25, 50 Hz). The force needed to evoke the first action potential was measured. Static mechanical stimulus: A ramp and hold stimulation was used with a constant fast ramp (1.5-2 mN/ms) and repeated with varying amplitude. Only spikes evoked during the static phase were analyzed.

6.3 5 Immunofluorescence staining protocols for skin

Tissue preparation and antibody incubation for whole mount or tissue section staining were performed according to the protocols described below.

Whole-mount skin staining protocol (5 days)

Day 1

1. Shave skin and clean off any loose hair. Dissect the skin sample and remove the hypodermis. Stretched out the sample using a small Sylgard Elastomer plate and insect needles.
2. Fix tissues in 4% PFA/PBS for 2h with rotation.
3. Rinse tissue and wash thrice for 10 minutes in PBS at RT with rotation.
4. Incubate with primary antibodies in blocking solution for 2-4 days at 4C with rotation.
    a. Block = 5% serum, 0.04% Triton X100, 0.5% Bovine. 20% DMSO optional.
    b. For 20ml block - 1ml serum, 80ul Triton, 100ug bovine, 19ml PBS (or 14ml PBS and 5ml DMSO)

Day 4

5. Rinse tissue and wash thrice for 30 minutes in PBS at RT with rotation.
6. Incubate with secondary antibodies in blocking solution at 4C overnight.

Day 5

7. Rinse tissue and wash thrice for 30 minutes in PBS at RT with rotation.
8. Optional - Wash for 1 hour in BABB (2:1 benzoate: alcohol)
9. Wash for 5 min in PBS, three times
10. Wash for 2 hours in 10% TDE / 25% PBS / 65% ddH2O

11. Wash for 2 hours in 25% TDE / 25% PBS / 50% ddH2O
12. Store in 50% TDE / 25% PBS / 25% ddH2O overnight or until imaging

Day 6

13. One hour before imaging, place tissue in 70-90% TDE (splash a bit of 100% TDE into 50% tubes).
14. Glue two silicon isolators on one slide and fill them with 97% TDE. Remove bubbles on the edge and place the sample inside. Make sure the TDE solution does not run over the isolator. Remove the plastic from the upper glue part of the silicon slide and carefully fix the coverslip by tilting it from one edge to the other. Try to avoid bubbles inside the sample and remove all excess TDE from the coverslip.

<u>Gelatine section staining protocol (6 days)</u>

Day 1

1. Dissect the skin sample and remove the hypodermis. Stretch out the sample using a small Sylgard Elastomer plate and insect needles.
1. Fix tissues in 4% PFA for 45 minutes at RT.
2. Cut small 2-3 small sections of skin per plastic cube. For glabrous skin, try to have 1-2 running pads per section.
3. Warm gelatine at 54 °C until liquid.
4. Transfer the gelatine into a plastic cube and immediately place the tissue samples upright at the bottom of the cube (cutting edge down). Keep tissue upright as the gelatine solidifies; use dry ice to speed up the solidification, but be careful of snap freezing.
5. Fix for 8 hours or overnight at 4 °C

Day 2

6. Cut 50-200µm thick sections using a vibratome. Start cutting at one of the angles of the block. 120µm thickness works well for glabrous skin and 150µm+ for hairy skin.
7. Rinse tissue and wash thrice for 30 minutes in PBS at RT with rotation.
8. Incubate with primary antibodies in a section-blocking solution at 4°C for 2-3 days.
    a. Block = 5% serum, 0.04% Triton X100, 0.5% Bovine. 20% DMSO optional.
    b. For 20ml block - 1ml serum, 80ul Triton, 100ug bovine, 19ml PBS (or 14ml PBS and 5ml DMSO)

Day 4

9. Rinse tissue and wash thrice for 30 minutes in PBS at RT with rotation.

10. Incubate with secondary antibodies in section-blocking solution at 4°C for 1 day/overnight

Day 5

11. Rinse tissue and wash thrice for 30 minutes in PBS at RT with rotation.
12. Wash for 2 hours in 10% TDE / 25% PBS / 65% ddH2O
13. Wash for 2 hours in 25% TDE / 25% PBS / 50% ddH2O
14. Store in 50% TDE / 25% PBS / 25% ddH2O overnight or until imaging

Day 6

15. One hour before imaging, place tissue in 70-90% TDE (splash a bit of 100% TDE into 50% tubes).
16. Mount to slide using 97% TDE/PBS and seal with a cover slip.

6.3.1 Immunohistochemistry and multiplex fluorescent *in situ* hybridization in DRGs

For both methods tissue sections of 16 µm were acquired on a cryostat, dried for 1 h, and directly used or frozen at -80°C. For immunohistochemistry, dry tissue sections were washed for 10 min with PBS followed by another 10 min incubation of 0.1 % Triton-X-100 in PBS (0.1 % PBST) for permeabilization. Primary antibodies were diluted in 0.1 % PBST and incubated O/N at 4°C. The next day, slides were washed three times for 5 minutes with 0.1% PBST followed by secondary antibody/DAPI incubation for 1 h at RT. After staining with secondary antibodies, slides were washed three times with 0.1 % PBST and subsequently mounted with Dako Mounting Medium.

For multiplex fluorescent *in situ* hybridization, the RNAscope Multiplex Fluorescent Kit v2 was used with a modified manufacturing protocol. Tissue sections were dried, fixed with ice-cold 4 % PFA in PBS for 15 min, and dehydrated in a series of 50 %, 70 %, and 100 % ethanol for 5 min each. Afterward, sections were treated with a hydrogen peroxide solution for 15 min at RT to block endogenous peroxidase activity followed by another wash with 100% ethanol for 5 min. Next, Protease III was applied for 30 min at RT. After three washes with PBS, probes were applied and hybridization was carried out in a humified oven at 40°C for 2 h. Following hybridization, amplification was performed using Amp1, Amp2, and Amp3 each for 30 min at 40°C. For detection, each section was treated sequentially with channel-specific HRP (HRP-C1, HRP-C1, HRP-C3) for 15 min, followed by TSA-mediated fluorophore binding for 30 min and final HRP blocking for 15 min (all steps at 40°C). For quantification of RNAscope

experiments, neurons (evaluated by DAPI staining) with ≥ 5 puncta/neuron were considered positive. Images were obtained using a confocal microscope (Carl-Zeiss, catalog no. LSM700) using Zen 2011 software.

6.3.2 Molecular biology

Preparation of DNA plasmids

N3HA-mscib2 and pCMV6_Kcnq4 (Myc-DDK-tagged) plasmids were PCR amplified using Phusion High-Fidelity DNA Polymerase (NEB) and *Kcnq4* or *Cib2* primers (Table 3.4). PCR products were gel purified (Wizard SV Gel and PCR Clean-Up System, Promega) and analyzed by sequencing (LGC Genomics). Sub-cloning experiments were performed using the above PCR products and the vectors pRK8-IRES-DSRed and pRK8-IRES-GFP to construct pRK8-Kcnq4IRES-GFP and pRK8-cib2-IRES-DSRed with T4 DNA ligase. DNA constructs containing Cib2 and Kcnq4 were purified from transformed bacteria grown in large-scale bacterial culture (50 mL Midiprep, PureYield™ Plasmid Midiprep System, Promega). The midi preps were made according to the manufacturer's protocol. DNA quantification was measured using a NanoDrop 2000 (Thermofisher Scientific).

Gene	**Primers**		**Annealing T (°C)**
Kcnq4	Forward	CTGCACCTCGGTTCTATGCCACCATGGCCGAGGCCCCCC	66
	Reverse	CAGAAGCTTAATTCAATTTAGTCCATGTTGGTGCTGACTGAGCG	
Cib2	Forward	CCCCATCGATATGGGGAACAAGCAGACC	68
	Reverse	GCTCTAGACTATTAGATTCGAATGTGGAAGGTG	

Table 2. Primers for CIB2 and KCNQ4 plasmids construct

6.3.3 Cell culture

In the present study, the CHO cell line was used. Cells were grown in DMEM/F12 - Dulbecco's Modified Eagle Medium: Nutrient Mixture F-12 medium supplemented with 10% fetal bovine serum (FBS) and 1% of the antibiotics Penicillin/Streptomycin at 37°C and 5% CO2 levels.

CHO cells were transiently transfected using FuGeneHD (Promega, Madison). Briefly, a mix of 100 µL of Opti-MEM, 3 µL of FuGeneHD, and 1 µg of DNA were incubated for 10 min at room
temperature. The mix was added to CHO cells cultured in 30 mm x 15 mm Petri dishes and 900 µL of media containing DMEM/F12 without serum or antibiotic was added for an Overnight transfection. Electrophysiological recordings were made 18-24 h post-transfection.

6.3.4 Whole-cell patch clamp

Whole-cell patch clamp experiments were made from CHO cell line which was transiently transfected. By using pulled and heat-polished borosilicate glass pipettes (Harvard apparatus,1.17 mm x 0.87 mm) with a resistance of 3-6 MΩ. The pipettes were pulled using a DMZ puller (Germany), and filled with a solution containing (in mM): 110 KCl, 10 NaCl, 1 MgCl2, 1 EGTA, and 10 HEPES. The pH was adjusted to 7.3 with KOH.The extracellular solution contained (in mM): 140 NaCl,4 KCl, 2 CaCl2, 1 MgCl2, 4 Glucose and 10 HEPES. The pH was adjusted to 7.4 with NaOH.Pipette and membrane capacitance was compensated using the auto-function of Patchmaster (HEKA, Elektronik GmbH, Germany) and series resistance was compensated to minimize voltage errors. Currents were evoked in response to 800 ms test pulses of 10 mV steps from a holding potential of -60mV in a voltage range from -100mV up to +80 Mv.

6.3.5 Behavioral assays

All behavior experiments were performed on adult male mice (>8–10 weeks of age). For controls, littermates without Cre were used. The experimenter was always blind to the genotype of the mice. Mice were habituated to the testing environment for 30 min each day for 3 d before testing. Mice were placed in individual Plexiglas cubicles on an elevated mesh platform

Cotton swab assay

Response to a gentle stroke was assessed by stroking a cotton swab in the heel-to-toe direction on the plantar surface of the hind paw. Mice were acclimated for 1 hour in von Frey

chambers. A cotton swab was puffed out about three times. A paw withdrawal motion in response to a stroke of the swab underneath the mouse paw was scored. Five sweeps were performed with at least 10 s between each. The number of withdrawals out of five trials was counted and reported as a percentage of withdrawal for each mouse.

Brush assay:

The left hind paw was stroked from heel to toe with a paint brush 5× with 10 s between each. The percentage of withdrawals was calculated similarly to cotton swab assay.

von Frey experiments

Using calibrated von Frey filaments (Aesthesio®, USA), mechanical nocifensive withdrawal thresholds were determined. The 50% paw withdrawal threshold was calculated using the Up-down approach. The "up-down approach" establishes the stimulus weight that elicits a reaction in 50% of animals (Chaplan et al., 1994; Christensen et al., 2020; Dixon, 1980). Von Frey filaments in the range of 0.008, 0.02, 0.04, 0.07, 0.16, 0.4, 0.6, 1.0, 1.4, and 2 g were used to stimulate the hind paws for roughly 1 to 3 seconds. At intervals of 3-5 minutes, Von Frey filaments were introduced perpendicular to the hind paws. Depending on the animal's reaction, the more or lesser force was delivered to the hind paw to induce a sequence of six to nine positive or negative withdrawal reflexes. When the paw was retracted, a positive reaction was evaluated. The testing began with the 0.4 g filament. A stronger stimulus was provided in the absence of paw withdrawal (a negative reaction, O). A lesser stimulus was evaluated while observing paw withdrawal (positive reaction, X). According to (Christensen et al., 2020), XO-response patterns of each animal were submitted to https://bioapps.shinyapps.io/von frey app/ to determine the 50% PWT as previously described (Chaplan et al., 1994; Dixon, 1980).

Tape response assay

Mice were acclimated in multi conditioning system for 10 min. 4cm piece of laboratory tape was placed gently on the center of the mouse’s back. Mice were observed for 5 min, and the total number of bouts in response to the tape was recorded and reported. In addition, the duration and the latency of the response were measured. Biting or scratching of the tape was scored as a response.

Digging behavior testing

The experimental device was a normal mouse cage with 4 cm of compacted wood chip bedding. Individually, mice were examined in the equipment for three minutes without food or drink. Before the tests, mice were acclimated for 30 minutes in their home cages in the room. The length of digging was defined as the time spent actively dislodging bedding with paws The tests were recorded for 3 min, and the length and the bouts of digging were recorded and reported.

6.3.6 Statistical analysis

All data analyses were performed using GraphPad Prism and all data sets were tested for normality. Data sets were compared using a two-tailed and unpaired T-test or Mann-Whitney U-test, one-way analysis of variance (ANOVA), or Kruskal-Wallice test with Bonferroni multiple comparison test. When required two-way repeated-measures analysis of variance (ANOVA) and posthoc tests were performed with Bonferroni's multiple comparisons test. Significance values are reported as: * denotes P value < 0.05; ** denotes P value < 0.005; *** denotes P value < 0.0005. All error bars are standard errors of the mean (SEM).

7 Results

7.1 Neuroanatomical distribution of CIB2 in the DRGs

Sensory neurons are pseudo-unipolar neurons that are tuned to distinct modalities of sensory stimuli like touch, temperature, and nociception. Their soma resides in the dorsal root ganglia whereas their axons extend to the periphery. According to their morphology and level of myelination, large-soma and thickly myelinated neurons are considered mechanoreceptors while small-soma and thinly or no myelinated axons as nociceptors. In a single-cell RNA sequencing study, *Cib2* was found to be expressed mainly in peptidergic nociceptors and myelinated mechanoreceptors (Usoskin et al., 2015) which I aimed to validate at the protein level using immunohistochemistry of lumbar DRG sections from C57BL/6 mice.

CIB2 cell size distribution was measured by the cross-sectional area in μm^2 (n=405) (Fig. 8F). CIB2 expression was evident in small-size neurons as 68% of CIB2 positive neurons had a cross-sectional area between 100 and 300 μm^2. The remaining 32% of CIB2 positive neurons had medium to large soma size (300-700 μm^2). The CIB2 antibody was combined with antibodies against the marker of myelinated afferents, neurofilament 200 (NF200) and it was found that approximately 40% of the CIB2-positive neurons also express NF200 (Fig. 8A, E) while ~20% were co-stained with TrkC (Fig. 8B, E), a marker for low threshold mechanoreceptors (LTMRs). Interestingly CIB2 was expressed in a large subset of neurons which were also positive for the nociceptive markers TrkA and TRPV1. CIB2-positive neurons were co-stained with ~80 % TrkA and ~70% with TRPV1 (Fig. 8C, D, E). These results are in agreement with the single-cell data and suggest that CIB2 could have a functional role in mechanoreceptors and nociceptors.

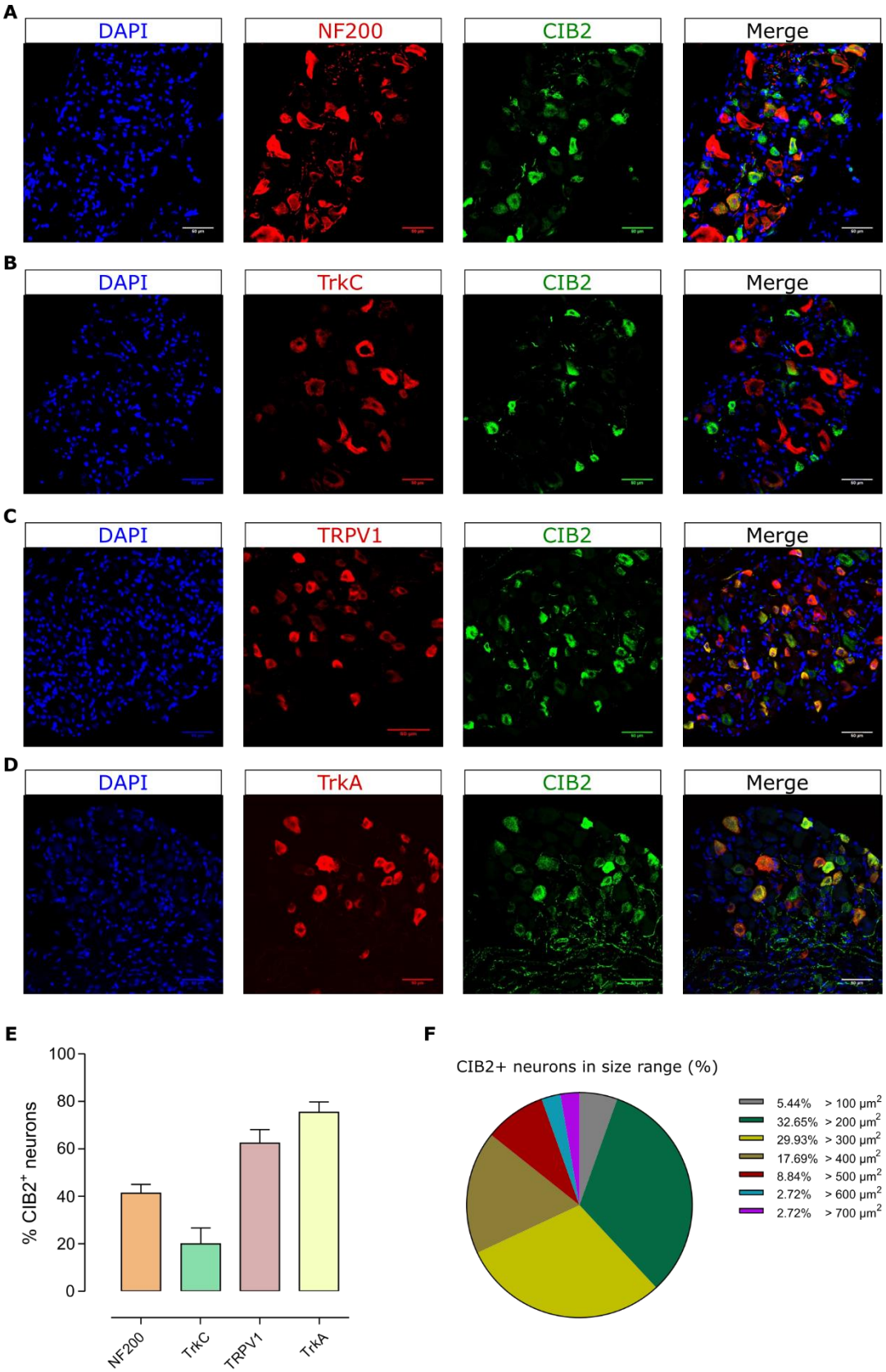

Figure 8. CIB2 is expressed in Mechanoreceptors and Nociceptors in DRG mouse sections. A. NF200 is expressed in about 40% of CIB2⁺ DRG neurons. **B.** A small portion of DRG neurons that express CIB2 also express TrkC **C.** TRPV1 expression in CIB2 positive neurons **D.** Almost all CIB2⁺ DRG neurons express TrkA. **E.** Quantification of A-D (number of mice=3) **F**. Quantitative analysis of the size of the CIB2⁺ neurons based on the cross-sectional area. Data are represented as means ± SEM. Scale bar = 50 µm. (n of animals = 2- 3)

7.2 CIB2 protein in Mechanosensory Organs in the skin

The detection of diverse stimuli from the environment relies on the activation of mechanosensory neurons that innervate the skin and are associated with cutaneous tactile end-organs (Barr-Gillespie et al., 2001). To test if CIB2 is present in the sensory terminals innervating the skin I used thick sections from glabrous and whole-mount, cleared hairy skin. I focused on the distinct skin structures that are the major cutaneous end-organs of mechanoreceptors: Merkel cells, Meissner's corpuscles, and hair follicles. In whole-mount hairy skin, CIB2 immunofluorescence was present in deep nerve branches and at circumferential endings that surround the hair follicle which was co-stained with the NF200 marker (Fig. 9A). Hair follicle longitudinal lanceolate and circular nerve endings are structures formed by rapidly adapting Aβ-fibres mechanoreceptors (RAMs) in the hairy skin. The lanceolate structures are associated with terminal Schwann cells, thus, were visualized with the S100 Schwann cells marker. In oblique cross-sections of hind paw hairy skin, CIB2 did not co-localize with S100 rather suggesting that CIB2 is mainly expressed in the axons of the hair follicle (Fig. 9B). I then examined CIB2 in Meissner's corpuscles, which are localized at dermal papillae and are innervated by RAMs in glabrous skin. These sensory corpuscles consist of lamellar Schwann cells; therefore, I co-stained the S100 Schwann cell marker together with the CIB2 antibody (Fig. 9C). CIB2 immunostaining was found in the axon that innervates the capsule but not in the lamellar cells of Meissner's corpuscles which again suggests that CIB2 is not present at the lamellar cells but in RAMs axons. Merkel cells are localized at the stratum basale, right at the transition from the dermis to the epidermis, and are innervated by slowly adapting Aβ-fibres. By using the antibody against cytokeratin 20, which stains Merkel cells, I observed that CIB2 immunostaining was not associated with this neurite complex (Fig. 9D). These data indicate that CIB2 is mainly present in RAMs that innervate skin sensory end-organs.

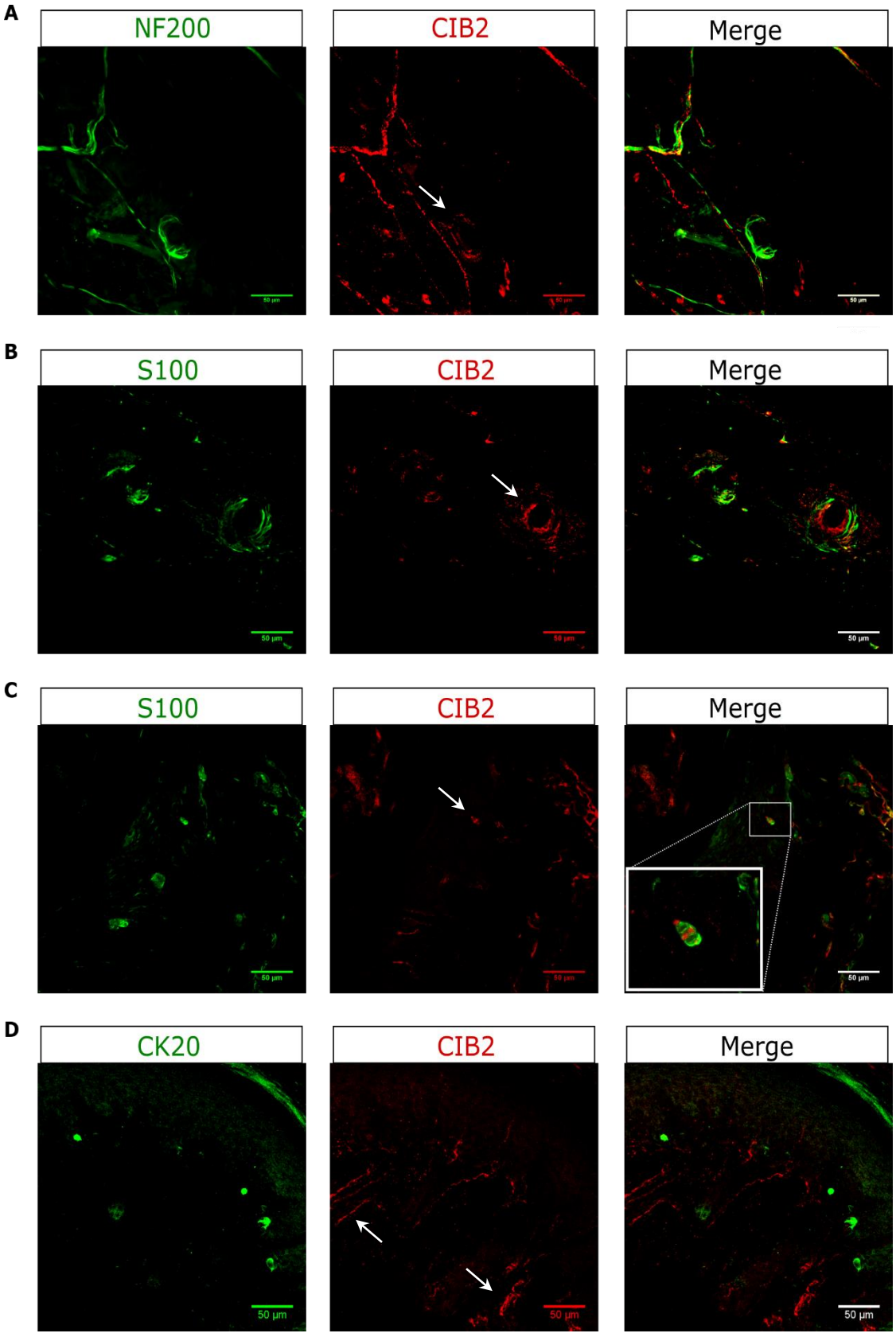

Figure 9. CIB2 is localised in mechanosensory organs in glabrous and hairy skin. Cutaneous nerve branch and circumferential endings surrounding the hair follicle in whole mount hind paw hairy skin **B.** Lanceolate endings and hair follicle in oblique cross-sections of hind paw hairy skin **C.**

Meissner's corpuscles of hind paw mouse glabrous skin **D.** Merkel cells of hind paw mouse glabrous skin. Arrows show CIB2 protein expression.

.

7.3 Role of CIB2 in Sensory fibre coding of mechanical stimuli

CIB2 was found to be expressed in the soma of sensory neurons and their terminals in the skin as well. To investigate the functional role of CIB2 in these cutaneous sensory fibres I used the well-established *ex vivo* skin nerve technique in both glabrous and hairy skin, recording from tibial and saphenous nerves respectively (Walcher et al., 2018; Koltzenburg and Lewin, 1997). For this purpose, I generated the *Wnt1-Cre; Cib2*$^{fl/\ fl}$ mice line in which CIB2 was conditionally knocked out in cells derived from the neural crest, like sensory neurons and glia cells (see methods) (Fig.10). In total, I obtained recordings from 65 Aβ-fibres in control mice and 64 in *Wnt1-Cre; Cib2*$^{fl/\ fl}$ (conduction velocities >10 m s−1), 44 and 32 Aδ-fibres, respectively (conduction velocities between 1.0 and 10 m s−1). Last, 17 c-fibers were recorded from control mice and 21 from *Wnt1-Cre; Cib2*$^{fl/\ fl}$ mice. (Data summarized in Table 3). Evaluation of the proportions and conduction velocities revealed no significant differences between the two genotypes (data not shown).

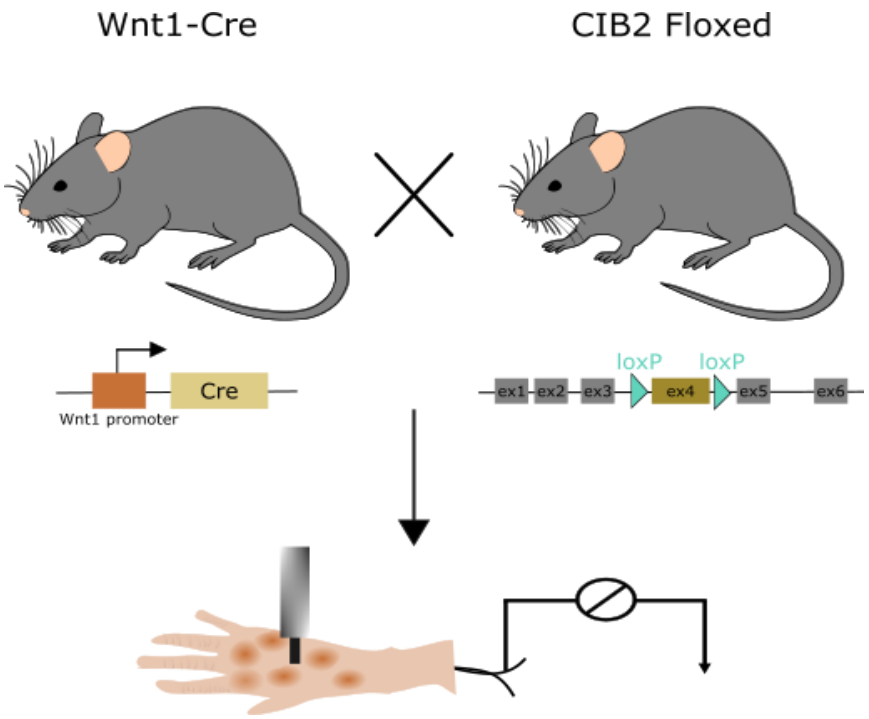

Figure 10. Cartoon representing the *Cib2*$^{fl/fl}$ crossed with *Wnt1-Cre* and skin nerve preparation in hind paw.

	Saphenous nerve Control	*Saphenous nerve Wnt1-Cre; Cib2$^{fl/fl}$*	*Tibial nerve Control*	*Tibial nerve Wnt1-Cre; Cib2$^{fl/fl}$*
Aβ-fibres				
Count (n)	47	47	18	17
Conduction velocity (m/ s)	12,7 ± 0,4	13 ± 0,5	10,8 ± 0,5	11,4 ± 0,3
RAMS				
Count (n)	23	20	11	11
Conduction velocity (m/ s)	11,3 ±0.4	13,2 ± 0,9	10,8 ± 0,5	11,6 ± 0,5
SAMS				
Count (n)	24	27	7	6
Conduction velocity (m/ s)	14 ± 0,7	12,8± 0,6	10,9 ± 1,4	11 ± 0,5
Aδ-fibres				
Count (n)	27	17	17	15
Conduction velocity (m/ s)	4,9 ± 0,4	5,2 ± 0,3	4,7 ± 0,4	4,1 ± 0,5
D-hair				
Count (n)	13	10	5	5
Conduction velocity (m/ s)	4,0 ± 0,5	4,2 ± 0,3	5,9 ± 0,3	4,8 ± 0,8
AM				
Count (n)	14	7	12	10
Conduction velocity (m/ s)	5,8 ± 0,6	6,5 ± 0,5	3,9 ± 0,6	3,7 ± 0,8
C-fibers				
Count (n)			17	21
Conduction velocity (m/ s)			0,6 ± 0,07	0,6 ± 0,07

Table 3. Numbers and conduction velocities of recorded primary afferents from saphenous (hair skin) and tibial (glabrous skin) nerve in control and *Wnt1-Cre; Cib2$^{fl/fl}$* mice. AM, Aδ-mechanonociceptor; RAM, rapidly adapting mechanoreceptor; SAM, slowly adapting mechanoreceptor.

7.4 Electrophysiological properties of Aβ-fibres in *Wnt1-Cre; Cib2$^{fl/fl}$* mice

7.4.1 Aβ-fibre rapidly adapting mechanoreceptors (RAMs)

Meissner ‘s corpuscles and hair follicles are innervated by RAMs in glabrous and hairy skin respectively. As CIB2 was found in association with these types of end organs I first focused on the investigation of its role in RAMs. These types of mechanoreceptors detect movement and low-frequency vibration. Thus, to activate RA mechanoreceptors a series of increasing ramp velocities (0.075 mm/s, 0.15 mm/s, 0.45 mm/s, 1.5 mm/s, and 15 mm/s) with a constant force (average force of 45 mN) was applied to the receptive field. Action potentials evoked in the dynamic phase of the stimulation were analyzed. In control mice, hair follicle RAMs,

respond during the dynamic phase of the fastest velocities with 1-3 spikes (Fig. 11E). Remarkably I found that afferents from mice that lack CIB2 display significantly increased firing rates in comparison to controls. During the slower velocities (0.075 – 0.045 mm/s), the responses of the RAMs lacking CIB2 were almost fivefold greater than those from control mice (Fig. 11A). In addition, RAMs from *Wnt1-Cre; Cib2*$^{fl/fl}$ exhibited shorter latencies in response to velocity stimuli, reflecting a lower mechanical threshold for activation (Fig. 11B). Particularly, between 0.075 – 0.045 mm/s velocity stimulation, RAMs from *Wnt1-Cre; Cib2*$^{fl/fl}$ displayed threefold faster responses in comparison to control mice (Fig. 11B). Meissner's corpuscles responses, similar to the hair follicle, showed elevated responses in *Wnt1-Cre; Cib2*$^{fl/fl}$ in comparison to control mice and significantly shorter latencies in response to velocity stimuli (Fig. 11B, D). In addition, the mechanical force required to elicit the first action potential was found to be significantly reduced in *Wnt1-Cre; Cib2*$^{fl/\ fl}$ in both hairy and glabrous skin (Fig. 11F, G).

RAMs derived from the hair follicle and the Meissner's corpuscle are also tuned to detect low-frequency vibrations (Heidenreich et al., 2012; Schwaller et al., 2021), therefore, I used a vibration stimulus of 6 increasing amplitudes at 5Hz, 25Hz, and 50 Hz frequencies. On average, hair follicle Aβ-fibre RAMs in *Wnt1-Cre; Cib2*$^{fl/\ fl}$ mice showed increased vibration sensitivity to 5-Hz and 25-Hz, but not to 50-Hz, compared to controls (Fig. 12A, B, C). RAMs in control mice responded with one spike per cycle while the neurons lacking CIB2 responded with 2 to 3 spikes per cycle (Fig. 12G). Meissner's corpuscle RAMs lacking CIB2 were also more responsive to 5 Hz and 25 Hz stimuli in comparison to control mice, but similarly to hair follicles, not to 50 Hz. These data support the hypothesis that CIB2 is involved in the regulation of RAMs and tunes their spike-frequency adaptation.

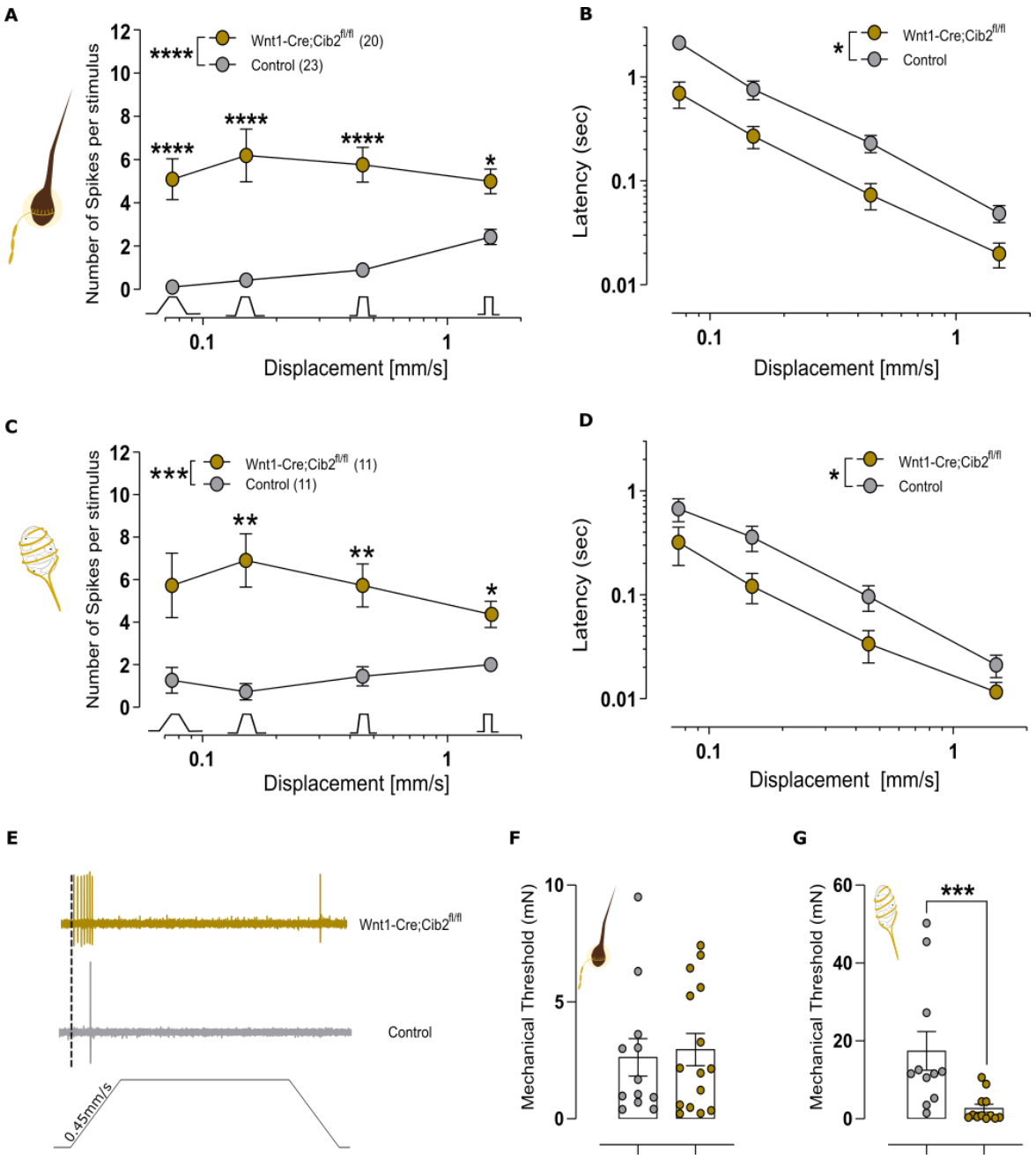

Figure 11. CIB2 modulates the excitability of RAMs. A. and C. RAMs innervating hair follicles and Meissner's corpuscles recorded using the *ex vivo*, hind paw, hairy skin-nerve preparation in *Wnt1-Cre; Cib2$^{fl/fl}$* mice had significantly increased firing activity compared with control mice (two-way repeated-measures ANOVA: asterisks indicate Bonferroni's posthoc analysis: ***P=0,0003, ****P < 0.0001)**. B and D.** Displacement-latency, showing that RAMs innervating Meissner's corpuscles from Wnt1-Cre; Cib2$^{fl/fl}$ are responding faster to mechanical stimuli (two-way ANOVA with Sídák post hoc analysis, *P= 0.0191) **E** Example ramp responses of individual RAMs from control and mutant mouse in hair follicle **F and G.** Mechanical Threshold (mN) (unpaired t-test with Welch's correction, ***P=0,0146). Data represent the mean ± s.e.m.

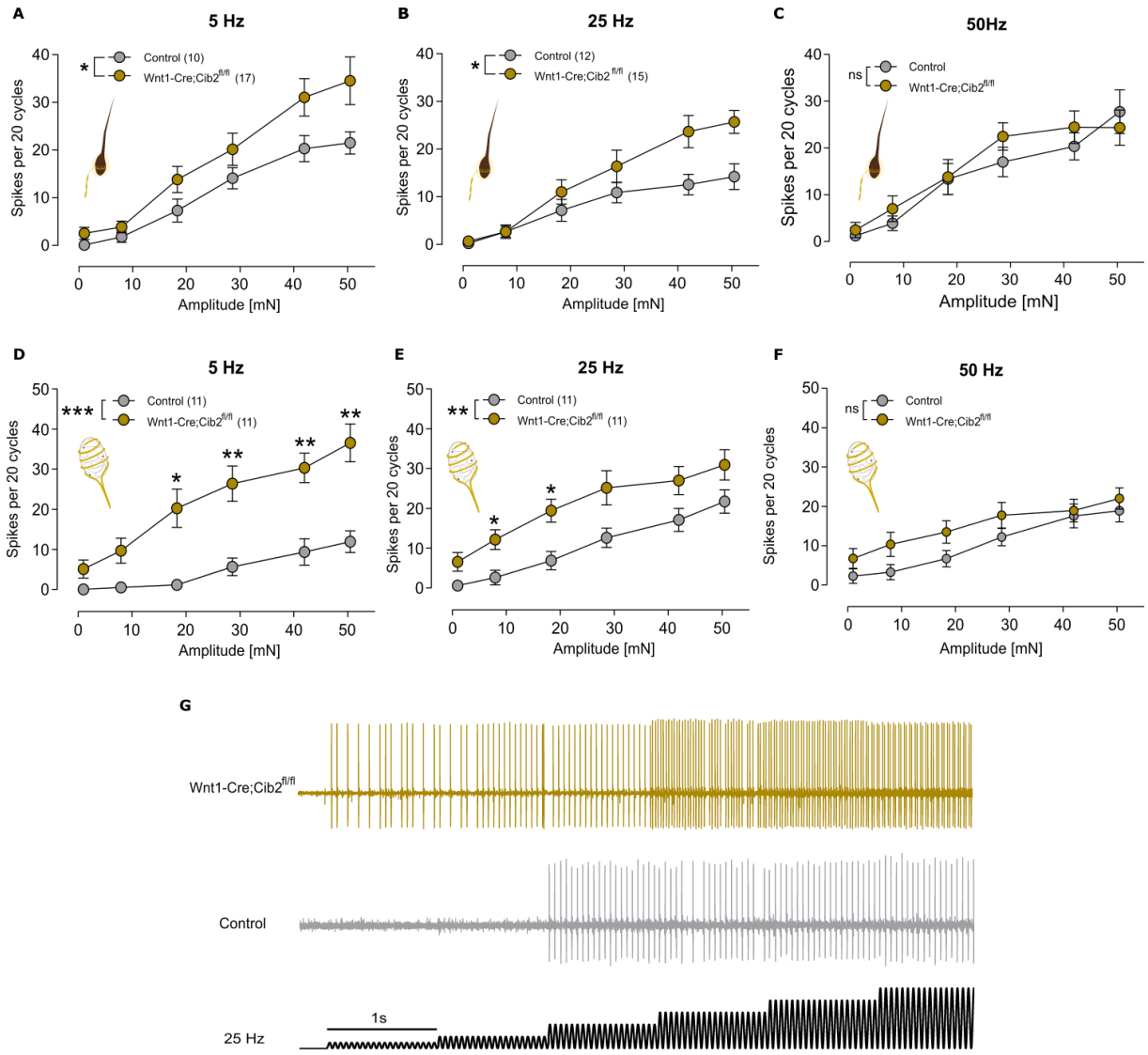

Figure 12. Vibration sensitivity was elevated in *Wnt1-Cre; Cib2$^{fl/fl}$* mice. A. 5Hz vibration-evoked firing activity from hair-follicle RAMs lacking CIB2 was significantly increased (two-way ANOVA with Sídák post hoc analysis, *P= 0,0463) **B,** 25 Hz (P=0.05) **C.** 50-Hz vibration sensitivity was not significantly different. **D** RAM Aβ-fibres innervating Meissner's corpuscles had increased vibration firing at 5 Hz (***P=0.0002). **E.** 25 Hz (**P=0.0067). **F.** 50-Hz vibration sensitivity was not significantly different**. G.** Example traces of single RAMs in *Wnt1-Cre; Cib2$^{fl/fl}$* (top) and control (bottom) mice in response to 25Hz vibration. Data represent the mean ± s.e.m.

7.4.2 Slowly adapting mechanoreceptors (SAMS)

Slowly adapting mechanoreceptors (SAMs) have Aβ-fibre axons with conduction velocities greater than 10m/s. SAMs are associated with Merkel's cell complexes and are tuned to detect the pressure, shape, and texture of objects. Each receptor was stimulated with the velocity protocol, as described in the previous section. SAMs respond rapidly to the dynamic phase

and then adapt slowly during the static phase (Fig. 13C). However, a difference in the responses from the dynamic phase between *Wnt1-Cre; Cib2*$^{fl/\ fl,}$ and controls, was not observed (Fig. 13A). In addition, a constant ramp velocity with increasing static displacements were used to analyze the responses to skin indentation. Here responses in the static phase were counted and compared between conditional *Cib2* knock-out mice and control mice but similar to velocity protocol the mechanosensitivity of SAMs was not altered between genotypes (Fig. 13B). SAMs are also vibration sensitive, but again the responses in *Wnt1-Cre; Cib2*$^{fl/\ fl}$ were unchanged in all frequencies (Fig. 13E, F, G) as well as the mechanical threshold (Fig. 13D) in comparison to control mice. These results are in agreement with the findings from immunofluorescence as *Cib2* was not detected in CK20 Merkel's cell complexes. Most importantly these results show the specificity of CIB2 in the regulation of RAM Aβ-fibres.

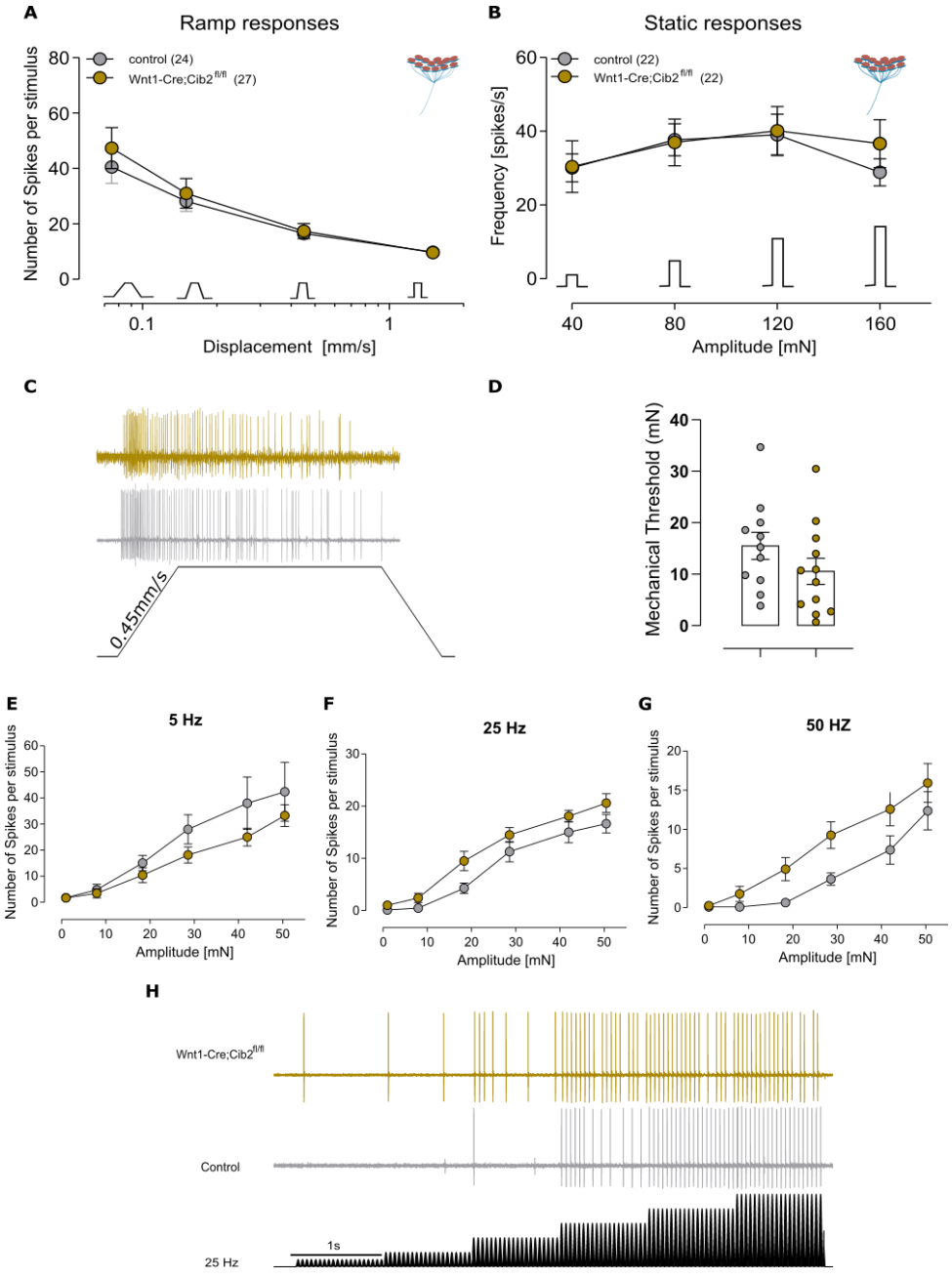

Figure 13. SAMs responses were unchanged in *Wnt1-Cre; Cib2$^{fl/fl}$ mice*. A. using ramp stimuli **B.** using the ramp and hold stimuli (two-way ANOVA with Bonferroni post-hoc analysis) **C**. Example ramp responses of individual of SAM Aβ fibres from *Wnt1-Cre; Cib2$^{fl/fl}$* and control mice in response to 0.45 mm/s **D.** Mechanical thresholds [mN] calculated from 25Hz vibration protocol were unaltered (Mann-Whitney test). **E.** 5Hz vibration, **F.** 25 HZ, and **G.** 50-Hz vibration sensitivity was not significantly different. **H**. Representative traces from of single SAM Aβ fibres from *Wnt1-Cre; Cib2$^{fl/fl}$* and control mice in response to vibration of 25 Hz. Data represents the mean ± s.e.m.

7.5 Electrophysiological properties of nociceptors in *Wnt1-Cre; Cib2$^{fl/ fl}$* mice

CIB2 was expressed in ~80% of TrKa and ~70% of TRPV1 peptidergic nociceptors which may indicate a role of this protein in nociception. These types of receptors are tuned to detect noxious stimuli from the environment and fall into two distinct fibre types, Aδ-mechanonociceptors and C-fibres.

C-fibres

C-fibre afferents terminate as free nerve endings in the periphery, closely associated with nociceptive Schwann cells (Abdo et al., 2019). C-fibre neurons have small axonal diameters and are non-myelinated, therefore displaying slower conduction velocities compared to Aβ fibres. These nociceptive afferents respond to increasing static forces in the noxious range (Lewin & Moshourab et al., 2004), therefore a ramp and hold stimuli of 10s with increasing force ranging from 50 to 230mN was used for characterizing their response properties. The speed of the ramp was constant at 2mm/s. The mechanical threshold for the response was measured from the first action potential of every indentation step. C-Fibres typically display slow adapting firing to sustained static force and an increase in force leads to a rise in receptor activation. Analyses of the static responses revealed no difference between the control and *Cib2*-deficient animals (Fig. 14A). In addition, the force needed for evoking the first action potential (threshold) was the same in control and mutant mice (Fig. 14B). These data indicate that CIB2 is not involved in setting the mechanical threshold in C-fibre nociceptors.

Interestingly, C-fibres lacking CIB2 exhibited significant continued firing following the removal of the mechanical stimulus, a characteristic seen at a considerably lesser level in fibres from control mice. (Fig. 14D). The after-charge responses of C-fibres from *Wnt1-Cre; Cib2$^{fl/ fl}$* animals were three times greater than those of the control mice (Fig. 14C). This finding was only obtained during the interstimulus phase of the procedure, since it was not observed before the initial stimulus, indicating that this event occurred only after the afferents had been activated. Along with the involvement of CIB2 in the firing rates of RAMs described above, it

seems that CIB2 regulates the excitability of C-fibres. C-fibres can respond both to thermal and mechanical stimuli (polymodal C-fibre) or can be activated only by noxious mechanical stimuli (C-M) (Smith & Lewin, 2009). The recorded C-fibres were sub-classified according to their thermal sensitivity to heat- and cold stimuli. Analyses of the static responses from polymodal or CM fibres showed no difference between genotypes (data not shown). However, after-charge responses from polymodal or CM fibres lacking CIB2, were increased compared to fibre from control mice which due to low numbers of recorded fibres was not significant (data not shown).

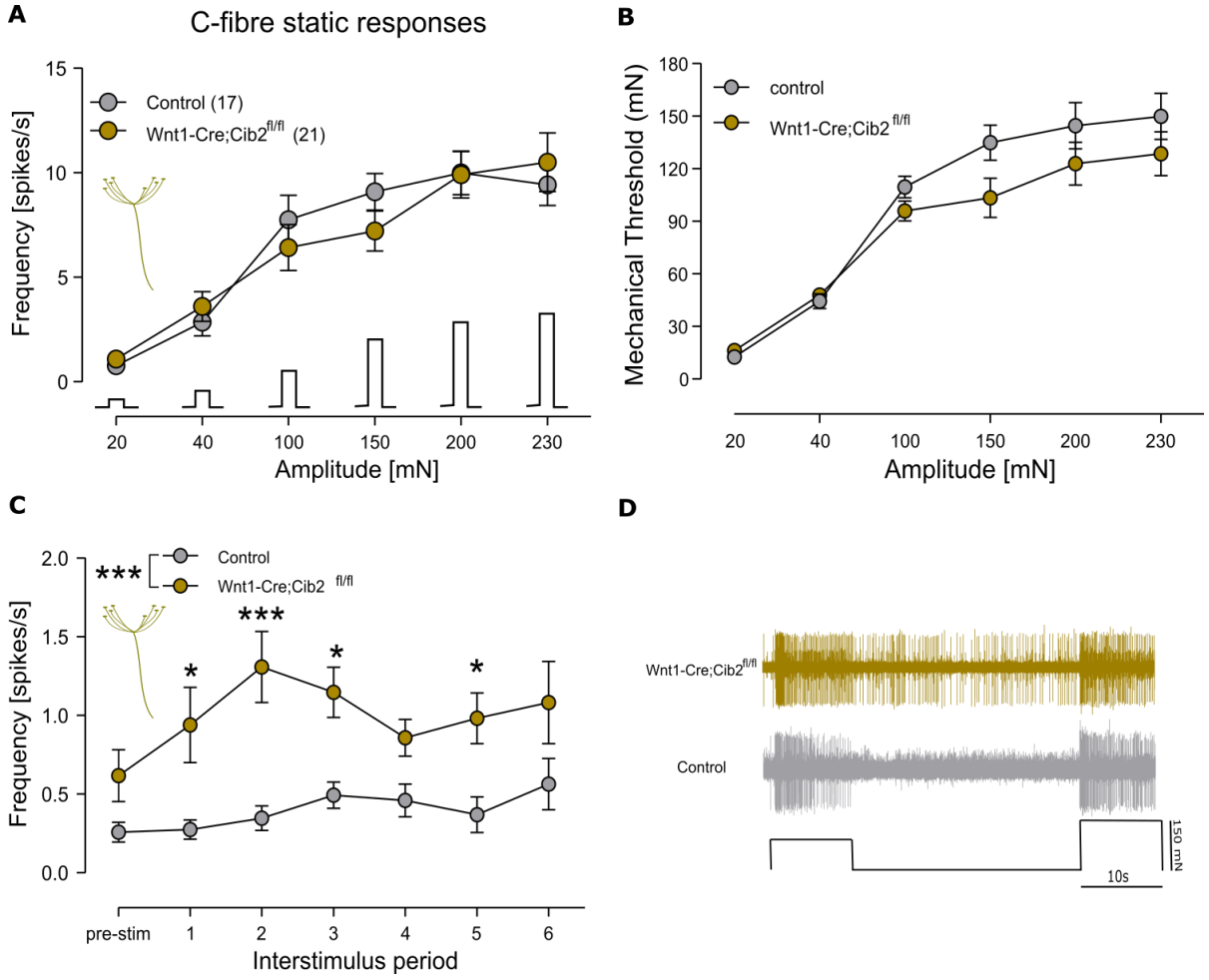

Figure 14. C-fibre responses. A. C-fibre static responses were unchanged in *Wnt1-Cre; Cib2$^{fl/fl}$* mice compared to control mice (two-way ANOVA with Sídák post hoc analysis) B. Mechanical threshold [mN] was unaltered, (unpaired t-test with Welch's correction) C. After charge responses from C-fibre were increased in the conditional CIB2 mice. (two-way ANOVA with Sídák post hoc analysis, ***P=0.0005) D. Representative traces from c-Fibre responses between two indentation stimuli (100 mN and 150 N).

Aδ-mechanonociceptors

Aδ-mechanonociceptors convey fast, mechanical pain (Ploner, 2002; Price, 1972, 1977). Aδ-mechanonociceptors have medium-sized soma and thinly myelinated axons, therefore their conduction velocity varies between more than 1m/s and less than 10 m/s (Lewin & Moshourab, 2004; Dubin & Patapoutian, 2010). Aδ-mechanonociceptors have an overlapping range of modalities with C-fibre and respond to the same type of stimuli (Lewin & Moshourab et al., 2004), therefore a ramp and hold stimuli of 10s with increasing force was used to probe their stimulus-response properties. Similarly, to C-fibre the firing rates in the static phase were analyzed, and was found that there was no difference in the responses from the mice lacking CIB2 in comparison to the control (Fig. 15A). Mean mechanical threshold was also unaltered in mutant mice in comparison to the control mice (Fig. 15B).

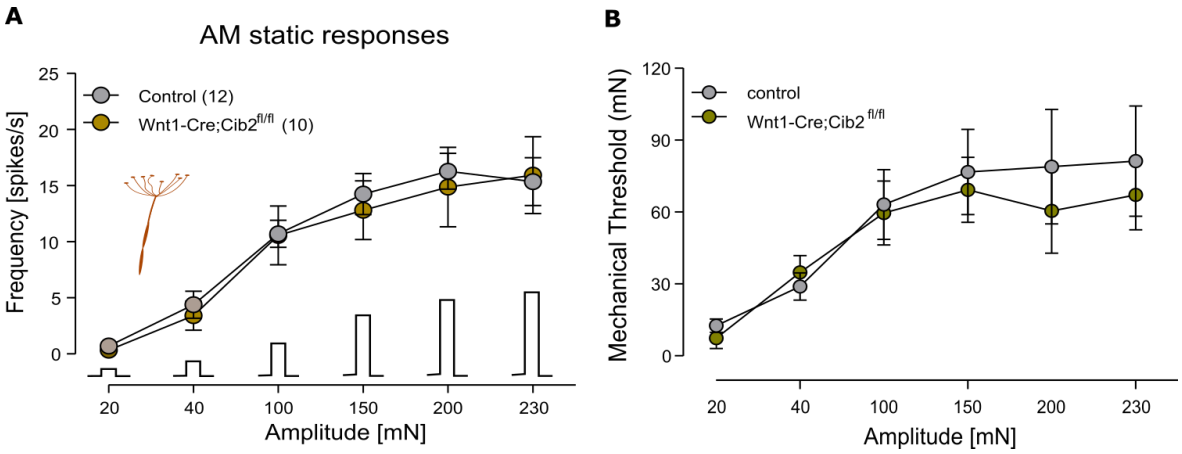

Figure 15. AMs responses. ***A.*** AMs static responses were unchanged in *Wnt1-Cre; Cib2*$^{fl/fl}$ mice compared to control mice (two-way ANOVA with Sídák post-hoc analysis**) B**. Mechanical threshold [mN] was unaltered, (unpaired t-test with Welch's correction)

7.6 Investigation of putative interaction of CIB2 with the potassium channel KCNQ4

Somatosensory neurons are tuned to detect a variety of stimuli and exhibit distinct firing patterns. Mechanosensitive channels are the major detectors and transducers of these stimuli but voltage-gated ion channels set and modulate the threshold and adaptation of the fibre responses (Du et al., 2014; Heidenreich et al., 2011; Muqeem et al., 2018). Potassium channels are widely expressed in the somatosensory system and they may modulate receptor properties and adaptation (Yang Zheng et al., 2019; Heidenreich et al., 2011). Members of the Kv7 (KCNQ) family are expressed in DRG neurons and exhibit a role in mechanosensation

and pain (Passmore et al., 2003; Linley et al., 2008; Heidenreich et al., 2011; Schütze et al., 2015). KCNQ channels are known for their role in regulating neuron excitability as they are the main contributors to the M-current (Brown and Adams, 1980; Brown, 1988; Zaika et al., 2006). Interestingly KCNQ4 channels, modulate the frequency responses of RAMs, reminiscent of what I observed with *Wnt1-Cre; Cib2* $^{fl/fl}$ mice. Genetic deletion of the *KCNQ4* gene or inhibition of the KCNQ4 protein in mice, exhibit increased RAM frequency responses (Heidenreich et al., 2011). KCNQ4 immunostainings have demonstrated that KCNQ4 is co-localized with NF200 in DRG neurons, and KCNQ4 is present in the same skin sensory terminals as CIB2 (Heidenreich et al., 2011). Furthermore, the CIB2 protein shows structural similarities with KChiP proteins, which are known to regulate Kv4.2 potassium channels (An et al., 2000; Wang, 2008). Thus, the hypothesis was that CIB2 could modulate the RAMs by interacting and regulating KCNQ4 channels.

I first tested if KCNQ4 is expressed in the same sensory neurons as CIB2. For this purpose, I used DRG sections from C57BL/6 mice and performed *in situ* hybridization (RNA scope) for the mRNA detection of *KCNQ4* and *Cib2.* The mRNA of *KCNQ4* was found in ~60% of Cib2 positive neurons (Fig. 16F) indicating co-localization and raising the question of whether these two proteins interact. *Cib2* expression was absent in DRG sections from *Wnt1-Cre; Cib2*$^{fl/fl}$ mice (Fig. 16E)

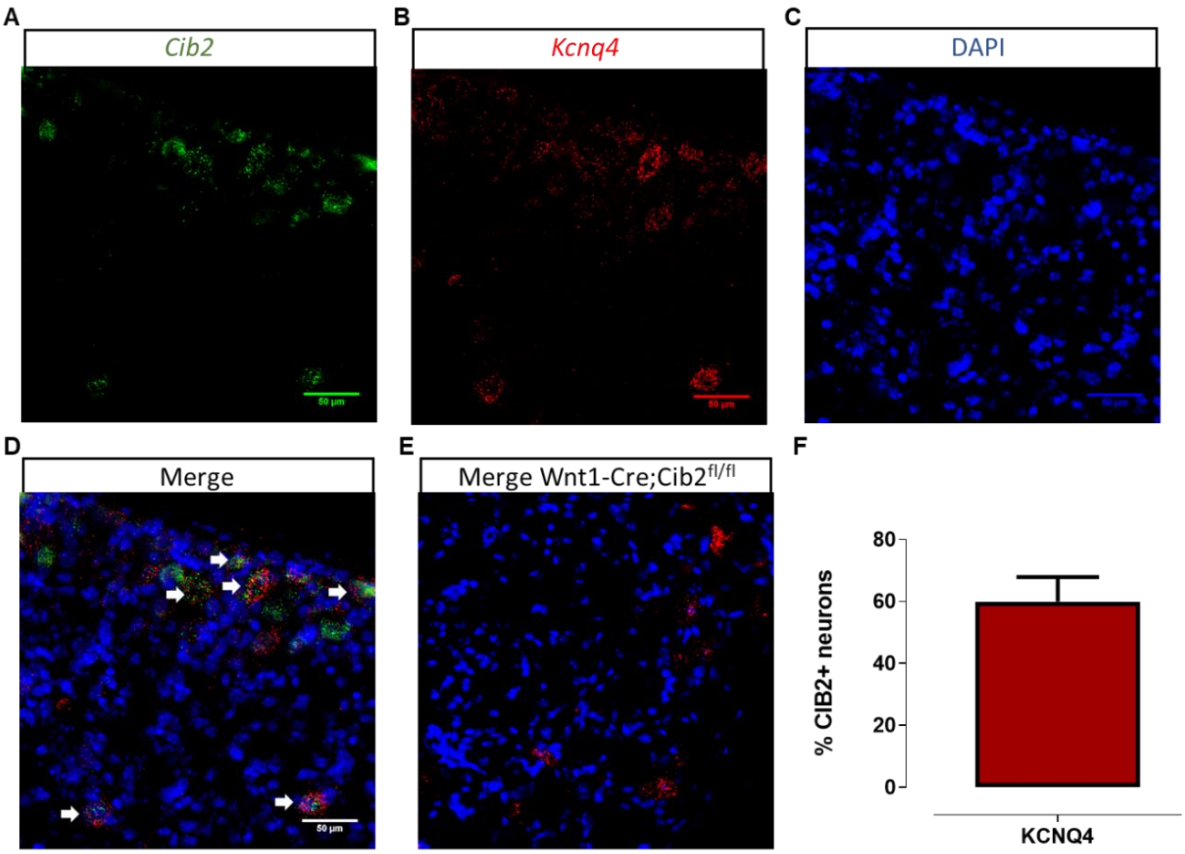

Figure 16. Expression of *KCNQ4* and *Cib2* in the same sensory neurons. A. *KCNQ4* mRNA **B.** *Cib2* mRNA **C**. DAPI. **D.** Merged picture showing the localization of *KCNQ4* and *Cib2* mRNA in the same neurons. **E**. Expression of *KCNQ4* and *Cib2* in *Wnt1-Cre; Cib2*$^{fl/fl}$ mice. **F.** Quantification (n of animals = 3)

To test the hypothesis that CIB2 regulates KCNQ4, I used the KCNQ inhibitor, linopirdine. If in *Cib2* mutant mice KCNQ4 is dysfunctional, blocking KCNQ4 would not affect the adaptation properties of RAMs, as it should in the wild type (Heidenreich et al., 2011). I performed skin nerve extracellular recordings in control and conditional knockout mice using a mechanical stimulus of 0.45 mm/s velocity followed by 400 µM of linopirdine. The inhibitor was introduced to the isolated receptor fields of the RAMs (Fig. 17A). As expected, responses from the control mice showed an increased firing rate from RAMs upon KCNQ4 block (Fig. 17B). These results validate the findings in Heidenreich study regarding the role of KCNQ channels in regulating the adaptation of RAMs (Heidenreich et al., 2011). RAM velocity responses in *Wnt1-Cre; Cib2*$^{fl/fl}$ mice did not change after the application of linopirdine (Fig. 17B). These data show that in fibres lacking CIB2, there is not an obvious KCNQ4 inhibition suggesting that when CIB2 protein is absent KCNQ4 channels are not functioning properly. Thus, KCNQ4 role as a brake on the excitation of RAMs is modulated by its interaction with CIB2.

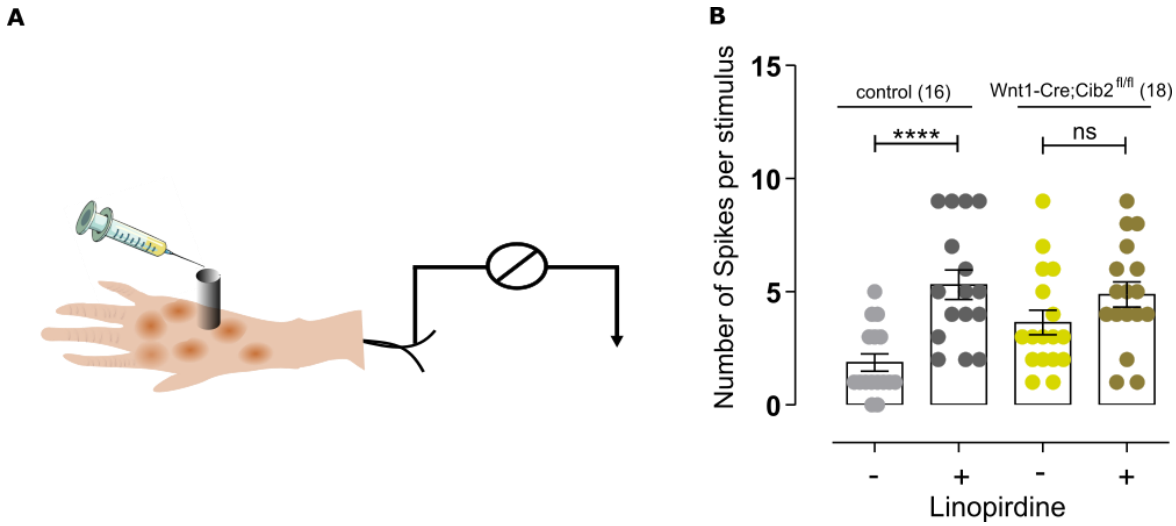

Figure 17. CIB2 is modulating KCNQ4. *A.* Illustration of *ex vivo* skin nerve with ring and linopirdine ***B***. Linopirdine effect in *Wnt1-Cre; Cib2* $^{fl/fl}$ was absent (Wilcoxon paired t-test ****P<0.0001)

KChiP proteins alter the kinetics of Kv4.2 currents (An et al., 2000) and therefore, CIB2 could similarly alter KCNQ4 function. Thus, I aimed to validate this hypothesis by testing if in the presence of CIB2 the biophysical properties of KCNQ4 in a heterologous system can be altered. For this purpose, I performed whole-cell patch clamp in a CHO cell line upon transient overexpression of CIB2 and KCNQ4. I used CHO cells since they show the following properties: an efficient exogenous expression of recombinant proteins, very low endogenous ionic currents, and good compatibility with patch-clamp (Gamper et al., 2005). I constructed a plasmid with the *Cib2* gene conjugated to a DSredMax fluorescence reporter, and another one with the *KCNQ4* gene conjugated to a GFP marker (Fig. 18A). I focused on the current density, resting membrane potential, and deactivation time and tested if CIB2 overexpression could alter these KCNQ4 properties. I used an activation protocol of test pulses of 10 mV steps from a holding potential of -20 mV in a voltage range from -60 up to +80 mV for 800 ms. The current density was analyzed from the ratio of peak current amplitude to the cell membrane capacitance (pA/pF). Deactivation properties were characterized by measuring the tail currents.

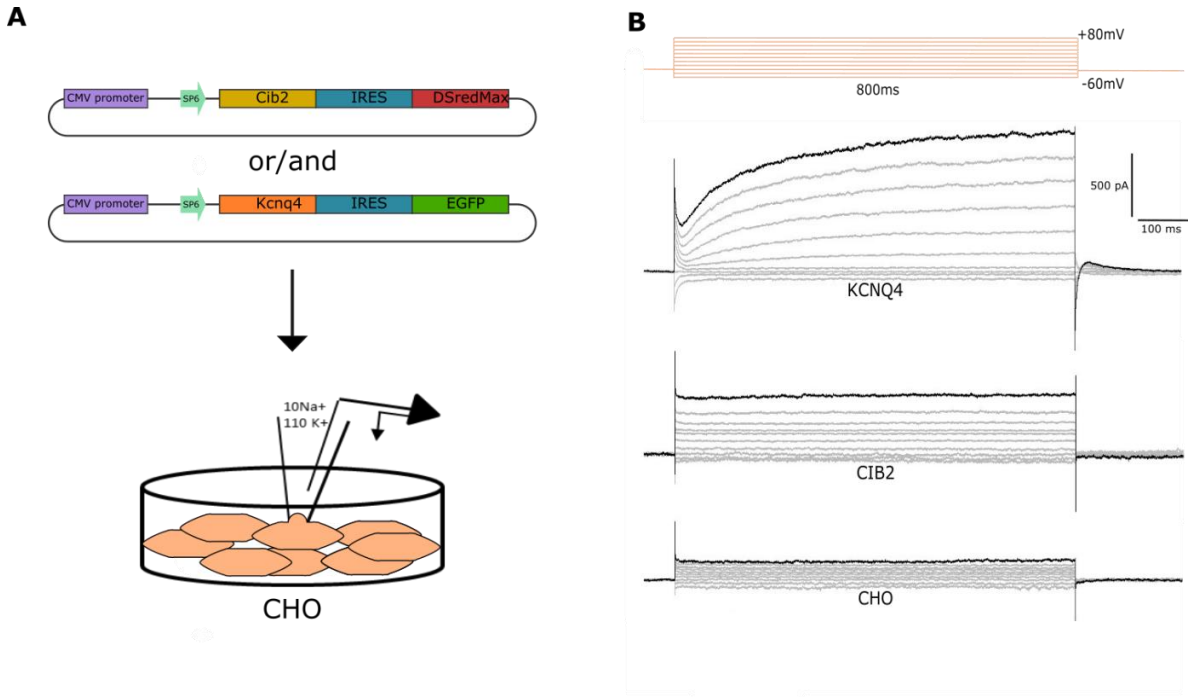

Figure 18. A. Scheme of the plasmids encoding for *Cib2* and *KCNQ4* and the CHO cells in a petri dish. **B.** Patch-clamp protocol and representative traces of K^+ currents in CHO cells (lower panel; CHO control, middle panel; cells were transfected with *Cib2*, upper panel; cells were transfected with *KCNQ4* plasmid.

When KCNQ4 was overexpressed, cells showed an increase in the outward currents which were significantly higher than the CHO endogenous K^+ currents. The I-V curve of KCNQ4 presented an activation threshold at around -40 mV and the mean current density was 10 ± 3 pA/pF which was 5-fold higher than in control cells (Fig. 19A). KCNQ4 overexpressing cells were 50% less depolarised in comparison to control cells (Fig. 19B). CHO cells overexpressing CIB2 exhibit a mean current density of 6 ± 2 pA/pF which was a 3-fold increase from the endogenous currents. Interestingly, the currents in CIB2 overexpressing cells were characteristically different from the KCNQ4 K^+ currents, which indicates that CIB2 is affecting endogenous K^+ channels of CHO cells (Fig. 19A). Co-transfection of the *KCNQ4* with the *Cib2* did not show any difference in the current density in comparison to currents derived from cells that expressed KCNQ4 only. The deactivation time of the KCNQ4 channel was 1 ± 0,25 ms. Upon overexpression of CIB2, KCNQ4 exhibits a threefold longer deactivation time (3,3 ± 0,83 ms) indicating that the channels close slower in the presence of CIB2 (Fig. 19C). These results show that CIB2 can alter the kinetics of the KCNQ4. CIB2 was unable to directly increase KCNQ4 current density. However, there is also a possibility of interference from endogenous CIB2 present in CHO cells, therefore creating a ceiling effect of CIB2-mediated KCNQ4 modulation. To rule out this alternative explanation, we would perform, siRNA experiments and knock down the *Cib2.*

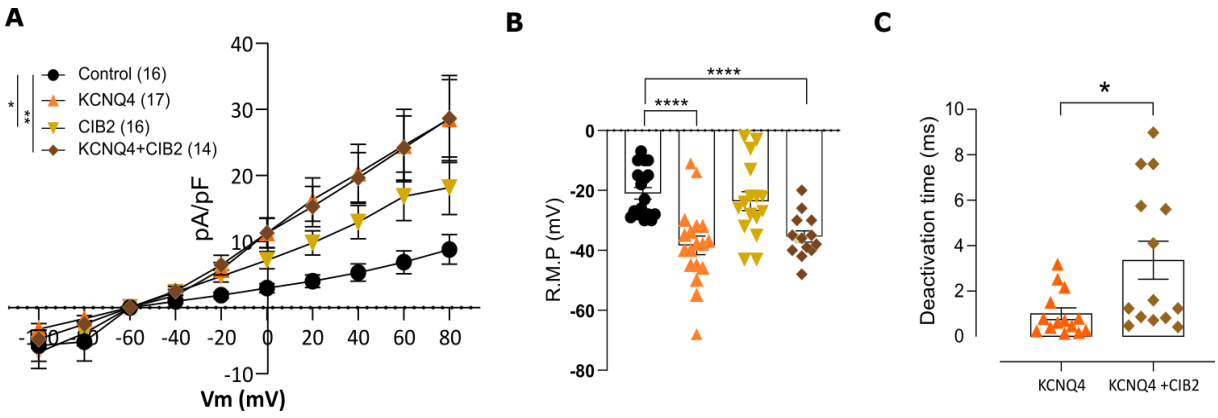

Figure 19. Whole-cell patch-clamp recordings from CHO cells. transfected with *Cib2, KCNQ4,* or *Cib2* and *KCNQ4* together, compared with non-transfected cells. A. Current density-voltage (I-V) curve for potassium currents (two-way ANOVA with Sídák post hoc analysis, **P= 0,0020), *P= 0,0262 **B.** Resting membrane potential (Unpaired t-test with Welch's correction ****P<0.0001) **C.** Deactivation time (unpaired t-test with Welch's correction, *P=0,0164)

7.7 Behavioural assessment of *Wnt1-Cre; Cib2$^{fl/fl}$* mice

Based on our skin-nerve electrophysiology data, we hypothesized that CIB2 has a behavioural impact on light touch and noxious stimulus detection. Innocuous mechanical stimuli were assessed by stroking the hind paw with a cotton swab/brush or applying tape on the back of the mouse. Mechanical nociceptive stimuli were applied and assessed by paw withdrawal responses using von Frey filaments. Interestingly, *Wnt1-Cre; Cib2$^{fl/fl}$* mice showed a decrease in the number of attempts and duration for removing the tape compared to the responses measured from the control mice (Fig. 20A, B). In addition, the percentage of paw withdrawal responses after stroking with cotton swab was also significantly lower in *Wnt1-Cre; Cib2$^{fl/fl}$* mice (Fig. 20C). No difference was observed after brush stimuli between mutant and control mice (Fig. 20D). Paw withdrawal responses were also assessed in response to a set of von Frey filaments of increasing force. However, the 50% paw withdrawal threshold was not significantly different between *Wnt1-Cre; Cib2$^{fl/fl,}$* and control mice, although mechanical thresholds in the mutant mice were slightly higher (Fig. 20E). Finally, a digging assay was performed. Digging is a natural behaviour together with burrowing and has been used to assess the well-being of the mouse and therefore, pain-like behaviours (Deacon, 2006; Jirkof, 2014; Shepherd et al., 2018; Chakrabarti et al., 2018). However, measuring the times that the mice were digging, I did not observe any difference between *Wnt1-Cre; Cib2$^{fl/fl}$* and control mice (Fig. 20F). These results suggest that the *Wnt1-Cre; Cib2$^{fl/fl}$* mice have an impaired ability to detect innocuous mechanical stimuli.

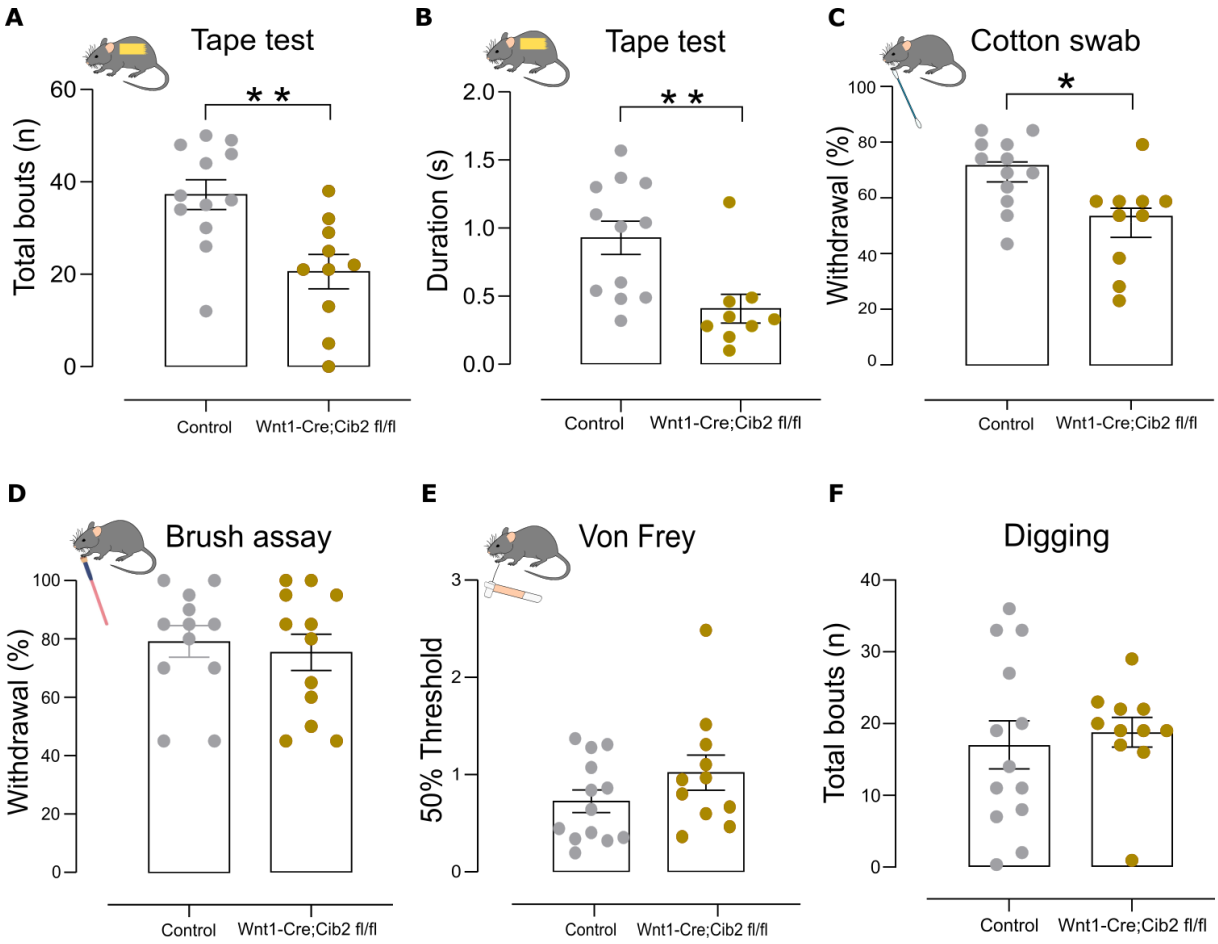

Figure 20. *Wnt1-Cre; Cib2$^{fl/fl}$* mice develop defects in innocuous touch sensation in behavioural assays. A. Number of tape bouts. (Unpaired t-test with Welch's correction, **P= 0,0032) **B.** Duration response in tape assay. (Unpaired t-test with Welch's correction, **P= 0,0045) **C, D**. Percent response to a cotton swab and brush stroke on the hind paw, respectively (Unpaired t-test with Welch's correction, *P= 0,0113) **E.** Mechanical threshold measured of a range of Von Frey filaments **F**. Digging assay. (Unpaired t-test with Welch's correction)

7.8 Electrical search in *Wnt1-Cre; Cib2$^{fl/fl}$* mice

The results from the behavioral assessment in *Wnt1-Cre; Cib2$^{fl/fl}$* mice showed an impairment of detection of innocuous touch in comparison to control mice, which was contrary to the observed increased sensitivity of RAMs. Therefore, I wanted to assess if this observation is due to a general decrease in the mechanosensitivity of Aβ-fibres. Thus, I performed an electrical search protocol of isolate Aβ-fibres and then assess if the same afferents can be also activated mechanically (Fig. 21A). Remarkably, 50% of the units; which fall in the Aβ-fibre category, according to their conductance velocity, were not responsive or responded with one spike and then became silent (tap units) (Fig. 21B): These results indicate that CIB2 is

important for mechanotransduction in a subset of Aβ-fibres as in *Wnt1-Cre; Cib2*$^{fl/\ fl}$ mice half of the Aβ-fibres lose their mechanosensitivity. Thus, these data along with our skin-nerve data described above suggest that deletion of *Cib2* in the peripheral somatosensory system has two seemingly opposite effects; On one hand lack of *Cib2* in RAMs leads to

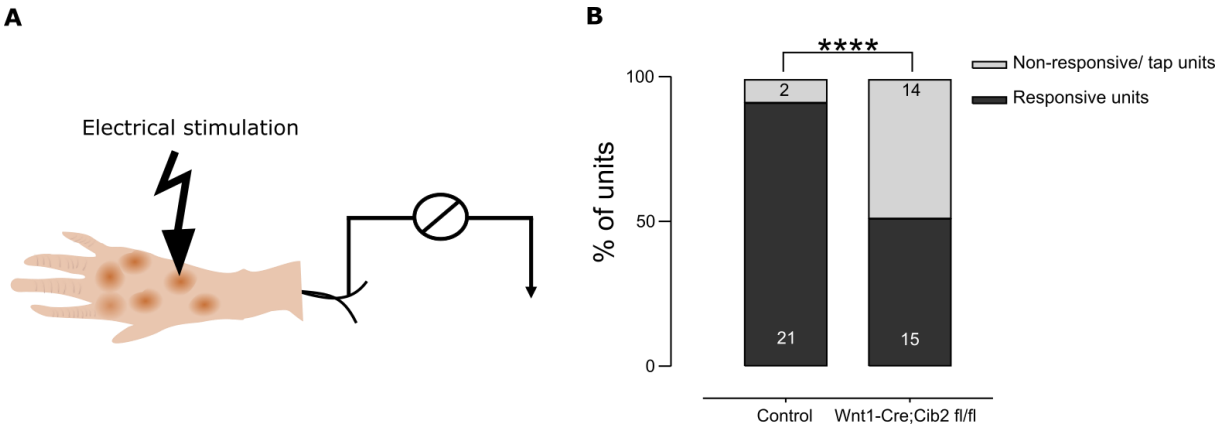

Figure 2110. *Wnt1-Cre; Cib2*$^{fl/\ fl}$ mice exhibit 50% of silent or tap units. A. Illustration of electrical stimulation in an *ex vivo* skin nerve preparation. **B.** Quantification of the percentage of units responding mechanically upon electrical stimulation in *Wnt1-Cre; Cib2*$^{fl/\ fl}$ and control mice (χ^2 test, ****P<0.0001)

8 Discussion

Hearing and touch are two distinct senses that rely on the conversion of mechanical force into electrical impulses in a process called mechanotransduction. Among all senses, the mechanism of mechanotransduction is important only for the somatosensory and auditory systems. Taste and olfaction respond to chemical stimuli and vision to light using a biochemical signal transduction cascade. On the other hand, hearing and touch detect mechanical stimuli from the environment. This could explain the expression of common genes in these two systems (Frenzel et al., 2012; Usoskin et al., 2015). Many of these genes have been discovered to contribute to hearing and touch in similar or opposite ways, implying a shared mechanism (de Nooij et al., 2015; Frenzel et al., 2012; Heidenreich et al., 2011, p. 4; Schwaller et al., 2021). Thus, finding more common genes will help us untangle the shared procedures manifest in auditory and touch and may facilitate the research of hearing disorders and fundamental biological understanding of mechanotransduction.

Here in this study, we investigate the role of the hearing gene, Calcium- and integrin-binding protein 2 (*Cib2*) in the somatosensory system. *Cib2* deficiency has been linked to isolated deafness, DFNB48, Usher syndrome type-IJ and plays an important role in mechanotransduction in the auditory system (Giese et al., 2017; Michel et al., 2017; Riazuddin et al., 2012; Y. Wang et al., 2017). In hair cells, CIB2 is distributed over the entire length of the stereocilia and gathered at the very tips of the shortest where the mechanotransduction complex is located (Giese et al., 2017). In a single-cell RNA sequencing study, *Cib2* was also found to be expressed in a subset of DRG sensory neurons (Usoskin et al., 2015). Recent studies have demonstrated that CIB2 is an auxiliary subunit of the mechanotransduction channel in worms and mice, that regulates channel function and affects its localization (Jeong et al., 2022; Liang et al., 2021). Thus, given the expression pattern of *Cib2* in DRG neurons, its role in the fundamental procedure of mechanotransduction, and its evolutionary-conserved role, we hypothesize a potential role for CIB2 also in the somatosensory system.

Transcriptomic data from DRG neurons showed the expression of *Cib2* in NF2 and NF3 clusters (Usoskin et al., 2015), which also include neurofilament-heavy chains associated with low threshold mechanoreceptors. In addition, in the same study, the mRNA of *Cib2* was also found in the cluster associated with peptidergic nociceptors, while a smaller amount was found in the TH cluster that corresponds to C-LTMRs. We verified these findings at the protein level, demonstrating that CIB2 protein is mostly found in peptidergic nociceptors using TRKA and TRPV1 as markers, as well as in a subgroup of mechanoreceptors expressing NF200 and TRKC. CIB2 was also present in the terminal endings of sensory neurons that innervate

specialized skin end organs. CIB2 was found in myelinated nerve fibers in the skin, where it co-localized with neurofilament-200 (NF200, a marker of myelinated sensory axons). Furthermore, CIB2 was present at cutaneous mechanosensory organs innervated by rapidly adapting Aβ-fibers mechanoreceptors (RAMs), which include Meissner corpuscle afferents, and hair follicle endings. However, *Cib2* was not detected in the Merkel cell-neurite complex, which is innervated by slowly adapting Aβ-fibers mechanoreceptors (SAMs). Notably, CIB2 protein was also detected in axons where NF200 was not expressed and was not associated with any obvious structure, which could be free endings of nociceptors reaching the skin. Its location, especially at regions close to RA mechanoreceptors, indicated a function for CIB2 in mechanotransduction or receptor potential modulation.

8.1 Regulation of RAMs by CIB2

RAMs are tailored to detect dynamic skin deformation, vibrations, and movement of individual hair follicles, depending on the end-organ they innervate (A. G. Brown & Iggo, 1967). Their responses are restricted to the stimulus's dynamic phase and they are insensitive to static indentation. RAMs are associated with guard and Awl/auchene hairs in the hairy skin, forming lanceolate structures parallel to the hair follicle's axis. RAMs also innervate Meissner's corpuscles in glabrous skin, which are activated by low-frequency vibrations (80 Hz) (Handler & Ginty, 2021). CIB2 was found in these structures, and *ex vivo* skin nerve experiments demonstrated that the CIB2 protein controls RAM responses. RAM firing rates represent velocity and they infrequently react to slow ramp stimuli. However, in mice lacking CIB2, RAMs responded to such stimuli and exhibited between three-and five-fold higher firing frequencies. The latencies measured during the ramp phases were shorter in the *Cib2* mutant compared to the control mice, reflecting a lower force threshold. Furthermore, *Cib2* conditional knockout mice displayed enhanced firing at 5 and 25 Hz but not at 50 Hz. Therefore, it seems that the presence of CIB2 sets the threshold for vibration detection in RAMs, such that low-frequency sinusoids < 50 Hz are less susceptible to detection than higher frequencies. High-frequency vibration <300Hz can be detected from Pacinian corpuscles associated with type II RAMs (Schwaller et al., 2021). These receptors are mostly found on the mouse's long bones' interosseous membrane. Due to technical limitations, we did not investigate the expression of CIB2 nor its role in these structures. However, the unchanged responses at 50 Hz vibration stimuli across control and mutant animals, on the other hand, demonstrate that CIB2 is essential for establishing vibration threshold at lower frequencies.

The elevated RAM firing responses might be explained by a lack of adaptation when *Cib2* is absent. Activation of voltage-gated inward currents at the point of impulse generation may enhance the length and size of the receptor potential (Hao et al., 2015). RAMs are tightly regulated by potassium channels, which play a critical role in their rapid adaptation to stimuli. This is evident from the voltage-gated channel expression pattern in the RAM sensory neuron subtype, where multiple potassium channel families are highly expressed in RAMs (Zheng et al., 2019). CIB2 is structurally similar to KChIP proteins (Liang et al., 2021). KChIP proteins, like CIB2, can bind both Ca^{2+} and Mg^{2+} through their EF hands. Furthermore, KChIP proteins are integral components of Kv4 channels and modulate their trafficking and kinetics by binding to their cytoplasmic N termini (An et al., 2000; K. Wang, 2008; Zhou et al., 2004). This led us to hypothesize that CIB2 influences RAM adaptation by interacting with and regulating a potassium channel.

Interestingly, previously in our lab, the significance of the KCNQ4 potassium channel in RAM responses has already been established (Heidenreich et al., 2011). KCNQ4 belongs to a group of five proteins that contribute to M-currents and control excitability in a range of central and peripheral neurons (Jentsch, 2000). Mice with *KCNQ4* mutations have a depolarized resting membrane potential closer to the action potential firing threshold, resulting in increased RAM firing responses; This appears to be a similar phenotype to that of RAMs from *Wnt1-Cre; Cib2*$^{fl/\ fl}$ mice. As a result, we tested the idea that was proposed that CIB2 may control the function of KCNQ4 in RAMs. *In situ* hybridization tests using RNAScope revealed that 60% of *Cib2* positive neurons also expressed *KCNQ4*. Linopirdine, a KCNQ4 inhibitor, caused enhanced RAM responses in extracellular recordings. The same inhibitor treatment had no effect on their responses in *Wnt1-Cre; Cib2*$^{fl/\ fl}$ mice. These findings imply that KCNQ4 does not function effectively in RAMs lacking CIB2. Because KChIP proteins modulate the kinetics of the kv4 channel, we attempted to assess the influence of CIB2 on the kinetics of KCNQ4 currents. In a heterologous system, we measured the current density, deactivation time, and resting membrane potential of KCNQ4 after CIB2 overexpression. The expression of KCNQ4 in combination with CIB2 influenced the deactivation time of KCNQ4, which was significantly slower, suggesting that CIB2 may modify the electrophysiological characteristics of KCNQ4. In the presence of CIB2, the current density of potassium currents remained unchanged. While the CHO cell line is a suitable model for ion channel investigations (Gamper et al., 2005), RNA-Seq Data has shown that there is significant endogenous CIB2 expression in CHO cell line (Singh et al., 2018), which might interfere and generate a ceiling effect of CIB2 mediated KCNQ4 regulation. We could do siRNA tests and knock down the endogenous *Cib2* to rule out this alternative interpretation. Although CHO cells had very low endogenous K^+ currents, when CIB2 was overexpressed, the current density of potassium currents rose dramatically.

These currents have distinctive properties from those of KCNQ4 currents, showing that CIB2 potentially controls additional potassium channels that are endogenously expressed in this cell line. An intriguing experiment would be to assess the membrane potential and potassium currents in isolated DRG neurons from *Cib2* mutant mice and determine whether the *Cib2* mutant DRG neurons are more depolarized than sensory neurons taken from control animals. KChIP proteins are known to affect kv4 surface expression and assembly. Furthermore, it was recently shown that CIB2 influences the positioning of the hair cell TMC1/2 mechanosensitive protein at the tip of stereocilia (Liang et al., 2021). Thus, CIB2 may function by maintaining channel transport and retention at the membrane. Therefore, KCNQ4 protein localization should be assessed in *Cib2* knockout mice.

KCNQ4 in the auditory system (Kharkovets et al., 2000). *KCNQ4* gene mutations cause autosomal dominant progressive deafness (DFNA2). KCNQ4 is involved in basolateral K^+ conductance, which is required for both electrical excitation and regulation of intracellular K^+. Prolonged K^+ excess leads to the degeneration of these cells (Kubisch et al., 1999). This might explain why DFNA2 mutations cause progressive hearing loss. The expression of CIB2 in hair cells was critical for the functioning and retention of stereocilia since the protein's absence significantly disturbs the staircase structure of the hair bundle. This resulted in deafness in mice and the elimination of mechanotransduction in auditory hair cells. CIB2 binds to the primary pore-forming unit TMC1/2 and is required for the mechanotransduction channel to function properly. Although interaction with KCNQ4 and modulation by CIB2 in hair cells have not been explored, it seems that CIB2's involvement in hair cells is centered on the mechanotransduction complex. Furthermore, CIB2 localization has been found along the stereocilia especially at the tip of the shorter stereocilia while KCNQ4, is localized in the basal membrane of outer mechanosensitive hair cells, making an interaction unlikely.

In our findings, CIB2 do not seem to regulate slowly adapting Aβ-fiber mechanoreceptors (SAMs) or contribute to their excitability. Merkel cells, which are keratinocyte-derived epidermal cells, are associated with SAM terminals. Maksimovic and colleagues (2014) demonstrated that optogenetic stimulation of Merkel cells causes slow adapting firing activity in Aβ-fibers. Both Merkel cells and terminal afferents contribute to the two distinct stages following observed upon indentation and stimulation of the complex. Sensory afferents carry out dynamic signals, whilst Merkel cells are tuned to detect static signals (Maksimovic et al., 2014). *Cib2* conditional knockout mice are absent in cells derived from the neural crest. As Merkel cells do not derive from neural crest but from epidermal lineage (Morrison et al., 2009)

our model cannot thoroughly study the function of CIB2 in these structures. However, in our immunostainings, CIB2 protein was not expressed or associated with Merkel cells.

The CIB2 protein may interact with and regulate other potassium channels involved in mechanosensation. Each sensory neuron subtype has a unique pattern of potassium channel expression, which supports subtype-specific intrinsic membrane properties and firing patterns (Du & Gamper, 2013; Zheng et al., 2019). The potassium current in Aβ-fibres is governed by the Kv1 and Kv3 channel families, which account for more than 80% of the total potassium current (Zheng et al., 2019). One research found that inhibiting Kv1 channels increased the firing of dynamic responses to velocity stimuli in Aβ-fibres, which we also found in our data. However, the impact was significantly weaker as compared to the fibre responses of CIB2 conditional knockout animals, and the mechanical threshold remained unchanged (Hao, Padilla, et al., 2013). However, CIB2 may control other potassium channels whose functions are unknown.

CIB2 interacts with the mechanosensory hair cell channel TMC1/2 and acts as an auxiliary subunit of the mechanotransduction complex (Jeong et al., 2022; Liang et al., 2021), raising the possibility of an interaction with a mechanosensitive channel in the somatosensory system. Indentation of the membrane of sensory neurons with a piezoelectric-driven blunt glass pipette during whole-cell recording is one of the most common techniques for analyzing mechanosensitive currents (Hao, Ruel, et al., 2013; Hu & Lewin, 2006)."Poking" experiments in isolated DRG neurons from CIB2 conditional knockout mice were performed to investigate the impact of CIB2 on mechanosensitive currents by Dr. Chakrabarti Sampurna in our lab. These preliminary data showed a lack of mechanosensitive currents or, in some cases, currents that did not follow the increasing stimuli but rather stayed the same or disappeared. As the number of neurons that were tested was really low, statistical analysis was not able to be performed. More experiments with DRG neurons from *Cib2* conditional knockout and control mice should be conducted to test the role of CIB2 in mechanosensitive currents.

TMC1/2 is expressed in DRG sensory neurons, albeit at low levels, and its significance in the somatosensory system is unknown (Sharma et al., 2020; Usoskin et al., 2015). A large proportion of DRG neurons express PIEZO2 channels, which convert mechanical inputs into mechanosensitive currents (Coste et al., 2010). PIEZO2 is found in the nerve terminals of sensory neurons that innervate both hairy and glabrous skin and functions as one of the primary mechanosensitive channels in LTMRs (Ranade et al., 2014). Mammalian PIEZO2 channels are voltage-regulated (Moroni et al., 2018), and mammalian PIEZO2 channel inactivation is voltage-dependent, with the channels inactivating slower or not at all at positive holding voltages compared to negative voltages. *Piezo2* gain of function mutations has

recently been studied in our group. These mutations cause a voltage relief in this channel, resulting in an enhanced open probability (Sánchez-Carranza O, thesis 2021). RAMs with these mutations exhibit stronger mechanosensitivity, with higher firing rates and vibrating sensitivity, almost similar to RAMs from *Cib2* mutant animals. Thus, by altering its voltage sensitivity, CIB2 might interact with PIEZO2 and function as a break in these channels, raising the activation and open probability thresholds. Future research might test this hypothesis by co-expressing *Cib2* and *Piezo2* in a heterologous system and measuring the impact of CIB2 on PIEZO2 mechanosensitivity.

8.2 Increased excitability in nociceptors from *Wnt1-Cre; Cib2$^{fl/fl}$* mice

Nociceptors protect mammals from potentially harmful or noxious stimuli and tissue damage. They are linked to thinly myelinated Aδ or C fibers and are tuned to detect painful stimuli such as noxious mechanical pressure, and chemical changes such as inflammatory cytokines, pH, and temperature (Smith & Lewin, 2009). Nociceptors exhibit high detection thresholds for mechanical stimuli. In this study, we discovered that CIB2-positive DRG neurons express a high level of nociceptive markers. TRPV1, which is triggered by noxious heat, pH, and capsaicin, was co-stained in 60% of the CIB2+ neurons, whereas TrkA (a high-affinity NGF receptor) was co-stained in 70%. TrkA and TRPV1 are mostly expressed in peptidergic nociceptors, indicating that cib2 is predominant in this subgroup of nociceptors. This discovery is consistent with the evidence from single-cell RNA sequencing and single-cell transcriptome analysis (Sharma et al., 2020; Usoskin et al., 2015). Furthermore, these results led us to test whether CIB2 plays a significant role in nociception. We studied the responses of Aδ and C nociceptors in conditional CIB2 knockout mice using the *ex-vivo* skin nerve approach. We used a series of increasing mechanical indentations. Typical nociceptors produce activity only during the static phase of stimulation and have slowly adapting features (Garell et al., 1996). We did not observe variations between the two genotypes in C or Aδ nociceptors during the static phase. Furthermore, the mechanical threshold for activation was unchanged. These findings suggest that CIB2 does not regulate the sensitivity of these kinds of nociceptors. However, we found a considerable increase in after-charge firing in C-fibers lacking the CIB2 protein. This result was not seen before the initial stimulation, showing that these fibers are not firing spontaneously but rather fail to stop firing after stimulus offset.

C-fibers have high expression of sodium channels such as Nav 1.8 and Nav1.9 that regulate their excitability (Zheng et al., 2019). However, nociceptors also express and are controlled

by potassium channels (Ocaña et al., 2004; Tsantoulas & McMahon, 2014). Thus, CIB2 may interact with a potassium channel in c-fibers, which modulates their excitability. Notably, the expression of KCNQ family members is expressed in small-diameter neuron subtypes and plays an important role in modulating the excitability of nociceptive neurons (Passmore et al., 2003). The activation of KCNQ2 channels by retigabine substantially and specifically lowers responses of nociceptive neurons in the rat dorsal root ganglia, a result that persists after nerve damage and provides analgesic activity in an animal model of inflammatory pain. Because the M-current is the major subthreshold current in small sensory neurons, it has a considerable influence on their excitability (Passmore et al., 2003). Furthermore, immunostaining for KCNQ2 reveals its expression in the peripheral terminals of nociceptive primary afferents (Passmore et al., 2012). CIB2 could regulate KCNQ2 function in nociceptors, and the lack of this M-channel may result in a lower threshold for spike formation and a preference for the generation of repetitive bursts of action potentials following the stimulus. Similar to our hypothesis for KCNQ4, CIB2 could modulate the location and kinetics of KCNQ2 channels in nociceptors.

Furthermore, DRG neurons express a variety of K^+ channels associated with nociception, including members of the Kv1 family. The excitability of c-fibers was shown to be regulated by the Kv1.1 mechanosensitive potassium channel. Kv1.1-1.2 raises the mechanical threshold for firing and shortens the duration of mechanically produced AP discharges. Thus, Kv1.1 controls generator potential by regulating the activity of mechanosensitive excitatory channels. In the same study, it was found that Kv1.1 inhibition could cause mechanical allodynia (Hao, Padilla, et al., 2013). However, Kv1.1 mutant mice did not display ongoing responses after stimulus as reported in our experiments, indicating that the CIB2 function may not occur via this channel.

PIEZO2 has recently been discovered to have a significant function in nociception. PIEZO2 is expressed in a large proportion of small neurons that express transient receptor potential cation channel V1 (TRPV1) and the PIEZO2 channel is required for mechanical allodynia in mice and humans (Eijkelkamp et al., 2013; Murthy, Loud, et al., 2018; Szczot et al., 2018). Recent findings in our lab on *Piezo2* gain of function mutations showed that the PIEZO2 channel plays a role in nociception. These mutations showed enhanced after-stimulus responses, similar to our findings with *Cib2* conditional knockout mice. Furthermore, nociceptors with a gain of function mutations had considerably lower mechanical thresholds for activation and enhanced static and ramp responses when compared to the wild type (Sánchez-Carranza O, thesis 2021). Although the impact of CIB2 in C-fibers is milder than that of PIEZO2, interaction and control of CIB2 with PIEZO2 is possible. StomL1 and StomL3 are known to modulate PIEZO2 activity by sensitizing PIEZO ion channel activity (Poole et al.,

2014). CIB2 may have an opposing regulating impact on PIEZO2 mechanosensitive channels, acting as a break in PIEZO2 sensitivity in both RAMs and c-fibers. The milder impact seen in C-fibers compared to the *Piezo2* mutation might be explained by PIEZO2 control by other molecules in these cells. Another possibility might be that additional members of the CIB family are expressed in C-fibers to compensate for the loss of CIB2; as was seen in hair cells (Liang et al., 2021; Sharma et al., 2020).

Abdo and colleagues (2019) have recently identified the nociceptive glia-neurite complex, which consists of epidermal Schwann cells creating a mesh-like network in tight functional interaction with what were previously thought to be free terminals of nociceptive sensory neurons (Abdo et al., 2019). Nociceptive Schwann cells serve as a staging point between noxious stimuli and terminal endings, are mechanosensitive, and are able to convey nociceptive information (Abdo et al., 2019). In our immunostaining, CIB2 did not co-localize with s100 staining, a marker for Schwann cells, suggesting that CIB2 does not play a function in these structures and that the finding we detect in nociceptor is likely associated with the axon rather than these end-organ like complexes.

8.3 Light-touch detection deficiency in *Wnt1-Cre; Cib2$^{fl/fl}$* mice

More prominent peripheral mechanoreceptor activation could translate into more pronounced behavioral responses to mechanical stimuli, so we sought to assess what were the behavioral consequences of peripheral *Cib2* deficiency in light touch. To our surprise, *Cib2* mutant mice were less able to detect innocuous touch compared to controls. Innocuous mechanical stimuli were applied to the glabrous skin of the mice with a dispersed cotton swab by softly stroking the bottom of their paws. In comparison to the control, *Cib2* mutant mice reacted significantly less to dynamic stroke. We also examined how *Wnt1-Cre; Cib2$^{fl/fl}$* mice reacted to mechanical stimuli applied to hairy skin. Therefore, a tape response assay to monitor the response of mice to adhesive tape attached to their backs was used. For the most part, *Wnt1-Cre; Cib2$^{fl/fl}$ mice* ignored the tape, and the overall number and length of efforts to remove the tape were much more reduced compared to control mice. These results contradicted our expectations based on our findings in *ex-vivo* experiments. The *Wnt1-Cre; Cib2$^{fl/fl}$* mice used in this work lack cib2 protein in cells derived from the neural crest, hence *Cib2* ablation occurs in sensory neurons and glial cells. Thus, the behavioral impact of *Cib2* mutant mice resulted from cib2's contribution from the periphery. We wanted to see whether this impact is related to a loss of mechanosensitivity of sensory fibers in the skin, so we performed an electrical search

experiment in *ex-vivo* skin nerve preparation to search for mechanically insensitive fibers (Ranade et al., 2014). 50% of the Aβ-fibers showed no detectable mechanosensitivity, compared to less than 10% of Aβ-fibers from the control mice. These findings imply that about half of the Aβ-fibers have lost their mechanosensitivity, which might affect the mouse's sense of light touch. Mutations in the *Cib2* gene induced hearing loss in humans and mice, which is due to CIB2 function as a regulator of both the assembly and activity of the mechanotransduction channel complex in hair cells. As previously stated, CIB2 proteins are structurally similar to another calcium sensor, KChIP proteins. Furthermore, the interaction of CIB2 with TMC1/2 is similar to that of KChIP proteins with Kv4 channels. We have shown that CIB2 regulates and maybe interacts with the KCNQ4 channel. Given the effect of CIB2 on TMC1/2 localization in stereocilia, the suggested explanation is that CIB2 interacts with KCNQ4 and monitors its surface location. The lack of mechanosensitivity of the aβ-fibers is associated with the dysfunction of a mechanosensitive channel. One potential explanation is that CIB2 regulates the location of a mechanosensitive channel in these fibers. PIEZO2 is a major mechanotransducer in LTMRs, and mice lacking *Piezo2* display 50% insensitive Aβ-fibers. Thus, CIB2 might interact with PIEZO2 and regulate its appropriate surface positioning and assembly.

8.4 Mild decrease of sensitivity to stimulus-evoked pain-like behavior in *Wnt1-Cre; Cib2$^{fl/\ fl}$* mice

To explore the role of CIB2 in mechanical pain sensitivity *in vivo*, we used a von Frey test where we examined paw withdrawal in response to punctate stimulation. Paw withdrawal thresholds were slightly elevated but not significantly in *Wnt1-Cre; Cib2$^{fl/\ fl}$* mice. Furthermore, in the digging experiment, which was used to detect pain-like behaviors, *Wnt1-Cre; Cib2$^{fl/\ fl}$* mice behaved similarly to control mice, indicating that these mice did not display any severe pain behavior. These findings suggest that CIB2 has a small influence on nociception, which is more visible in the excitability of the C-fiber, but does not affect pain detection. The slight increase in the von Frey threshold might imply a minimal change in the mechanosensitivity of these fibers in *Cib2* mutant mice. It is possible that some proportion of nociceptors lost their mechanosensitivity in *Cib2* mutant mice similar to Aβ-fibres. However, in this study, we did not investigate mechanical insensitive nociceptors by electrical search.

Recently, Elkin channels were identified (Patkunarajah et al., 2020). Elkin channels were discovered in a melanoma cell line, and evoked currents from cells expressing this channel

resulted in mechanosensitive intermediate adapting currents (Patkunarajah et al., 2020). According to current findings in our lab, Elkin is expressed in sensory neurons and has a crucial role in mechanotransduction in the LTMRS. PIEZO2 contributes to only 50% of the responses of Aβ-fibres. Therefore, Elkin or other channels could be involved. Further research into the interaction with Elkin channels with CIB2 might reveal whether CIB2 regulates this channel, which is implicated in A and C fiber mechanosensitivity.

9 Conclusions

Several lines of evidence indicate that the senses of hearing and touch have similar molecular and genetic components. In a study, a subset of congenitally deaf young people showed considerably diminished touch sensitivity, and a cohort of individuals with mutations in the *USH2A* gene, which causes deaf-blindness or Usher syndrome, displayed low touch sensitivity (Frenzel et al., 2012). *USH2A* is involved in vibration sensitivity in humans and mice, according to electrophysiological investigations of this gene (Schwaller et al., 2021). Furthermore, *KCNQ4* deficiency induces deafness mostly by causing sensory hair cell degeneration; it instead improves touch sensitivity at low frequencies (Heidenreich et al., 2011; Kubisch et al., 1999). Additionally, *whirlin* which encodes for a PDZ-scaffold protein involved in sensory transduction in auditory hair cells is also expressed by proprioceptive sensory neurons (de Nooij et al., 2015). Mice lacking *whirlin* in proprioceptors exhibit a reduction in stretch-evoked firing frequency (de Nooij et al., 2015).

In this study, we have shown that another hearing gene is essential for the appropriate function of the somatosensory system and mechanotransduction. We hypothesize that the CIB2 protein, like in the auditory system, is an auxiliary subunit of ion channels in the somatosensory system (potassium or mechanosensitive channels) ensuring their appropriate function and/or assembly. Therefore, CIB2 proteins play an important role in the mechanotransduction process.

10 Acknowledgments

The Ph.D. path has been the most challenging task I have ever experienced so far. It included excitement, disappointment, anxiety, pressure, tears, and laughter. It has made me more resistant, independent, and self-critical in both professional and personal aspects. I owe this to all the people I have been surrounded by who have inspired me and supported me.

First, I would like to express my gratitude to Prof. Dr. Gary Lewin for allowing me to pursue my Ph.D. in his lab. In particular, I want to thank Gary for sharing his knowledge of the field and enthusiasm with me and for many inspiring ideas and guidance. I appreciate that you always had an open door, but you also gave me the freedom to develop my ideas and skills.

I also would like to thank Prof. Dr. Ulrich Mueller for financially supporting my doctoral studies as well as mentoring me in the field of the auditory system.

I want to thank Ursula Koch for kindly agreeing to be my Doktormutter at the Freie Universität and evaluating my Ph.D. thesis.

I would also like to thank Dr. James Poulet and Dr. Niccolo Zampieri for being part of my committee meetings and helping me with their comments and suggestions for my project.

I thank all current and former members of the Lewin lab for technical and scientific support as well as for the funny moments and fruitful conversations inside and outside the lab.

I want to especially thank Dr. Jan Walcher for introducing me to the skin-nerve technique.

I thank Dr. Oscar Sanchez-Carranza (Oscar) for sharing his expertise in the patch-clamp technique and for being there from the start until the end.

Special thanks to Dr. Sampurna Chakrabarti (Sam) for many scientific discussions, and constructive criticisms which helped me finalize my thesis. I am also grateful for sharing with me her patch clamp rig.

I would like to thank my lovely Berlin family. This path would not be possible without you. A lot of dinners with nice food from Italy, Spain, and Greece, always with amazing wine. Exploring together what Berlin is made it more interesting and less boring. I especially want to thank Verus and Elisus for being such gracious hosts at their place. A lot of discussions, arguments, and laughs. Corona time would be (even more) a nightmare without you. Thank you, Silvi, for being an amazing flatmate and always being honest and loyal. Your food is almost as good as mine. Χρηστο thank you for being a good flatmate as well, but most importantly, you will always be my ΄΄διπλανος παγκος΄΄. The path of biology was much more fun, having you there from the very start. I also would like to thank Stephan for the discussions and many many

arguments that led to a good friendship. Thank you for always checking if I am alive when I disappear. You are all amazing scientists, but more importantly, you are great people.

To my friends who are far away, you always make me feel like I am there. Especially Ευη, Ναταλια, Παγωνα, Πενυ, Ρομινα you are great friends and support all these years. Special thanks to Ελενη, ευχαριστω που εισαι εκει χωρις να εισαι, που με καταλαβαινεις χωρις να μιλησω, που με κανεις να γελαω οταν θελω να κλαψω, που εισαι ο μονος ανθρωπος που μπορω να μιλαω μεχρι το πρωι και να εχω και αλλα να πω.

With all my heart, I would like to thank my family. Μαμα, Μπαμπα ευχαριστω που παντα με στηριζετε ακομα και ας ηταν δυσκολο. Εχετε βοηθησει σε πολλα σταδια αυτου του δυσκολου δρομου. Σας αγαπω. Γιαννη και Κατερινα ευχαριστω επισης. Η ζωη χωρις αδερφια θα ηταν βαρετη ακομα και οταν σου σπανε τα νευρα. Τελος ευχαριστω την Φλωρεντια που ειναι η μονη που ξερει απο την οικογενεια μου τι ακριβως κανω στο διδακτορικο μου. I love you all.

11 References

Abdo, H., Calvo-Enrique, L., Lopez, J. M., Song, J., Zhang, M.-D., Usoskin, D., El Manira, A., Adameyko, I., Hjerling-Leffler, J., & Ernfors, P. (2019). Specialized cutaneous Schwann cells initiate pain sensation. *Science (New York, N.Y.)*, *365*(6454), 695–699. https://doi.org/10.1126/science.aax6452

Abraira, V. E., & Ginty, D. D. (2013). The sensory neurons of touch. *Neuron*, *79*(4), 618–639. https://doi.org/10.1016/j.neuron.2013.07.051

Alagramam, K. N., Goodyear, R. J., Geng, R., Furness, D. N., van Aken, A. F. J., Marcotti, W., Kros, C. J., & Richardson, G. P. (2011). Mutations in Protocadherin 15 and Cadherin 23 Affect Tip Links and Mechanotransduction in Mammalian Sensory Hair Cells. *PLoS ONE*, *6*(4), e19183. https://doi.org/10.1371/journal.pone.0019183

Alonso-González, P., Cabo, R., San José, I., Gago, A., Suazo, I. C., García-Suárez, O., Cobo, J., & Vega, J. A. (2017). Human Digital Meissner Corpuscles Display Immunoreactivity for the Multifunctional Ion Channels Trpc6 and Trpv4. *Anatomical Record (Hoboken, N.J.: 2007)*, *300*(6), 1022–1031. https://doi.org/10.1002/ar.23522

An, W. F., Bowlby, M. R., Betty, M., Cao, J., Ling, H. P., Mendoza, G., Hinson, J. W., Mattsson, K. I., Strassle, B. W., Trimmer, J. S., & Rhodes, K. J. (2000). Modulation of A-type potassium channels by a family of calcium sensors. *Nature*, *403*(6769), 553–556. https://doi.org/10.1038/35000592

Arnadóttir, J., & Chalfie, M. (2010). Eukaryotic mechanosensitive channels. *Annual Review of Biophysics*, *39*, 111–137. https://doi.org/10.1146/annurev.biophys.37.032807.125836

Assad, J. A., Shepherd, G. M., & Corey, D. P. (1991). Tip-link integrity and mechanical transduction in vertebrate hair cells. *Neuron*, *7*(6), 985–994. https://doi.org/10.1016/0896-6273(91)90343-x

Ballesteros, A., Fenollar-Ferrer, C., & Swartz, K. J. (2018). Structural relationship between the putative hair cell mechanotransduction channel TMC1 and TMEM16 proteins. *ELife*, *7*, e38433. https://doi.org/10.7554/eLife.38433

Beaulieu-Laroche, L., Christin, M., Donoghue, A., Agosti, F., Yousefpour, N., Petitjean, H., Davidova, A., Stanton, C., Khan, U., Dietz, C., Faure, E., Fatima, T., MacPherson, A., Mouchbahani-Constance, S., Bisson, D. G., Haglund, L., Ouellet, J. A., Stone, L. S., Samson, J., … Sharif-Naeini, R. (2020). TACAN Is an Ion Channel Involved in Sensing Mechanical Pain. *Cell*, *180*(5), 956-967.e17. https://doi.org/10.1016/j.cell.2020.01.033

Bennett, D. L., Clark, A. J., Huang, J., Waxman, S. G., & Dib-Hajj, S. D. (2019). The Role of Voltage-Gated Sodium Channels in Pain Signaling. *Physiological Reviews*, *99*(2), 1079–1151. https://doi.org/10.1152/physrev.00052.2017

Berrier, C., Pozza, A., de Lacroix de Lavalette, A., Chardonnet, S., Mesneau, A., Jaxel, C., le Maire, M., & Ghazi, A. (2013). The purified mechanosensitive channel TREK-1 is directly sensitive to membrane tension. *The Journal of Biological Chemistry*, *288*(38), 27307–27314. https://doi.org/10.1074/jbc.M113.478321

Beurg, M., Barlow, A., Furness, D. N., & Fettiplace, R. (2019). A Tmc1 mutation reduces calcium permeability and expression of mechanoelectrical transduction channels in cochlear hair cells. *Proceedings of the National Academy of Sciences of the United States of America*, *116*(41), 20743–20749. https://doi.org/10.1073/pnas.1908058116

Beurg, M., Fettiplace, R., Nam, J.-H., & Ricci, A. J. (2009). Localization of inner hair cell mechanotransducer channels using high-speed calcium imaging. *Nature Neuroscience*, *12*(5), 553–558. https://doi.org/10.1038/nn.2295

Beurg, M., Goldring, A. C., & Fettiplace, R. (2015). The effects of Tmc1 Beethoven mutation on mechanotransducer channel function in cochlear hair cells. *The Journal of General Physiology*, *146*(3), 233–243. https://doi.org/10.1085/jgp.201511458

Beurg, M., Schimmenti, L. A., Koleilat, A., Amr, S. S., Oza, A., Barlow, A. J., Ballesteros, A., & Fettiplace, R. (2021). New Tmc1 Deafness Mutations Impact Mechanotransduction in Auditory Hair Cells. *The Journal of Neuroscience: The Official Journal of the Society for Neuroscience*, *41*(20), 4378–4391. https://doi.org/10.1523/JNEUROSCI.2537-20.2021

Beurg, M., Xiong, W., Zhao, B., Müller, U., & Fettiplace, R. (2015). Subunit determination of the conductance of hair-cell mechanotransducer channels. *Proceedings of the National Academy of Sciences of the United States of America*, *112*(5), 1589–1594. https://doi.org/10.1073/pnas.1420906112

Bird, E. V., Christmas, C. R., Loescher, A. R., Smith, K. G., Robinson, P. P., Black, J. A., Waxman, S. G., & Boissonade, F. M. (2013). Correlation of Nav1.8 and Nav1.9 sodium channel expression with neuropathic pain in human subjects with lingual nerve neuromas. *Molecular Pain*, *9*, 52. https://doi.org/10.1186/1744-8069-9-52

Blazejczyk, M., Sobczak, A., Debowska, K., Wisniewska, M. B., Kirilenko, A., Pikula, S., Jaworski, J., Kuznicki, J., & Wojda, U. (2009). Biochemical characterization and expression analysis of a novel EF-hand Ca2+ binding protein calmyrin2 (Cib2) in brain indicates its function in NMDA receptor mediated Ca2+ signaling. *Archives of Biochemistry and Biophysics*, *487*(1), 66–78. https://doi.org/10.1016/j.abb.2009.05.002

Bolz, H., von Brederlow, B., Ramírez, A., Bryda, E. C., Kutsche, K., Nothwang, H. G., Seeliger, M., del C-Salcedó Cabrera, M., Vila, M. C., Molina, O. P., Gal, A., & Kubisch, C. (2001). Mutation of CDH23, encoding a new member of the cadherin gene family, causes Usher syndrome type 1D. *Nature Genetics*, *27*(1), 108–112. https://doi.org/10.1038/83667

Booth, K. T., Kahrizi, K., Babanejad, M., Daghagh, H., Bademci, G., Arzhangi, S., Zareabdollahi, D., Duman, D., El-Amraoui, A., Tekin, M., Najmabadi, H., Azaiez, H., &

Smith, R. J. (2018). Variants in CIB2 cause DFNB48 and not USH1J. *Clinical Genetics*, *93*(4), 812–821. https://doi.org/10.1111/cge.13170

Bork, J. M., Peters, L. M., Riazuddin, S., Bernstein, S. L., Ahmed, Z. M., Ness, S. L., Polomeno, R., Ramesh, A., Schloss, M., Srisailpathy, C. R., Wayne, S., Bellman, S., Desmukh, D., Ahmed, Z., Khan, S. N., Kaloustian, V. M., Li, X. C., Lalwani, A., Riazuddin, S., … Morell, R. J. (2001). Usher syndrome 1D and nonsyndromic autosomal recessive deafness DFNB12 are caused by allelic mutations of the novel cadherin-like gene CDH23. *American Journal of Human Genetics*, *68*(1), 26–37. https://doi.org/10.1086/316954

Breitkreutz, D., Mirancea, N., & Nischt, R. (2009). Basement membranes in skin: Unique matrix structures with diverse functions? *Histochemistry and Cell Biology*, *132*(1), 1–10. https://doi.org/10.1007/s00418-009-0586-0

Brown, A. G., & Iggo, A. (1967). A quantitative study of cutaneous receptors and afferent fibres in the cat and rabbit. *The Journal of Physiology*, *193*(3), 707–733. https://doi.org/10.1113/jphysiol.1967.sp008390

Brown, D. A. (1988). M currents. *Ion Channels*, *1*, 55–94. https://doi.org/10.1007/978-1-4615-7302-9_2

Brown, D. A., & Adams, P. R. (1980). Muscarinic suppression of a novel voltage-sensitive K+ current in a vertebrate neurone. *Nature*, *283*(5748), 673–676. https://doi.org/10.1038/283673a0

Cabo, R., Alonso, P., Viña, E., Vázquez, G., Gago, A., Feito, J., Pérez-Moltó, F. J., García-Suárez, O., & Vega, J. A. (2015). ASIC2 is present in human mechanosensory neurons of the dorsal root ganglia and in mechanoreceptors of the glabrous skin. *Histochemistry and Cell Biology*, *143*(3), 267–276. https://doi.org/10.1007/s00418-014-1278-y

Cain, D. M., Khasabov, S. G., & Simone, D. A. (2001). Response properties of mechanoreceptors and nociceptors in mouse glabrous skin: An *in vivo* study. *Journal of Neurophysiology*, *85*(4), 1561–1574. https://doi.org/10.1152/jn.2001.85.4.1561

Cauna, N. (1956). Nerve supply and nerve endings in Meissner's corpuscles. *The American Journal of Anatomy*, *99*(2), 315–350. https://doi.org/10.1002/aja.1000990206

Cavanaugh, D. J., Lee, H., Lo, L., Shields, S. D., Zylka, M. J., Basbaum, A. I., & Anderson, D. J. (2009). Distinct subsets of unmyelinated primary sensory fibers mediate behavioral responses to noxious thermal and mechanical stimuli. *Proceedings of the National Academy of Sciences of the United States of America*, *106*(22), 9075–9080. https://doi.org/10.1073/pnas.0901507106

Chalfie, M. (2009). Neurosensory mechanotransduction. *Nature Reviews. Molecular Cell Biology*, *10*(1), 44–52. https://doi.org/10.1038/nrm2595

Chen, C.-C., & Wong, C.-W. (2013). Neurosensory mechanotransduction through acid-sensing ion channels. *Journal of Cellular and Molecular Medicine*, *17*(3), 337–349. https://doi.org/10.1111/jcmm.12025

Chesler, A. T., Szczot, M., Bharucha-Goebel, D., Čeko, M., Donkervoort, S., Laubacher, C., Hayes, L. H., Alter, K., Zampieri, C., Stanley, C., Innes, A. M., Mah, J. K., Grosmann, C. M., Bradley, N., Nguyen, D., Foley, A. R., Le Pichon, C. E., & Bönnemann, C. G. (2016). The Role of PIEZO2 in Human Mechanosensation. *The New England Journal of Medicine*, *375*(14), 1355–1364. https://doi.org/10.1056/NEJMoa1602812

Chung, W.-H., Kim, K. R., Cho, Y.-S., Cho, D.-Y., Woo, J. H., Ryoo, Z. Y., Cho, K. I., & Hong, S. H. (2007). Cochlear pathology of the circling mouse: A new mouse model of DFNB6. *Acta Oto-Laryngologica*, *127*(3), 244–251. https://doi.org/10.1080/00016480600827071

Corey, D. P., & Hudspeth, A. J. (1979). Response latency of vertebrate hair cells. *Biophysical Journal*, *26*(3), 499–506. https://doi.org/10.1016/S0006-3495(79)85267-4

Coste, B., Mathur, J., Schmidt, M., Earley, T. J., Ranade, S., Petrus, M. J., Dubin, A. E., & Patapoutian, A. (2010). Piezo1 and Piezo2 are essential components of distinct mechanically activated cation channels. *Science (New York, N.Y.)*, *330*(6000), 55–60. https://doi.org/10.1126/science.1193270

Cunningham, C. L., Qiu, X., Wu, Z., Zhao, B., Peng, G., Kim, Y.-H., Lauer, A., & Müller, U. (2020). TMIE Defines Pore and Gating Properties of the Mechanotransduction Channel of Mammalian Cochlear Hair Cells. *Neuron*, *107*(1), 126-143.e8. https://doi.org/10.1016/j.neuron.2020.03.033

Cunningham, C., O' Sullivan, R., Caserotti, P., & Tully, M. A. (2020). Consequences of physical inactivity in older adults: A systematic review of reviews and meta-analyses. *Scandinavian Journal of Medicine & Science in Sports*, *30*(5), 816–827. https://doi.org/10.1111/sms.13616

de Nooij, J. C., Simon, C. M., Simon, A., Doobar, S., Steel, K. P., Banks, R. W., Mentis, G. Z., Bewick, G. S., & Jessell, T. M. (2015). The PDZ-domain protein Whirlin facilitates mechanosensory signaling in mammalian proprioceptors. *The Journal of Neuroscience: The Official Journal of the Society for Neuroscience*, *35*(7), 3073–3084. https://doi.org/10.1523/JNEUROSCI.3699-14.2015

Delmas, P., & Brown, D. A. (2005). Pathways modulating neural KCNQ/M (Kv7) potassium channels. *Nature Reviews. Neuroscience*, *6*(11), 850–862. https://doi.org/10.1038/nrn1785

Delmas, P., & Coste, B. (2013). Mechano-gated ion channels in sensory systems. *Cell*, *155*(2), 278–284. https://doi.org/10.1016/j.cell.2013.09.026

Dib-Hajj, S. D., Black, J. A., & Waxman, S. G. (2015). NaV1.9: A sodium channel linked to human pain. *Nature Reviews. Neuroscience*, *16*(9), 511–519. https://doi.org/10.1038/nrn3977

Du, X., & Gamper, N. (2013). Potassium channels in peripheral pain pathways: Expression, function and therapeutic potential. *Current Neuropharmacology*, *11*(6), 621–640. https://doi.org/10.2174/1570159X113119990042

Du, X., Gao, H., Jaffe, D., Zhang, H., & Gamper, N. (2018). M-type K+ channels in peripheral nociceptive pathways. *British Journal of Pharmacology*, *175*(12), 2158–2172. https://doi.org/10.1111/bph.13978

Eijkelkamp, N., Linley, J. E., Torres, J. M., Bee, L., Dickenson, A. H., Gringhuis, M., Minett, M. S., Hong, G. S., Lee, E., Oh, U., Ishikawa, Y., Zwartkuis, F. J., Cox, J. J., & Wood, J. N. (2013). A role for Piezo2 in EPAC1-dependent mechanical allodynia. *Nature Communications*, *4*, 1682. https://doi.org/10.1038/ncomms2673

Frenzel, H., Bohlender, J., Pinsker, K., Wohlleben, B., Tank, J., Lechner, S. G., Schiska, D., Jaijo, T., Rüschendorf, F., Saar, K., Jordan, J., Millán, J. M., Gross, M., & Lewin, G. R. (2012). A genetic basis for mechanosensory traits in humans. *PLoS Biology*, *10*(5), e1001318. https://doi.org/10.1371/journal.pbio.1001318

Gamper N, Shapiro MS. (2015). *KCNQ Channels In: Zheng J, Trudeau MC. (eds). Handbook of Ion Channels*.

Gamper, N., Stockand, J. D., & Shapiro, M. S. (2005). The use of Chinese hamster ovary (CHO) cells in the study of ion channels. *Journal of Pharmacological and Toxicological Methods*, *51*(3), 177–185. https://doi.org/10.1016/j.vascn.2004.08.008

García-Mesa, Y., García-Piqueras, J., García, B., Feito, J., Cabo, R., Cobo, J., Vega, J. A., & García-Suárez, O. (2017). Merkel cells and Meissner's corpuscles in human digital skin display Piezo2 immunoreactivity. *Journal of Anatomy*, *231*(6), 978–989. https://doi.org/10.1111/joa.12688

Garell, P. C., McGillis, S. L., & Greenspan, J. D. (1996). Mechanical response properties of nociceptors innervating feline hairy skin. *Journal of Neurophysiology*, *75*(3), 1177–1189. https://doi.org/10.1152/jn.1996.75.3.1177

Giese, A. P. J., Tang, Y.-Q., Sinha, G. P., Bowl, M. R., Goldring, A. C., Parker, A., Freeman, M. J., Brown, S. D. M., Riazuddin, S., Fettiplace, R., Schafer, W. R., Frolenkov, G. I., & Ahmed, Z. M. (2017). CIB2 interacts with TMC1 and TMC2 and is essential for mechanotransduction in auditory hair cells. *Nature Communications*, *8*(1), 43. https://doi.org/10.1038/s41467-017-00061-1

Gillespie, P. G., & Müller, U. (2009). Mechanotransduction by hair cells: Models, molecules, and mechanisms. *Cell*, *139*(1), 33–44. https://doi.org/10.1016/j.cell.2009.09.010

Gleason, M. R., Nagiel, A., Jamet, S., Vologodskaia, M., López-Schier, H., & Hudspeth, A. J. (2009). The transmembrane inner ear (Tmie) protein is essential for normal hearing and balance in the zebrafish. *Proceedings of the National Academy of Sciences of the United States of America*, *106*(50), 21347–21352. https://doi.org/10.1073/pnas.0911632106

Häger, M., Bigotti, M. G., Meszaros, R., Carmignac, V., Holmberg, J., Allamand, V., Akerlund, M., Kalamajski, S., Brancaccio, A., Mayer, U., & Durbeej, M. (2008). Cib2 binds integrin alpha7Bbeta1D and is reduced in laminin alpha2 chain-deficient muscular dystrophy. *The Journal of Biological Chemistry*, *283*(36), 24760–24769. https://doi.org/10.1074/jbc.M801166200

Hammami, S., Willumsen, N. J., Olsen, H. L., Morera, F. J., Latorre, R., & Klaerke, D. A. (2009). Cell volume and membrane stretch independently control K+ channel activity. *The Journal of Physiology*, *587*(Pt 10), 2225–2231. https://doi.org/10.1113/jphysiol.2008.163550

Handler, A., & Ginty, D. D. (2021). The mechanosensory neurons of touch and their mechanisms of activation. *Nature Reviews. Neuroscience*, *22*(9), 521–537. https://doi.org/10.1038/s41583-021-00489-x

Hao, J., Bonnet, C., Amsalem, M., Ruel, J., & Delmas, P. (2015). Transduction and encoding sensory information by skin mechanoreceptors. *Pflugers Archiv: European Journal of Physiology*, *467*(1), 109–119. https://doi.org/10.1007/s00424-014-1651-7

Hao, J., Padilla, F., Dandonneau, M., Lavebratt, C., Lesage, F., Noël, J., & Delmas, P. (2013). Kv1.1 channels act as mechanical brake in the senses of touch and pain. *Neuron*, *77*(5), 899–914. https://doi.org/10.1016/j.neuron.2012.12.035

Hao, J., Ruel, J., Coste, B., Roudaut, Y., Crest, M., & Delmas, P. (2013). Piezo-electrically driven mechanical stimulation of sensory neurons. *Methods in Molecular Biology (Clifton, N.J.)*, *998*, 159–170. https://doi.org/10.1007/978-1-62703-351-0_12

Hartschuh, W., & Weihe, E. (1980). Fine structural analysis of the synaptic junction of Merkel cell-axon-complexes. *The Journal of Investigative Dermatology*, *75*(2), 159–165. https://doi.org/10.1111/1523-1747.ep12522555

Heidenreich, M., Lechner, S. G., Vardanyan, V., Wetzel, C., Cremers, C. W., De Leenheer, E. M., Aránguez, G., Moreno-Pelayo, M. Á., Jentsch, T. J., & Lewin, G. R. (2011). KCNQ4 K(+) channels tune mechanoreceptors for normal touch sensation in mouse and man. *Nature Neuroscience*, *15*(1), 138–145. https://doi.org/10.1038/nn.2985

Hitchcock, I. S., Genever, P. G., & Cahusac, P. M. B. (2004). Essential components for a glutamatergic synapse between Merkel cell and nerve terminal in rats. *Neuroscience Letters*, *362*(3), 196–199. https://doi.org/10.1016/j.neulet.2004.02.071

Hoffman, B. U., Baba, Y., Griffith, T. N., Mosharov, E. V., Woo, S.-H., Roybal, D. D., Karsenty, G., Patapoutian, A., Sulzer, D., & Lumpkin, E. A. (2018). Merkel Cells Activate Sensory Neural Pathways through Adrenergic Synapses. *Neuron*, *100*(6), 1401-1413.e6. https://doi.org/10.1016/j.neuron.2018.10.034

Holton, T., & Hudspeth, A. J. (1986). The transduction channel of hair cells from the bull-frog characterized by noise analysis. *The Journal of Physiology*, *375*(1), 195–227. https://doi.org/10.1113/jphysiol.1986.sp016113

Hu, J., Chiang, L.-Y., Koch, M., & Lewin, G. R. (2010). Evidence for a protein tether involved in somatic touch. *The EMBO Journal*, *29*(4), 855–867. https://doi.org/10.1038/emboj.2009.398

Hu, J., & Lewin, G. R. (2006). Mechanosensitive currents in the neurites of cultured mouse sensory neurones. *The Journal of Physiology*, *577*(Pt 3), 815–828. https://doi.org/10.1113/jphysiol.2006.117648

Hudspeth, A. J. (2014). Integrating the active process of hair cells with cochlear function. *Nature Reviews. Neuroscience*, *15*(9), 600–614. https://doi.org/10.1038/nrn3786

Hudspeth, A. J., & Corey, D. P. (1977). Sensitivity, polarity, and conductance change in the response of vertebrate hair cells to controlled mechanical stimuli. *Proceedings of the National Academy of Sciences of the United States of America*, *74*(6), 2407–2411. https://doi.org/10.1073/pnas.74.6.2407

Hudspeth, A. J., & Jacobs, R. (1979). Stereocilia mediate transduction in vertebrate hair cells (auditory system/cilium/vestibular system). *Proceedings of the National Academy of Sciences of the United States of America*, *76*(3), 1506–1509. https://doi.org/10.1073/pnas.76.3.1506

Iggo, A., & Muir, A. R. (1969). The structure and function of a slowly adapting touch corpuscle in hairy skin. *The Journal of Physiology*, *200*(3), 763–796. https://doi.org/10.1113/jphysiol.1969.sp008721

Ikeda, R., Cha, M., Ling, J., Jia, Z., Coyle, D., & Gu, J. G. (2014). Merkel cells transduce and encode tactile stimuli to drive Aβ-afferent impulses. *Cell*, *157*(3), 664–675. https://doi.org/10.1016/j.cell.2014.02.026

Jacoszek, A., Pollak, A., Płoski, R., & Ołdak, M. (2017). Advances in genetic hearing loss: CIB2 gene. *European Archives of Oto-Rhino-Laryngology: Official Journal of the European Federation of Oto-Rhino-Laryngological Societies (EUFOS): Affiliated with*

the German Society for Oto-Rhino-Laryngology - Head and Neck Surgery, *274*(4), 1791–1795. https://doi.org/10.1007/s00405-016-4330-9

Jenkins, B. A., & Lumpkin, E. A. (2017). Developing a sense of touch. *Development (Cambridge, England)*, *144*(22), 4078–4090. https://doi.org/10.1242/dev.120402

Jentsch, T. J. (2000). Neuronal KCNQ potassium channels: Physiology and role in disease. *Nature Reviews. Neuroscience*, *1*(1), 21–30. https://doi.org/10.1038/35036198

Jeong, H., Clark, S., Goehring, A., Dehghani-Ghahnaviyeh, S., Rasouli, A., Tajkhorshid, E., & Gouaux, E. (2022). Structures of the TMC-1 complex illuminate mechanosensory transduction. *Nature*. https://doi.org/10.1038/s41586-022-05314-8

Jia, Y., Zhao, Y., Kusakizako, T., Wang, Y., Pan, C., Zhang, Y., Nureki, O., Hattori, M., & Yan, Z. (2020). TMC1 and TMC2 Proteins Are Pore-Forming Subunits of Mechanosensitive Ion Channels. *Neuron*, *105*(2), 310-321.e3. https://doi.org/10.1016/j.neuron.2019.10.017

Johansson, O., Fantini, F., & Hu, H. (1999). Neuronal structural proteins, transmitters, transmitter enzymes and neuropeptides in human Meissner's corpuscles: A reappraisal using immunohistochemistry. *Archives of Dermatological Research*, *291*(7–8), 419–424. https://doi.org/10.1007/s004030050432

Johnson, K. O. (2001). The roles and functions of cutaneous mechanoreceptors. *Current Opinion in Neurobiology*, *11*(4), 455–461. https://doi.org/10.1016/s0959-4388(00)00234-8

Kandel, E.R. (2000). *Principles of neural science*.

Kawashima, Y., Géléoc, G. S. G., Kurima, K., Labay, V., Lelli, A., Asai, Y., Makishima, T., Wu, D. K., Della Santina, C. C., Holt, J. R., & Griffith, A. J. (2011). Mechanotransduction in mouse inner ear hair cells requires transmembrane channel-like genes. *The Journal of Clinical Investigation*, *121*(12), 4796–4809. https://doi.org/10.1172/JCI60405

Kharkovets, T., Dedek, K., Maier, H., Schweizer, M., Khimich, D., Nouvian, R., Vardanyan, V., Leuwer, R., Moser, T., & Jentsch, T. J. (2006). Mice with altered KCNQ4 K+ channels implicate sensory outer hair cells in human progressive deafness. *The EMBO Journal*, *25*(3), 642–652. https://doi.org/10.1038/sj.emboj.7600951

Kharkovets, T., Hardelin, J. P., Safieddine, S., Schweizer, M., El-Amraoui, A., Petit, C., & Jentsch, T. J. (2000). KCNQ4, a K+ channel mutated in a form of dominant deafness, is expressed in the inner ear and the central auditory pathway. *Proceedings of the National Academy of Sciences of the United States of America*, *97*(8), 4333–4338. https://doi.org/10.1073/pnas.97.8.4333

Kim, K. X., & Fettiplace, R. (2013). Developmental changes in the cochlear hair cell mechanotransducer channel and their regulation by transmembrane channel-like proteins. *The Journal of General Physiology*, *141*(1), 141–148. https://doi.org/10.1085/jgp.201210913

Kindt, K. S., Finch, G., & Nicolson, T. (2012). Kinocilia mediate mechanosensitivity in developing zebrafish hair cells. *Developmental Cell*, *23*(2), 329–341. https://doi.org/10.1016/j.devcel.2012.05.022

Koltzenburg, M., Stucky, C. L., & Lewin, G. R. (1997). Receptive properties of mouse sensory neurons innervating hairy skin. *Journal of Neurophysiology*, *78*(4), 1841–1850. https://doi.org/10.1152/jn.1997.78.4.1841

Kros, C. J., Rüsch, A., & Richardson, G. P. (1992). Mechano-electrical transducer currents in hair cells of the cultured neonatal mouse cochlea. *Proceedings. Biological Sciences*, *249*(1325), 185–193. https://doi.org/10.1098/rspb.1992.0102

Kubisch, C., Schroeder, B. C., Friedrich, T., Lütjohann, B., El-Amraoui, A., Marlin, S., Petit, C., & Jentsch, T. J. (1999). KCNQ4, a novel potassium channel expressed in sensory outer hair cells, is mutated in dominant deafness. *Cell*, *96*(3), 437–446. https://doi.org/10.1016/s0092-8674(00)80556-5

Kurima, K., Peters, L. M., Yang, Y., Riazuddin, S., Ahmed, Z. M., Naz, S., Arnaud, D., Drury, S., Mo, J., Makishima, T., Ghosh, M., Menon, P. S. N., Deshmukh, D., Oddoux, C., Ostrer, H., Khan, S., Riazuddin, S., Deininger, P. L., Hampton, L. L., … Griffith, A. J. (2002). Dominant and recessive deafness caused by mutations of a novel gene, TMC1, required for cochlear hair-cell function. *Nature Genetics*, *30*(3), 277–284. https://doi.org/10.1038/ng842

Lacour, J. P., Dubois, D., Pisani, A., & Ortonne, J. P. (1991). Anatomical mapping of Merkel cells in normal human adult epidermis. *The British Journal of Dermatology*, *125*(6), 535–542. https://doi.org/10.1111/j.1365-2133.1991.tb14790.x

Lang, P. M., Fleckenstein, J., Passmore, G. M., Brown, D. A., & Grafe, P. (2008). Retigabine reduces the excitability of unmyelinated peripheral human axons. *Neuropharmacology*, *54*(8), 1271–1278. https://doi.org/10.1016/j.neuropharm.2008.04.006

Leem, J. W., Willis, W. D., & Chung, J. M. (1993). Cutaneous sensory receptors in the rat foot. *Journal of Neurophysiology*, *69*(5), 1684–1699. https://doi.org/10.1152/jn.1993.69.5.1684

Lewin, G. R., & Moshourab, R. (2004). Mechanosensation and pain. *Journal of Neurobiology*, *61*(1), 30–44. https://doi.org/10.1002/neu.20078

Li, L., Rutlin, M., Abraira, V. E., Cassidy, C., Kus, L., Gong, S., Jankowski, M. P., Luo, W., Heintz, N., Koerber, H. R., Woodbury, C. J., & Ginty, D. D. (2011). The functional organization of cutaneous low-threshold mechanosensory neurons. *Cell*, *147*(7), 1615–1627. https://doi.org/10.1016/j.cell.2011.11.027

Liang, X., Qiu, X., Dionne, G., Cunningham, C. L., Pucak, M. L., Peng, G., Kim, Y.-H., Lauer, A., Shapiro, L., & Müller, U. (2021). CIB2 and CIB3 are auxiliary subunits of the mechanotransduction channel of hair cells. *Neuron*, *109*(13), 2131-2149.e15. https://doi.org/10.1016/j.neuron.2021.05.007

Löken, L. S., Wessberg, J., Morrison, I., McGlone, F., & Olausson, H. (2009). Coding of pleasant touch by unmyelinated afferents in humans. *Nature Neuroscience*, *12*(5), 547–548. https://doi.org/10.1038/nn.2312

Longo-Guess, C. M., Gagnon, L. H., Cook, S. A., Wu, J., Zheng, Q. Y., & Johnson, K. R. (2005). A missense mutation in the previously undescribed gene Tmhs underlies deafness in hurry-scurry (hscy) mice. *Proceedings of the National Academy of Sciences of the United States of America*, *102*(22), 7894–7899. https://doi.org/10.1073/pnas.0500760102

Lumpkin, E. A., & Caterina, M. J. (2007). Mechanisms of sensory transduction in the skin. *Nature*, *445*(7130), 858–865. https://doi.org/10.1038/nature05662

Maingret, F., Fosset, M., Lesage, F., Lazdunski, M., & Honoré, E. (1999). TRAAK is a mammalian neuronal mechano-gated K+ channel. *The Journal of Biological Chemistry*, *274*(3), 1381–1387. https://doi.org/10.1074/jbc.274.3.1381

Maksimovic, S., Baba, Y., & Lumpkin, E. A. (2013). Neurotransmitters and synaptic components in the Merkel cell-neurite complex, a gentle-touch receptor. *Annals of the New York Academy of Sciences*, *1279*, 13–21. https://doi.org/10.1111/nyas.12057

Maksimovic, S., Nakatani, M., Baba, Y., Nelson, A. M., Marshall, K. L., Wellnitz, S. A., Firozi, P., Woo, S.-H., Ranade, S., Patapoutian, A., & Lumpkin, E. A. (2014). Epidermal Merkel cells are mechanosensory cells that tune mammalian touch receptors. *Nature*, *509*(7502), 617–621. https://doi.org/10.1038/nature13250

Maljevic, S., Wuttke, T. V., & Lerche, H. (2008). Nervous system KV7 disorders: Breakdown of a subthreshold brake. *The Journal of Physiology*, *586*(7), 1791–1801. https://doi.org/10.1113/jphysiol.2008.150656

Marcotti, W., Corns, L. F., Desmonds, T., Kirkwood, N. K., Richardson, G. P., & Kros, C. J. (2014). Transduction without tip links in cochlear hair cells is mediated by ion channels with permeation properties distinct from those of the mechano-electrical transducer

channel. *The Journal of Neuroscience: The Official Journal of the Society for Neuroscience*, *34*(16), 5505–5514. https://doi.org/10.1523/JNEUROSCI.4086-13.2014

Maricich, S. M., Morrison, K. M., Mathes, E. L., & Brewer, B. M. (2012). Rodents rely on Merkel cells for texture discrimination tasks. *The Journal of Neuroscience: The Official Journal of the Society for Neuroscience*, *32*(10), 3296–3300. https://doi.org/10.1523/JNEUROSCI.5307-11.2012

Maricich, S. M., Wellnitz, S. A., Nelson, A. M., Lesniak, D. R., Gerling, G. J., Lumpkin, E. A., & Zoghbi, H. Y. (2009). Merkel cells are essential for light-touch responses. *Science (New York, N.Y.)*, *324*(5934), 1580–1582. https://doi.org/10.1126/science.1172890

Marshall, K. L., & Lumpkin, E. A. (2012). The molecular basis of mechanosensory transduction. *Advances in Experimental Medicine and Biology*, *739*, 142–155. https://doi.org/10.1007/978-1-4614-1704-0_9

McGlone, F., & Reilly, D. (2010). The cutaneous sensory system. *Neuroscience and Biobehavioral Reviews*, *34*(2), 148–159. https://doi.org/10.1016/j.neubiorev.2009.08.004

McPherson, D. R. (2018). Sensory Hair Cells: An Introduction to Structure and Physiology. *Integrative and Comparative Biology*, *58*(2), 282–300. https://doi.org/10.1093/icb/icy064

Meaud, J., & Grosh, K. (2010). The effect of tectorial membrane and basilar membrane longitudinal coupling in cochlear mechanics. *The Journal of the Acoustical Society of America*, *127*(3), 1411–1421. https://doi.org/10.1121/1.3290995

Meyer, R. A., Davis, K. D., Cohen, R. H., Treede, R. D., & Campbell, J. N. (1991). Mechanically insensitive afferents (MIAs) in cutaneous nerves of monkey. *Brain Research*, *561*(2), 252–261. https://doi.org/10.1016/0006-8993(91)91601-v

Michel, V., Booth, K. T., Patni, P., Cortese, M., Azaiez, H., Bahloul, A., Kahrizi, K., Labbé, M., Emptoz, A., Lelli, A., Dégardin, J., Dupont, T., Aghaie, A., Oficjalska-Pham, D., Picaud, S., Najmabadi, H., Smith, R. J., Bowl, M. R., Brown, S. D., … El-Amraoui, A. (2017). CIB2, defective in isolated deafness, is key for auditory hair cell mechanotransduction and survival. *EMBO Molecular Medicine*, *9*(12), 1711–1731. https://doi.org/10.15252/emmm.201708087

Milenkovic, N., Wetzel, C., Moshourab, R., & Lewin, G. R. (2008). Speed and temperature dependences of mechanotransduction in afferent fibers recorded from the mouse saphenous nerve. *Journal of Neurophysiology*, *100*(5), 2771–2783. https://doi.org/10.1152/jn.90799.2008

Mitchem, K. L., Hibbard, E., Beyer, L. A., Bosom, K., Dootz, G. A., Dolan, D. F., Johnson, K. R., Raphael, Y., & Kohrman, D. C. (2002). Mutation of the novel gene Tmie results in sensory cell defects in the inner ear of spinner, a mouse model of human hearing loss DFNB6. *Human Molecular Genetics*, *11*(16), 1887–1898. https://doi.org/10.1093/hmg/11.16.1887

Moll, I., & Moll, R. (1992). Early development of human Merkel cells. *Experimental Dermatology*, *1*(4), 180–184. https://doi.org/10.1111/j.1600-0625.1992.tb00186.x

Moroni, M., Servin-Vences, M. R., Fleischer, R., Sánchez-Carranza, O., & Lewin, G. R. (2018). Voltage gating of mechanosensitive PIEZO channels. *Nature Communications*, *9*(1), 1096. https://doi.org/10.1038/s41467-018-03502-7

Morrison, K. M., Miesegaes, G. R., Lumpkin, E. A., & Maricich, S. M. (2009). Mammalian Merkel cells are descended from the epidermal lineage. *Developmental Biology*, *336*(1), 76–83. https://doi.org/10.1016/j.ydbio.2009.09.032

Munger, B. L., & Ide, C. (1988). The structure and function of cutaneous sensory receptors. *Archives of Histology and Cytology*, *51*(1), 1–34. https://doi.org/10.1679/aohc.51.1

Muqeem, T., Ghosh, B., Pinto, V., Lepore, A. C., & Covarrubias, M. (2018). Regulation of Nociceptive Glutamatergic Signaling by Presynaptic Kv3.4 Channels in the Rat Spinal Dorsal Horn. *The Journal of Neuroscience: The Official Journal of the Society for Neuroscience*, *38*(15), 3729–3740. https://doi.org/10.1523/JNEUROSCI.3212-17.2018

Murthy, S. E., Dubin, A. E., Whitwam, T., Jojoa-Cruz, S., Cahalan, S. M., Mousavi, S. A. R., Ward, A. B., & Patapoutian, A. (2018). OSCA/TMEM63 are an Evolutionarily Conserved Family of Mechanically Activated Ion Channels. *ELife*, *7*, e41844. https://doi.org/10.7554/eLife.41844

Murthy, S. E., Loud, M. C., Daou, I., Marshall, K. L., Schwaller, F., Kühnemund, J., Francisco, A. G., Keenan, W. T., Dubin, A. E., Lewin, G. R., & Patapoutian, A. (2018). The mechanosensitive ion channel Piezo2 mediates sensitivity to mechanical pain in mice. *Science Translational Medicine*, *10*(462), eaat9897. https://doi.org/10.1126/scitranslmed.aat9897

Naik, U. P., Patel, P. M., & Parise, L. V. (1997). Identification of a novel calcium-binding protein that interacts with the integrin alphaIIb cytoplasmic domain. *The Journal of Biological Chemistry*, *272*(8), 4651–4654. https://doi.org/10.1074/jbc.272.8.4651

Neubarth, N. L., Emanuel, A. J., Liu, Y., Springel, M. W., Handler, A., Zhang, Q., Lehnert, B. P., Guo, C., Orefice, L. L., Abdelaziz, A., DeLisle, M. M., Iskols, M., Rhyins, J., Kim, S. J., Cattel, S. J., Regehr, W., Harvey, C. D., Drugowitsch, J., & Ginty, D. D. (2020). Meissner corpuscles and their spatially intermingled afferents underlie gentle touch perception. *Science (New York, N.Y.)*, *368*(6497), eabb2751. https://doi.org/10.1126/science.abb2751

Nikolaev, Y. A., Feketa, V. V., Anderson, E. O., Schneider, E. R., Gracheva, E. O., & Bagriantsev, S. N. (2020). Lamellar cells in Pacinian and Meissner corpuscles are touch sensors. *Science Advances*, *6*(51), eabe6393. https://doi.org/10.1126/sciadv.abe6393

Niu, Y., Tao, X., Vaisey, G., Olinares, P. D. B., Alwaseem, H., Chait, B. T., & MacKinnon, R. (2021). Analysis of the mechanosensor channel functionality of TACAN. *ELife*, *10*, e71188. https://doi.org/10.7554/eLife.71188

Ocaña, M., Cendán, C. M., Cobos, E. J., Entrena, J. M., & Baeyens, J. M. (2004). Potassium channels and pain: Present realities and future opportunities. *European Journal of Pharmacology*, *500*(1–3), 203–219. https://doi.org/10.1016/j.ejphar.2004.07.026

Omerbašić, D., Schuhmacher, L.-N., Bernal Sierra, Y.-A., Smith, E. S. J., & Lewin, G. R. (2015). ASICs and mammalian mechanoreceptor function. *Neuropharmacology*, *94*, 80–86. https://doi.org/10.1016/j.neuropharm.2014.12.007

Pan, B., Akyuz, N., Liu, X.-P., Asai, Y., Nist-Lund, C., Kurima, K., Derfler, B. H., György, B., Limapichat, W., Walujkar, S., Wimalasena, L. N., Sotomayor, M., Corey, D. P., & Holt, J. R. (2018). TMC1 Forms the Pore of Mechanosensory Transduction Channels in Vertebrate Inner Ear Hair Cells. *Neuron*, *99*(4), 736-753.e6. https://doi.org/10.1016/j.neuron.2018.07.033

Pan, B., Géléoc, G. S., Asai, Y., Horwitz, G. C., Kurima, K., Ishikawa, K., Kawashima, Y., Griffith, A. J., & Holt, J. R. (2013). TMC1 and TMC2 are components of the mechanotransduction channel in hair cells of the mammalian inner ear. *Neuron*, *79*(3), 504–515. https://doi.org/10.1016/j.neuron.2013.06.019

Passmore, G. M., Reilly, J. M., Thakur, M., Keasberry, V. N., Marsh, S. J., Dickenson, A. H., & Brown, D. A. (2012). Functional significance of M-type potassium channels in nociceptive cutaneous sensory endings. *Frontiers in Molecular Neuroscience*, *5*, 63. https://doi.org/10.3389/fnmol.2012.00063

Passmore, G. M., Selyanko, A. A., Mistry, M., Al-Qatari, M., Marsh, S. J., Matthews, E. A., Dickenson, A. H., Brown, T. A., Burbidge, S. A., Main, M., & Brown, D. A. (2003). KCNQ/M currents in sensory neurons: Significance for pain therapy. *The Journal of*

Neuroscience: The Official Journal of the Society for Neuroscience, *23*(18), 7227–7236.

Patel, K., Giese, A. P., Grossheim, J. M., Hegde, R. S., Hegde, R. S., Delio, M., Samanich, J., Riazuddin, S., Frolenkov, G. I., Cai, J., Ahmed, Z. M., & Morrow, B. E. (2015). A Novel C-Terminal CIB2 (Calcium and Integrin Binding Protein 2) Mutation Associated with Non-Syndromic Hearing Loss in a Hispanic Family. *PloS One*, *10*(10), e0133082. https://doi.org/10.1371/journal.pone.0133082

Patkunarajah, A., Stear, J. H., Moroni, M., Schroeter, L., Blaszkiewicz, J., Tearle, J. L., Cox, C. D., Fürst, C., Sánchez-Carranza, O., Ocaña Fernández, M. D. Á., Fleischer, R., Eravci, M., Weise, C., Martinac, B., Biro, M., Lewin, G. R., & Poole, K. (2020). TMEM87a/Elkin1, a component of a novel mechanoelectrical transduction pathway, modulates melanoma adhesion and migration. *ELife*, *9*, e53308. https://doi.org/10.7554/eLife.53308

Perry, M. J., & Lawson, S. N. (1998). Differences in expression of oligosaccharides, neuropeptides, carbonic anhydrase and neurofilament in rat primary afferent neurons retrogradely labelled via skin, muscle or visceral nerves. *Neuroscience*, *85*(1), 293–310. https://doi.org/10.1016/s0306-4522(97)00629-5

Petit, C., & Richardson, G. P. (2009). Linking genes underlying deafness to hair-bundle development and function. *Nature Neuroscience*, *12*(6), 703–710. https://doi.org/10.1038/nn.2330

Pickles, J. O. (2012). *An introduction to the physiology of hearing*. Emerald Group Publishing.

Poole, K., Herget, R., Lapatsina, L., Ngo, H.-D., & Lewin, G. R. (2014). Tuning Piezo ion channels to detect molecular-scale movements relevant for fine touch. *Nature Communications*, *5*, 3520. https://doi.org/10.1038/ncomms4520

Ranade, S. S., Syeda, R., & Patapoutian, A. (2015). Mechanically Activated Ion Channels. *Neuron*, *87*(6), 1162–1179. https://doi.org/10.1016/j.neuron.2015.08.032

Ranade, S. S., Woo, S.-H., Dubin, A. E., Moshourab, R. A., Wetzel, C., Petrus, M., Mathur, J., Bégay, V., Coste, B., Mainquist, J., Wilson, A. J., Francisco, A. G., Reddy, K., Qiu, Z., Wood, J. N., Lewin, G. R., & Patapoutian, A. (2014). Piezo2 is the major transducer of mechanical forces for touch sensation in mice. *Nature*, *516*(7529), 121–125. https://doi.org/10.1038/nature13980

Riazuddin, S., Belyantseva, I. A., Giese, A. P. J., Lee, K., Indzhykulian, A. A., Nandamuri, S. P., Yousaf, R., Sinha, G. P., Lee, S., Terrell, D., Hegde, R. S., Ali, R. A., Anwar, S., Andrade-Elizondo, P. B., Sirmaci, A., Parise, L. V., Basit, S., Wali, A., Ayub, M., … Ahmed, Z. M. (2012). Alterations of the CIB2 calcium- and integrin-binding protein cause Usher syndrome type 1J and nonsyndromic deafness DFNB48. *Nature Genetics*, *44*(11), 1265–1271. https://doi.org/10.1038/ng.2426

Rivera-Arconada, I., & Lopez-Garcia, J. A. (2005). Effects of M-current modulators on the excitability of immature rat spinal sensory and motor neurones. *The European Journal of Neuroscience*, *22*(12), 3091–3098. https://doi.org/10.1111/j.1460-9568.2005.04507.x

Rutlin, M., Ho, C.-Y., Abraira, V. E., Cassidy, C., Bai, L., Woodbury, C. J., & Ginty, D. D. (2014). The cellular and molecular basis of direction selectivity of Aδ-LTMRs. *Cell*, *159*(7), 1640–1651. https://doi.org/10.1016/j.cell.2014.11.038

Schmidt, R., Schmelz, M., Forster, C., Ringkamp, M., Torebjörk, E., & Handwerker, H. (1995). Novel classes of responsive and unresponsive C nociceptors in human skin. *The Journal of Neuroscience: The Official Journal of the Society for Neuroscience*, *15*(1 Pt 1), 333–341.

Schwaller, F., Bégay, V., García-García, G., Taberner, F. J., Moshourab, R., McDonald, B., Docter, T., Kühnemund, J., Ojeda-Alonso, J., Paricio-Montesinos, R., Lechner, S. G., Poulet, J. F. A., Millan, J. M., & Lewin, G. R. (2021). USH2A is a Meissner's corpuscle protein necessary for normal vibration sensing in mice and humans. *Nature Neuroscience*, *24*(1), 74–81. https://doi.org/10.1038/s41593-020-00751-y

Seco, C. Z., Giese, A. P., Shafique, S., Schraders, M., Oonk, A. M. M., Grossheim, M., Oostrik, J., Strom, T., Hegde, R., van Wijk, E., Frolenkov, G. I., Azam, M., Yntema, H. G., Free, R. H., Riazuddin, S., Verheij, J. B. G. M., Admiraal, R. J., Qamar, R., Ahmed, Z. M., & Kremer, H. (2016). Novel and recurrent CIB2 variants, associated with nonsyndromic deafness, do not affect calcium buffering and localization in hair cells. *European Journal of Human Genetics: EJHG*, *24*(4), 542–549. https://doi.org/10.1038/ejhg.2015.157

Shabbir, M. I., Ahmed, Z. M., Khan, S. Y., Riazuddin, S., Waryah, A. M., Khan, S. N., Camps, R. D., Ghosh, M., Kabra, M., Belyantseva, I. A., Friedman, T. B., & Riazuddin, S. (2006). Mutations of human TMHS cause recessively inherited non-syndromic hearing loss. *Journal of Medical Genetics*, *43*(8), 634–640. https://doi.org/10.1136/jmg.2005.039834

Sharma, N., Flaherty, K., Lezgiyeva, K., Wagner, D. E., Klein, A. M., & Ginty, D. D. (2020). The emergence of transcriptional identity in somatosensory neurons. *Nature*, *577*(7790), 392–398. https://doi.org/10.1038/s41586-019-1900-1

Siemens, J., Lillo, C., Dumont, R. A., Reynolds, A., Williams, D. S., Gillespie, P. G., & Müller, U. (2004). Cadherin 23 is a component of the tip link in hair-cell stereocilia. *Nature*, *428*(6986), 950–955. https://doi.org/10.1038/nature02483

Singh, A., Kildegaard, H. F., & Andersen, M. R. (2018). An Online Compendium of CHO RNA-Seq Data Allows Identification of CHO Cell Line-Specific Transcriptomic Signatures. *Biotechnology Journal*, *13*(10), e1800070. https://doi.org/10.1002/biot.201800070

Smith, E. S. J., & Lewin, G. R. (2009). Nociceptors: A phylogenetic view. *Journal of Comparative Physiology. A, Neuroethology, Sensory, Neural, and Behavioral Physiology*, *195*(12), 1089–1106. https://doi.org/10.1007/s00359-009-0482-z

Sneddon, L. U. (2015). Pain in aquatic animals. *The Journal of Experimental Biology*, *218*(Pt 7), 967–976. https://doi.org/10.1242/jeb.088823

Srinivasan, M. A., Whitehouse, J. M., & LaMotte, R. H. (1990). Tactile detection of slip: Surface microgeometry and peripheral neural codes. *Journal of Neurophysiology*, *63*(6), 1323–1332. https://doi.org/10.1152/jn.1990.63.6.1323

Sukharev, S. I., Blount, P., Martinac, B., Blattner, F. R., & Kung, C. (1994). A large-conductance mechanosensitive channel in E. coli encoded by mscL alone. *Nature*, *368*(6468), 265–268. https://doi.org/10.1038/368265a0

Sundt, D., Gamper, N., & Jaffe, D. B. (2015). Spike propagation through the dorsal root ganglia in an unmyelinated sensory neuron: A modeling study. *Journal of Neurophysiology*, *114*(6), 3140–3153. https://doi.org/10.1152/jn.00226.2015

Szczot, M., Liljencrantz, J., Ghitani, N., Barik, A., Lam, R., Thompson, J. H., Bharucha-Goebel, D., Saade, D., Necaise, A., Donkervoort, S., Foley, A. R., Gordon, T., Case, L., Bushnell, M. C., Bönnemann, C. G., & Chesler, A. T. (2018). PIEZO2 mediates injury-induced tactile pain in mice and humans. *Science Translational Medicine*, *10*(462), eaat9892. https://doi.org/10.1126/scitranslmed.aat9892

Takahashi-Iwanaga, H. (2000). Three-dimensional microanatomy of longitudinal lanceolate endings in rat vibrissae. *The Journal of Comparative Neurology*, *426*(2), 259–269. https://doi.org/10.1002/1096-9861(20001016)426:2<259::aid-cne7>3.0.co;2-n

Takahashi-Iwanaga, H., & Shimoda, H. (2003). The three-dimensional microanatomy of Meissner corpuscles in monkey palmar skin. *Journal of Neurocytology*, *32*(4), 363–371. https://doi.org/10.1023/B:NEUR.0000011330.57530.2f

Tang, Y.-Q., Lee, S. A., Rahman, M., Vanapalli, S. A., Lu, H., & Schafer, W. R. (2020). Ankyrin Is An Intracellular Tether for TMC Mechanotransduction Channels. *Neuron*, *107*(1), 112-125.e10. https://doi.org/10.1016/j.neuron.2020.03.026

Tsantoulas, C., & McMahon, S. B. (2014). Opening paths to novel analgesics: The role of potassium channels in chronic pain. *Trends in Neurosciences*, *37*(3), 146–158. https://doi.org/10.1016/j.tins.2013.12.002

Tsantoulas, C., Zhu, L., Shaifta, Y., Grist, J., Ward, J. P. T., Raouf, R., Michael, G. J., & McMahon, S. B. (2012). Sensory neuron downregulation of the Kv9.1 potassium channel subunit mediates neuropathic pain following nerve injury. *The Journal of Neuroscience: The Official Journal of the Society for Neuroscience*, *32*(48), 17502–17513. https://doi.org/10.1523/JNEUROSCI.3561-12.2012

Usoskin, D., Furlan, A., Islam, S., Abdo, H., Lönnerberg, P., Lou, D., Hjerling-Leffler, J., Haeggström, J., Kharchenko, O., Kharchenko, P. V., Linnarsson, S., & Ernfors, P. (2015). Unbiased classification of sensory neuron types by large-scale single-cell RNA sequencing. *Nature Neuroscience*, *18*(1), 145–153. https://doi.org/10.1038/nn.3881

Vega, J. A., Haro, J. J., & Del Valle, M. E. (1996). Immunohistochemistry of human cutaneous Meissner and pacinian corpuscles. *Microscopy Research and Technique*, *34*(4), 351–361. https://doi.org/10.1002/(SICI)1097-0029(19960701)34:4<351::AID-JEMT6>3.0.CO;2-R

Vega-Bermudez, F., & Johnson, K. O. (1999). Surround suppression in the responses of primate SA1 and RA mechanoreceptive afferents mapped with a probe array. *Journal of Neurophysiology*, *81*(6), 2711–2719. https://doi.org/10.1152/jn.1999.81.6.2711

Vetter, I., Hein, A., Sattler, S., Hessler, S., Touska, F., Bressan, E., Parra, A., Hager, U., Leffler, A., Boukalova, S., Nissen, M., Lewis, R. J., Belmonte, C., Alzheimer, C., Huth, T., Vlachova, V., Reeh, P. W., & Zimmermann, K. (2013). Amplified cold transduction in native nociceptors by M-channel inhibition. *The Journal of Neuroscience: The Official Journal of the Society for Neuroscience*, *33*(42), 16627–16641. https://doi.org/10.1523/JNEUROSCI.1473-13.2013

Waguespack, J., Salles, F. T., Kachar, B., & Ricci, A. J. (2007). Stepwise Morphological and Functional Maturation of Mechanotransduction in Rat Outer Hair Cells. *Journal of Neuroscience*, *27*(50), 13890–13902. https://doi.org/10.1523/JNEUROSCI.2159-07.2007

Walcher, J., Ojeda-Alonso, J., Haseleu, J., Oosthuizen, M. K., Rowe, A. H., Bennett, N. C., & Lewin, G. R. (2018). Specialized mechanoreceptor systems in rodent glabrous skin. *The Journal of Physiology*, *596*(20), 4995–5016. https://doi.org/10.1113/JP276608

Wang, K. (2008). Modulation by clamping: Kv4 and KChIP interactions. *Neurochemical Research*, *33*(10), 1964–1969. https://doi.org/10.1007/s11064-008-9705-x

Wang, R., & Lewin, G. R. (2011). The Cav3.2 T-type calcium channel regulates temporal coding in mouse mechanoreceptors. *The Journal of Physiology*, *589*(Pt 9), 2229–2243. https://doi.org/10.1113/jphysiol.2010.203463

Wang, Y., Li, J., Yao, X., Li, W., Du, H., Tang, M., Xiong, W., Chai, R., & Xu, Z. (2017). Loss of CIB2 Causes Profound Hearing Loss and Abolishes Mechanoelectrical Transduction in Mice. *Frontiers in Molecular Neuroscience*, *10*, 401. https://doi.org/10.3389/fnmol.2017.00401

Waxman, S. G., & Zamponi, G. W. (2014). Regulating excitability of peripheral afferents: Emerging ion channel targets. *Nature Neuroscience*, *17*(2), 153–163. https://doi.org/10.1038/nn.3602

Wellnitz, S. A., Lesniak, D. R., Gerling, G. J., & Lumpkin, E. A. (2010). The regularity of sustained firing reveals two populations of slowly adapting touch receptors in mouse hairy skin. *Journal of Neurophysiology*, *103*(6), 3378–3388. https://doi.org/10.1152/jn.00810.2009

Werner, G., & Mountcastle, V. B. (1965). NEURAL ACTIVITY IN MECHANORECEPTIVE CUTANEOUS AFFERENTS: STIMULUS-RESPONSE RELATIONS, WEBER FUNCTIONS, AND INFORMATION TRANSMISSION. *Journal of Neurophysiology*, *28*, 359–397. https://doi.org/10.1152/jn.1965.28.2.359

Woo, S.-H., Ranade, S., Weyer, A. D., Dubin, A. E., Baba, Y., Qiu, Z., Petrus, M., Miyamoto, T., Reddy, K., Lumpkin, E. A., Stucky, C. L., & Patapoutian, A. (2014). Piezo2 is

required for Merkel-cell mechanotransduction. *Nature*, *509*(7502), 622–626. https://doi.org/10.1038/nature13251

Wu, H., Williams, J., & Nathans, J. (2012). Morphologic diversity of cutaneous sensory afferents revealed by genetically directed sparse labeling. *ELife*, *1*, e00181. https://doi.org/10.7554/eLife.00181

Xiong, W., Grillet, N., Elledge, H. M., Wagner, T. F. J., Zhao, B., Johnson, K. R., Kazmierczak, P., & Müller, U. (2012). TMHS is an integral component of the mechanotransduction machinery of cochlear hair cells. *Cell*, *151*(6), 1283–1295. https://doi.org/10.1016/j.cell.2012.10.041

Zhao, B., Wu, Z., Grillet, N., Yan, L., Xiong, W., Harkins-Perry, S., & Müller, U. (2014). TMIE is an essential component of the mechanotransduction machinery of cochlear hair cells. *Neuron*, *84*(5), 954–967. https://doi.org/10.1016/j.neuron.2014.10.041

Zheng, Y., Liu, P., Bai, L., Trimmer, J. S., Bean, B. P., & Ginty, D. D. (2019). Deep Sequencing of Somatosensory Neurons Reveals Molecular Determinants of Intrinsic Physiological Properties. *Neuron*, *103*(4), 598-616.e7. https://doi.org/10.1016/j.neuron.2019.05.039

Zhou, W., Qian, Y., Kunjilwar, K., Pfaffinger, P. J., & Choe, S. (2004). Structural insights into the functional interaction of KChIP1 with Shal-type K(+) channels. *Neuron*, *41*(4), 573–586. https://doi.org/10.1016/s0896-6273(04)00045-5

Zimmerman, A., Bai, L., & Ginty, D. D. (2014). The gentle touch receptors of mammalian skin. *Science (New York, N.Y.)*, *346*(6212), 950–954. https://doi.org/10.1126/science.1254229